

A MULTI-MEDIA BIOASSAY-DIRECTED INVESTIGATION OF  
THE HAMILTON HARBOUR AREA OF WESTERN LAKE ONTARIO

By

C.H. MARVIN, B.Sc., M.Sc.

A Thesis

Submitted to the School of Graduate Studies  
in Partial Fulfilment of the Requirements  
for the Degree

Doctor of Philosophy

McMaster University

(c) Copyright by C.H. Marvin 1994

BIOASSAY-DIRECTED INVESTIGATION OF HAMILTON HARBOUR

DOCTOR OF PHILOSOPHY (1994)      McMASTER UNIVERSITY  
(Chemistry)                              Hamilton, Ontario

**TITLE:**                              A Multi-Media Bioassay-Directed Investigation of  
the Hamilton Harbour Area of Western Lake  
Ontario.

**AUTHOR:**                            Christopher H. Marvin, B.Sc. (University of  
Waterloo), M.Sc. (Brock University)

**SUPERVISOR:**                      Dr. B.E. McCarry

**NUMBER OF PAGES:**      XXI,185

PREFACE

Parts of the text, figures and tables in this academic thesis have previously been published in the following scientific journals.

\*Marvin, C.H., Allan, L., McCarry, B.E. and Bryant, D.W. A comparison of ultrasonic extraction and Soxhlet extraction of polycyclic aromatic hydrocarbons from sediments and air particulate material. International Journal of Environmental Analytical Chemistry, Volume 49, pp. 221-230, 1992.

\*Marvin, C.H., Allan, L., McCarry, B.E. and Bryant, D.W. Chemical/Biological investigation of contaminated sediment from the Hamilton Harbour area of western Lake Ontario. Environmental and Molecular Mutagenesis, Volume 22, pp. 61-70, 1993.

This research was undertaken and compiled in written and graphical form entirely by the principal author under the supervision of Drs. B.E. McCarry and D.W. Bryant.

## ABSTRACT

A methodology for the extraction, clean-up and compound class fractionation of complex environmental mixtures was developed and tested using standard reference materials and sediment from Hamilton Harbour. Samples were extracted using a Soxhlet apparatus or an ultrasonication apparatus and the resulting organic solvent extracts were fractionated into compound classes using an alumina/Sephadex LH20 clean-up procedure and high performance liquid chromatographic techniques.

In the next phase of the study, sediment samples, sediment trap samples, and air particulate material from the Hamilton Harbour area of western Lake Ontario were fractionated using the developed methodology. These samples were chosen with the aim of evaluating the contributions of a variety of sources to chemical and genotoxic contamination in the harbour. The resulting fractions were analyzed by chromatographic techniques and tested for genotoxicity using the Ames *Salmonella*/microsome assay with TA98-like and TA100-like bacterial strains modified by the inclusion of genes for the activating enzymes nitroreductase and O-acetyltransferase. These data were used to construct chemical and biological profiles of the samples and to identify specific compounds and compound classes responsible for mutagenic activity observed in the sample extracts.

The majority of the mutagenic activity displayed by a Randle Reef sediment sample extract was found to be present in the fraction containing the polycyclic aromatic

hydrocarbons (PAH). Extracts of the PAH-containing fraction displayed dramatically higher responses with the TA100-type strains with metabolic activation. The PAH fraction was further fractionated and analysed to identify the compound(s) responsible for the mutagenic activity. The biological activity of this PAH-containing fraction was found to co-elute with compounds of molecular mass 252, 276, 278, and 302 amu.

In contrast to the results obtained from the investigation of the Randle Reef sediment sample, extracts of sediment trap samples displayed significantly higher responses with the TA98-type strains. The compound(s) responsible for this biological activity were contained in the more polar polycyclic aromatic compound (PAC) fractions and did not require oxidative metabolism to manifest their activity. Further separation of the most biologically active fraction from the sediment trap samples revealed that the biological activity was contained in a very narrow elution time range in the reversed-phase high performance liquid chromatography (RP-HPLC) chromatogram. This narrow band of activity was collected and analysed using gas chromatography-mass spectrometry (GC-MS). While alkyl-benzocarbazole derivatives were identified in these fractions, they were not considered to be the agents responsible for the observed biological activity.

The use of ultrasonic extraction and the alumina/Sephadex LH20 clean-up and normal phase HPLC compound class fractionation procedures were found to be effective for the preparation of a number of complex environmental samples. The chemical and biological profiles of the harbour sediment and suspended sediments indicate that PAH from resuspended coal tar contaminated sediment is a principal contributor to the

iv

chemical profile of suspended sediments in the harbour and a significant contributor to the genotoxicity of extracts of these samples. However, the biological profiles of the suspended sediments indicate the presence of additional mutagens other than PAH that are not present in the Randle Reef sediment sample. A comparison of the biological profiles of extracts of suspended sediments and air particulate material indicate that there may be a common mutagenic contaminant in both of these sample matrices.

vi

## ACKNOWLEDGEMENTS

I would like to express my sincere appreciation to Drs. Brian E. McCarty and Douglas W. Bryant for their supervision, advice, expertise, and friendship during the course of this study. I am also indebted to the third member of my supervisory committee, Dr. O.E. Hileman Jr., with whom I have also had the pleasure of working in the undergraduate laboratories.

I would also like to acknowledge the guidance of Dr A.D. Bain and Dr A. Corsini, from whom I have learned a great deal about the field of analytical chemistry.

Thanks also to Leah Allan, Mr. Faj Ramalen and Dr. R. Smith for technical support, and my co-worker Arnold Legzdins.

I would like to thank Dr. Bill Morris and J. Ken Versteeg of the Department of Geology, with whom I have enjoyed two years of collaborative research.

The technical support of Drs. Murray Charlton, Andrew Peters and Mike Fox of the Canada Center for Inland Waters, and the financial support of the Great Lakes University Research Fund and the Natural Science and Engineering Research Council is greatly appreciated.

vii



LIST OF FIGURES

		Page
Figure 1.	Map of Hamilton Harbour showing sites selected for sample collection.	2
Figure 2.	Structures of polycyclic aromatic hydrocarbons.	4
Figure 3.	Sediment trap mooring.	11
Figure 4.	Sediment trap.	12
Figure 5.	Sample clean-up and fractionation scheme.	19
Figure 6.	RP-HPLC chromatogram of Randle Reef sediment crude extract.	26
Figure 7.	Comparison of RP-HPLC chromatograms of Randle Reef sediment crude extract prepared by (A) ultrasonication and (B) by a Soxhlet apparatus.	28
Figure 8.	Comparison of RP-HPLC chromatograms of the PAH fraction (fraction N1) of the Randle Reef sediment sample prepared using (A) ultrasonication and (B) a Soxhlet apparatus.	30
Figure 9.	Sample clean-up and fractionation scheme with weights of material contained in each fraction of the Randle Reef sediment sample.	37
Figure 10.	RP-HPLC chromatogram of fraction A45 of the Randle Reef sediment sample.	39
Figure 11.	GC-FID chromatogram of fraction A1 of the Randle Reef sediment sample.	40
Figure 12.	GC-MS chromatogram of fraction A23/LH20 of the Randle Reef sediment sample.	41

Figure 13.	RP-HPLC chromatogram of fraction A23/LH20 of the Randle Reef sediment sample.	42
Figure 14.	NP-HPLC chromatogram of the Randle Reef sediment sample.	45
Figure 15.	RP-HPLC chromatogram of fraction N1 of the Randle Reef sediment sample.	47
Figure 16.	RP-HPLC chromatogram of fraction N2 of the Randle Reef sediment sample.	48
Figure 17.	GC-MS chromatogram of fraction N2 of the Randle Reef sediment sample.	49
Figure 18.	RP-HPLC chromatogram of fraction N3 of the Randle Reef sediment sample.	51
Figure 19.	GC-MS chromatogram of fraction N3 of the Randle Reef sediment sample.	52
Figure 20.	RP-HPLC chromatogram of fraction A23/LH20 of the station 910 sediment sample.	53
Figure 21.	Comparison of GC-MS chromatograms of Randle Reef and station 53 sediment traps fraction A23/LH20.	56
Figure 22.	Comparison of RP-HPLC chromatograms of Randle Reef and station 53 sediment traps fraction A23/LH20.	57
Figure 23.	GC-MS chromatogram of station 53 middle sediment trap fraction A23/LH20.	59
Figure 24.	GC-MS chromatogram of station 50 top sediment trap fraction A23/LH20.	64
Figure 25.	GC-MS chromatogram of station 53 top sediment trap fraction N2.	66
Figure 26.	GC-MS chromatogram of station 53 top sediment trap fraction N3.	67

		Page
Figure 27.	GC-MS SIM chromatogram of station 50 bottom sediment trap fraction N2.	68
Figure 28.	Dose response curves exhibited by Randle Reef sediment crude extract when assayed with strains YG1020 and YG1025.	70
Figure 29.	GC-MS SIM chromatogram of Randle Reef sediment fraction N2.	73
Figure 30.	Dose response curves exhibited by Randle Reef sediment fraction A23/LH20 when assayed with TA98-like strains.	74
Figure 31.	Dose response curves exhibited by Randle Reef sediment fraction A23/LH20 when assayed with TA100-like strains.	75
Figure 32.	Dose response curves exhibited by Randle Reef sediment fraction A45 when assayed with strains YG1020 and YG1025.	77
Figure 33.	Dose response curves exhibited by Randle Reef sediment N fractions when assayed with strain YG1020.	78
Figure 34.	Dose response curves exhibited by Randle Reef sediment N fractions when assayed with strain YG1025.	79
Figure 35.	Dose response curves exhibited by Randle Reef sediment N fractions when assayed with strain YG1024.	80
Figure 36.	Diagram showing relative contributions of Randle Reef sediment N fractions to the mutagenic activity in fraction A23/LH20 when assayed with strain YG1025+S9.	82
Figure 37.	Randle Reef sediment fraction N1 mutachromatogram.	84
Figure 38.	GC-MS chromatogram of the combined active subfractions from the Randle Reef sediment fraction N1 mutachromatogram.	87
Figure 39.	GC-MS SIM chromatogram of the combined active subfractions from the Randle Reef sediment fraction N1	88

		Page
	mutachromatogram.	
Figure 40.	Dose response curves exhibited by station 50 sediment trap fraction A23/LH20 when assayed with strain YG1025.	90
Figure 41.	Dose response curves exhibited by station 53 sediment trap fraction A23/LH20 when assayed with strain YG1025.	91
Figure 42.	Comparison of strain YG1025+S9 dose response curves of station 53 sediment traps and the Randle Reef sediment fraction A23/LH20 normalized for PAH content.	95
Figure 43.	Comparison of strain YG1025+S9 dose response curves of station 50 sediment traps and the Randle Reef sediment fraction A23/LH20 normalized for PAH content.	96
Figure 44.	Comparison of strain YG1024 dose response curves of station 53 sediment traps and Randle Reef sediment fraction A23/LH20.	98
Figure 45.	Dose response curves exhibited by station 53 top sediment trap N fractions when assayed with strain YG1024.	99
Figure 46.	Dose response curves exhibited by station 53 middle sediment trap N fractions when assayed with strain YG1024.	100
Figure 47.	Dose response curves exhibited by station 53 bottom sediment trap N fractions when assayed with strain YG1024.	101
Figure 48.	Dose response curves exhibited by station 50 sediment traps fraction A23/LH20 when assayed with strain YG1024.	103
Figure 49.	Dose response curves exhibited by station 50 top sediment trap N fractions when assayed with strain YG1024.	104
Figure 50.	Dose response curves exhibited by station 50 bottom sediment trap N fractions when assayed with strain	105

	Page
YG1024.	
Figure 51. Dose response curves exhibited by Randle Reef sediment N fractions when assayed with strain YG1024.	106
Figure 52. Dose response curves exhibited by station 51 sediment trap A23/LH20 fractions.	107
Figure 53. Dose response curves exhibited by station 50 top sediment trap fraction A45 when assayed with strain YG1024.	109
Figure 54. Dose response curves exhibited by station 50 bottom sediment trap A45 fractions when assayed with strain YG1024.	110
Figure 55. Station 50 top sediment trap fraction N3 mutachromatogram.	112
Figure 56. GC-MS chromatogram of the pooled active subfractions from the station 50 top sediment trap fraction N3 mutachromatogram.	114
Figure 57. Station 53 sediment trap fraction N3 mutachromatogram.	116
Figure 58. GC-MS chromatogram of the most active subfraction from the station 53 sediment trap fraction N3 mutachromatogram.	117
Figure 59. Mass spectrum of the molecular weight 231 compounds observed in the GC-MS chromatogram of the most active subfraction from the station 53 sediment trap fraction N3 mutachromatogram and the library spectrum of methylbenzo[c]carbazole.	118
Figure 60. GC-MS TIC and m/z 231 ion chromatogram from the analysis of the pooled active subfractions from the station 50 top sediment trap fraction N3 mutachromatogram.	119
Figure 61. GC-MS chromatograms from the analyses of the thirty second subfractions from the station 53 sediment trap N3	120

xvi

	Page
mutachromatogram.	
Figure 62. Plot of m/z 231 ion abundances from the analyses of the thirty second subfractions from the station 53 N3 mutachromatogram.	124
Figure 63. GC-MS m/z 231 ion chromatogram from the analysis of the Randle Reef sediment sample fraction N3.	125
Figure 64. Dose response curves exhibited by the pooled subfractions of the station 50 top sediment trap fraction N3 mutachromatogram when assayed with strain YG1024 and strain DNF <sub>6</sub> .	127
Figure 65. Dose response curves exhibited by fractions A23/LH20 and A45 of the CCIW air particulate extract.	130
Figure 66. Dose response curves exhibited by N fractions of the CCIW air particulate extract.	131
Figure 67. Mutachromatograms of air particulate extract N fractions.	134
Figure 68. Map of Hamilton Harbour showing Zebra mussel sample sites.	138
Figure 69. GC-MS SIM chromatogram of Zebra mussel extract fraction A23/LH20.	140
Figure 70. PAH concentrations in Zebra mussel extracts normalized to benzo[e]pyrene.	143
Figure 71. Dose response curves exhibited by Zebra mussel extract A23/LH20 fractions	144
Figure 72. Map of Hamilton Harbour showing PAH levels and mutagenic activities of extracts of samples from each site.	151
Figure 73. Schematic of the sample clean-up and fractionation procedure.	159
Figure 74. Representation of the bioassay procedure.	166

xvii

	Page
Figure 75. Dose response curves exhibited by standard mutagens when assayed with <u>Salmonella typhimurium</u> strains.	167

xviii

#### LIST OF TABLES

	Page
Table 1. Comparison of PAH levels determined in SRM1649 in samples prepared by ultrasonic extraction with the certified values.	33
Table 2. Common PAH determined in the Randle Reef sediment sample.	43
Table 3. Common PAH determined in Hamilton Harbour sediment traps.	61
Table 4. Weight of material contained in sediment trap sample extracts.	62
Table 5. Concentrations of PAH normalized to chrysene.	63
Table 6. Mutagenic potency of Randle Reef sediment sample extract.	71
Table 7. Mutagenic potency of station 53 sediment trap sample extracts.	92
Table 8. Mutagenic potency of station 50 sediment trap sample extracts.	93
Table 9. Mutagenic potency of CCIW air particulate extract.	132
Table 10. Concentrations of PAH determined in extracts of Zebra mussels.	141
Table 11. Mutagenic potencies of Zebra mussel extracts.	146

xix

## LIST OF ABBREVIATIONS

amu	Atomic mass units
CCIW	Canada Center for Inland Waters
DMSO	Dimethylsulfoxide
DNA	Deoxyribonucleic acid
FID	Flame ionization detection
GC-MS	Gas chromatography-mass spectrometry
g	Gram
HPLC	High performance liquid chromatography
mg	Milligram
m/z	Mass to charge ratio
ng	Nanogram
NIST	National Institute of Standards and Technology
NP	Normal phase
PAH	Polycyclic aromatic hydrocarbons
PAC	Polycyclic aromatic compounds
pg	Picogram
rev.	Revertants
RP	Reversed phase
S9	Rat liver supernatant

xx

SIM	Selected ion monitoring
SFE	Supercritical fluid extraction
SRM	Standard reference material
TIC	Total ion chromatogram
UV	Ultraviolet
µg	Microgram

xxi

1

## I. INTRODUCTION

### 1.1 Hamilton Harbour Geography and Environmental Status

Hamilton Harbour, an embayment located at the western end of Lake Ontario, has an area of 40 km<sup>2</sup> and acts as a receiving body for a watershed of some 900 km<sup>2</sup> (Figure 1). The average water depth in the harbour is 13 m and the maximum depth is 26 m. The east end of the harbour is joined to Lake Ontario by the Burlington ship canal and the west end of the harbour is joined to the Cootes Paradise conservation area by the Desjardins canal.

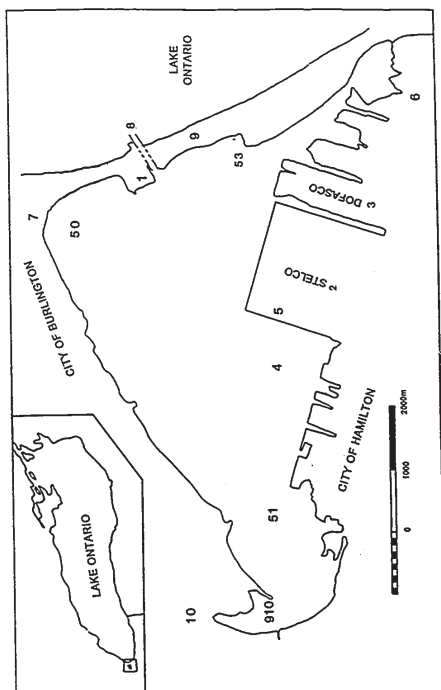
Major sources of contaminants in the harbour include industrial effluents, roadway runoff, and treated municipal sewage from a metropolitan area including the cities of Hamilton, Dundas, and Burlington with a combined population of about 500,000 people. The southeast shore of the harbour is dominated by the Steel Company of Canada (Stelco) and Dominion Foundry and Steel Company (Dofasco) steel mills; these are two of the largest steel operations in the nation. Hamilton Harbour has been designated as an area of concern by the Water Quality Board of the International Joint Commission.

High levels of contaminants including polychlorinated biphenyls (PCB), heavy metals, and PAH have been determined in Hamilton Harbour sediments (1,2). Figure 2 shows the structures of a number of homocyclic PAH that are commonly identified in

2

Figure 1. Map of Hamilton Harbour showing sites selected for sample collection. The following legend identifies key landmarks and sampling sites corresponding to the numbers on the map.

1. Canada Center for Inland Waters
2. Steel Co. of Canada (Stelco)
3. Dominion Foundry and Steel Co. (Dofasco)
4. Randle Reef
5. Stelco coking pier
6. Hamilton sewage treatment plant
7. Burlington sewage treatment plant
8. Ship canal
9. J. Allan Burlington/Hamilton Skyway, Queen Elizabeth Way
10. Cootes Paradise Conservation Area
50. Station 50 sediment trap sample site
51. Station 51 sediment trap sample site
53. Station 53 sediment trap sample site
910. Station 910 sediment sample site



harbour sediments. These ubiquitous compounds are the result of incomplete combustion of organic material. Several of these compounds have been implicated in the etiology of some human cancers. High levels of total dissolved solids, zinc, ammonia, phosphorus, iron, cyanide, and phenolic compounds have been determined in the harbour waters, particularly near the steel mills (3).

The concentrations of PAH in extracts of sediment sampled from the Randle Reef area of the harbour (Figure 1) have been observed to be as high as 1400  $\mu\text{g/g}$  (2). The high PAH levels in sediment samples taken from the harbour may arise principally from resuspension and transport of sediments from sites with extensive coal tar contamination such as the Randle Reef area (2). This transport phenomenon is thought to be responsible for similar PAH profiles in extracts of sediments collected at many locations within the harbour. The dynamics of the harbour result in non-uniform PAH concentrations in sediments sampled over small areas. Methodologies to remove or treat the grossly PAH-contaminated sediments of the Randle Reef area are currently being considered and tested. Atmospheric deposition, urban runoff, and the sewage treatment plants in the harbour watershed are considered to be more minor contributors to PAH contamination in the harbour. Poulton (1) found the total PAH levels (defined as the sum of individual PAH concentrations) at most sampling locations within Hamilton Harbour to be comparable to those determined by Black (4) in sediments taken from the Buffalo river, an area of heavy urban activity and industrialization.

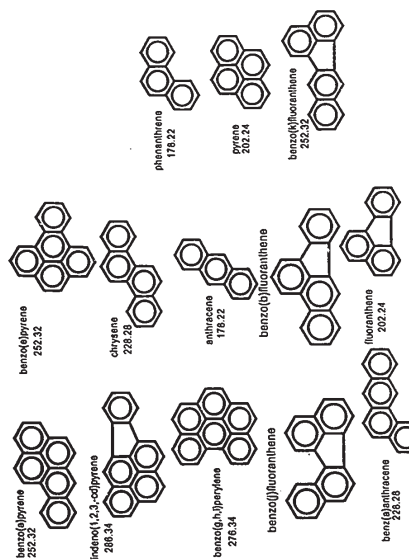


Figure 2. Structures and molecular weights of common homocyclic polycyclic aromatic hydrocarbons determined in Hamilton Harbour sediments.

## L2 Impact of Chemical Contamination on Aquatic Life

The determination of chemical contaminants in the aquatic environment is of importance not only because of the adverse effects on the ecosystem, but because of the potential of fish and wildlife to convey these contaminants to the human population. The observance of neoplasia in fish is considered to be evidence of the presence of carcinogens in the aquatic environment (5,6). The complex role of these chemical contaminants in the etiology of tumours in fish has previously been reviewed (5,6).

Hayes *et al* (7) described an increased prevalence of skin and liver neoplasms in white suckers (*Catostomus commersoni*) and brown bullheads (*Ictalurus nebulosus*) collected from industrially polluted areas in the western region of Lake Ontario, including Hamilton Harbour. In a similar study, Smith and Ferguson (8) reported a two to three-fold increase in the frequency of epidermal papillomas among white suckers and brown bullheads from Hamilton Harbour, as compared to similar fish from other areas of Lake Ontario. Metcalfe *et al* (9,10) have investigated the association between chemical contamination in Hamilton Harbour sediments and the high prevalence of fish tumours. These authors found that organic solvent extracts of sediments from Hamilton Harbour induced hepatocellular carcinomas in trout using a sac fry microinjection assay. High concentrations of polychlorinated biphenyls (PCB's), organochlorine pesticides and polycyclic aromatic hydrocarbons (PAH) were quantified in the sediment sample extracts.

The determination of high levels of chemical contaminants in sediments located near fish populations with high tumour frequencies has been used to support the

association between chemical contamination and fish tumours (11). Chemical contaminants have been determined in tissues of fish exhibiting tumours (12) and extensive epidemiological studies by Myers *et al* (13) and Stein *et al* (14) have confirmed an association between exposure to PAH and hepatic neoplasms in English sole from Puget Sound, Washington. Baumann (15) has observed that documented cases of cancer in wild freshwater fish populations in Lake Ontario increase in areas contaminated by industrial effluents.

### I.3 Hamilton Harbour Wildlife Status

There are approximately 60 species of fish in Hamilton Harbour but the fishery is dominated by carp (*Cyprinus carpio*) and brown bullhead (*Ictalurus nebulosus*). In Hamilton Harbour, these fish have been observed to experience higher incidences of tumours and skin papillomas than fish sampled from other areas in the Great Lakes less impacted by urbanization and/or industrialization (3). Consumption advisories are in effect for 5 of the 12 sport fish in the harbour. Snapping turtles, algae and zooplankton, and bottom fauna have all been observed to be affected by the contaminants in the water, sediments, or in organisms that these species feed on (3). Restrictions on fish and wildlife consumption, degraded fish and wildlife, fish tumours and other deformities, wildlife deformities or reproductive problems, degradation of benthos, eutrophication, and restrictions on drinking water consumption are all impairments to the harbour resulting from industrial and urban activity.

The documentation of increased occurrences of tumours and other deformities in fish in Hamilton Harbour (7,8) has led to investigations of the association of these deformities with chemical contamination (9,10,12,15). These studies have stopped short of identifying the specific compounds potentially responsible for these effects. An extensive chemico/biological investigation of sediment and sediment trap material using the developed extraction and bioassay-directed fractionation methodology could lead to the identification of individual compounds or compound classes responsible for the genotoxicity observed in extracts of these samples.

### I.5 Methodology

#### I.5.1 Sampling Locations and Methods

To fully assess the potential input of genotoxic contaminants into the harbour from a variety of sources, material was sampled from the bottom of the harbour, from the harbour water column, and from an air sampling site on the east shore. The samples and sample sites selected for this study (Figure 1) and the methods of collection are described in the following sections.

##### I.5.1.1 Randle Reef Sediment Sample

A grossly coal tar-contaminated sediment sample was obtained from an area east

### I.4 Summary of Research Objectives.

The hypothesis that the extraction of organic material from complex environmental samples using ultrasonic extraction is as efficient as extraction using a Soxhlet apparatus will be tested. The extraction efficiency of PAH from a Randle Reef sediment sample and from an urban dust SRM using ultrasonication will be evaluated and compared with those results obtained using a Soxhlet apparatus. A favourable statistical comparison between the efficiencies of the two techniques would support the hypothesis that ultrasonication is a feasible alternative to Soxhlet extraction and illustrate the efficiency of the clean-up and fractionation procedure for sample matrices other than airborne particulate material.

The hypothesis that the high PAH levels determined in extracts of sediment and suspended sediment samples taken from Hamilton Harbour arise principally from resuspension and transport of sediments from sites with extensive coal tar contamination will be tested. The resuspension and transport mechanisms could be responsible for similar PAH profiles in extracts of sediments collected at many locations within the harbour. A comparison of the analytical chemistry and genetic toxicology data of the sediment trap samples, sediment samples, and samples of air particulate material from the Hamilton Harbour area will be used to test the hypothesis and provide an estimate of the contribution of the resuspended contaminated sediments to the overall genotoxic burden on the harbour. This data may also indicate contamination by mutagenic compounds derived from other sources.

of the Randle Reef area of Hamilton Harbour. This site, also known as the Hamilton Harbour "hot spot" or "tar pit", is in close proximity to the principal coking pier of one of the largest steel mills in Canada. Resuspended sediments from this site have been implicated as one of the principal sources of PAH contamination in the harbour (2). Total PAH levels at this site are on the order of 500-1400 µg/g of dry sediment (2). Murphy *et al* (2) concluded that the PAH in extracts of sediments from this site were derived from coal tar contamination from known discharges of coke oven by-products. This site was chosen for sediment sampling because of the potential contribution of resuspended material from this site to the high levels of PAH found in sediments elsewhere in the harbour. Sediments were also sampled from the westernmost area of the harbour (station 910 near Carrolls Point, Figure 1) where the PAH concentrations in sediments are relatively low.

##### I.5.1.2 Hamilton Harbour Sediment Traps.

Particulate material was collected from sediment traps located at three locations within the harbour. Suspended solids are important contributors to the mechanisms of contaminant partitioning in the water column. Sediment traps are simple yet efficient apparatus for the collection of particle fluxes over long periods of time (16,17). Resuspended sediment, material from discharges into the harbour and material from airborne deposition can all contribute to the material collected in a sediment trap. A sediment trap and associated apparatus are illustrated in Figures 3 and 4. Material collected



Figure 3. Diagram of sediment trap mooring (courtesy of M. Charlton, Canada Center for Inland Waters).

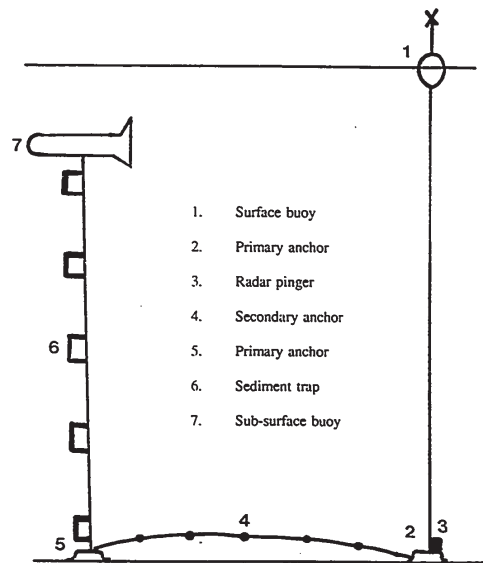
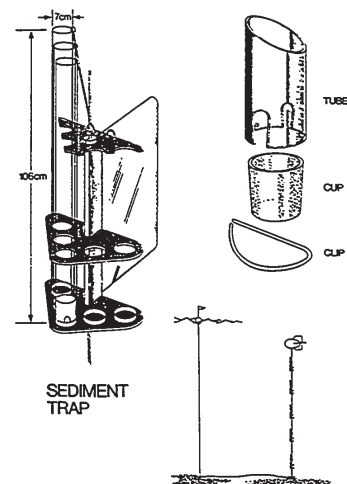


Figure 4. Diagram of sediment trap with sampling tube and cup (courtesy of M. Charlton, Canada Center for Inland Waters).



in sediment traps may differ significantly from material isolated from the water column using instantaneous collection methods such as filtration or centrifugation techniques. Eadie *et al* (18) and Baker *et al* (19) have studied resuspension and recycling of chemical contaminants in the Great Lakes using sediment trap samples. The sediment trap samples used in this study were collected over an 8 month winter period (October/1990 to May/1991) affording approximately 5-10 gram accumulations of material (dry weight) in each tube of the trap (Figure 4). Sediment traps were placed at 2 depths (approximately 3m from the surface and approximately 3m from the bottom) with the exception of station 53, where three traps were located (including a sediment trap at an intermediate depth) because of the increased depth of the water at this site. The station 50 site is near the outfall of the sewage treatment plant for the city of Burlington, Ontario (Figure 1). The station 53 site is near the mouth of the Windermere Arm, a body of water through which water from the Windermere Basin flows. The Windermere Basin is another area of Hamilton Harbour that has been shown to exhibit high levels of chemical contamination (2).

### 1.5.3 CCIW Air Sample

Respirable air particulate material was sampled using a PM-10 type air sampler located at the dock of the Canada Center for Inland Waters (CCIW) in Burlington, Ontario (Figure 1). The PM-10 sampler collects particulate material smaller than 10 microns in diameter. The bulk of the PAC and the mutagenicity/carcinogenicity exhibited

by air sample extracts is associated with this smaller diameter material (20). In addition, particulate material of less than 10 microns in diameter can be readily inhaled and deposited in the respiratory tract. CCIW is located on the east shore of the harbour, immediately beneath the Hamilton-Burlington skyway bridge on the Queen Elizabeth Way (QEW) highway. The QEW is the major traffic artery connecting the Golden Horseshoe area of Southern Ontario with the Northeastern United States. A large number of gasoline and diesel powered vehicles travel the skyway on a daily basis.

### 1.5.2 Analytical and Biological Analyses

#### 1.5.2.1 Short-Term Biological Testing

A variety of methodologies have been used to assess the impact of individual chemicals or complex environmental mixtures on fish populations in fresh water and marine environments. To complement epidemiological studies, short term bioassays such as the *Salmonella typhimurium*/microsome assay (Ames assay), or the detection of DNA adducts in affected fish (10), have been employed as indicators of contamination of bottom sediments by mutagenic and/or carcinogenic compounds. Not all chemical carcinogens are detected by short term mutagenicity assays but short term biological tests can provide a rapid means for assessing the potential genotoxicity of an individual chemical or a complex mixture (21). Bacterial mutagenicity assays have played a critical role in the detection of mutagens and in the analysis of the ability of aquatic organisms

to convert inert chemicals to genotoxic products (22).

Salmonella typhimurium is the most widely used species of bacteria for mutagenicity testing. The bacterial strains used for mutagenicity testing have been engineered without the ability to produce the amino-acid histidine and will not grow in a medium unless this compound is supplied to them. In the presence of a mutagenic agent, the bacterial DNA can be mutated to form a functional histidine gene resulting in the ability of the bacteria to grow independently of an external supply of histidine. The number of bacteria that have undergone mutation is reflected in the number of bacterial revertant colonies present on a minimal glucose plate (petri dish). The number of revertants obtained is a function of the mutagenic potency of the test compound(s) and the concentration(s) of the test compound(s) in the test medium.

The Salmonella/microsome assay can also be used to detect potentially mutagenic compounds that require metabolic activation to be transformed into a genotoxic product. A mammalian liver homogenate (rat liver supernatant S9) is added to simulate the metabolism that compounds undergo in mammalian bodies. Many compound classes, such as PAH, are only effective mutagens after transformation to reactive electrophiles by liver microsomes. The biotransformation of benzo[a]pyrene to a potent carcinogenic and mutagenic diol-epoxide intermediate by liver enzymes is well documented (14,23).

The Salmonella bacterial strains have also been engineered to increase their sensitivity to mutagenic agents. Defects have been incorporated into the bacterial cell walls that allow chemicals, particularly those of larger molecular weight, to more easily penetrate the cell wall of the bacteria. There are deficiencies in the DNA repair

positive dose/response relationship. A positive response was not observed with the TA98 strain and high doses of the sediment extract were toxic to both bacterial strains.

Metcalfe *et al* (10) could not conclude that PAH were responsible for the genotoxic and mutagenic activity in the sediment extract because of the observance of a mutagenic response without the addition of microsomal enzymes. As mentioned previously, PAH require oxidative transformation by liver microsomes to become effective mutagens. The potential presence of direct-acting frameshift mutagens such as nitro-polycyclic aromatic compounds (PAC) was discussed, but no mutagenic response was observed in the TA98 strain.

#### 1.5.2.2 Bioassay-Directed Fractionation

A bioassay-directed fractionation approach (28) was used to examine the samples selected for the study. This technique is a versatile and powerful experimental methodology that combines the disciplines of analytical chemistry and genetic toxicology in order to characterize and identify the key biologically active compounds or compound classes in extracts of complex mixtures. Fractionation of extracts of environmental samples is necessary given their complexity. The development of the Ames Salmonella bacterial mutation assay has resulted in the ability to subject selected fractions from environmental samples to simple, rapid, and inexpensive short-term testing. The identification of mutagenic fractions allows the potential determination of the compounds or compound classes responsible for the observed activity.

mechanisms that increase the probability that the DNA damage will be forced through mutation-prone pathways. The strains also carry a plasmid DNA (pKM101) that markedly increases the sensitivity of the bacteria to mutagens.

Two types of point mutations can be detected using the TA98-like and TA100-like Salmonella strains. The TA98-like strains detect frameshift mutations which occur when bases are deleted or added in a strand of DNA. This results in incorrect transcription of the DNA after the point of insertion or deletion. The TA100-like strains detect base-pair substitution mutations which arise when an incorrect base is added during DNA replication. The incorrect base then lines up with its counterpart base during the next replication resulting in an altered base-pair.

Mutagenicity and genotoxicity testing of sediments in the Great Lakes region using the Salmonella typhimurium assay has focussed on highly industrialized areas, including the Black river (24), the Aberjona watershed (25), the Detroit river (26), and several Great Lakes tributaries (27).

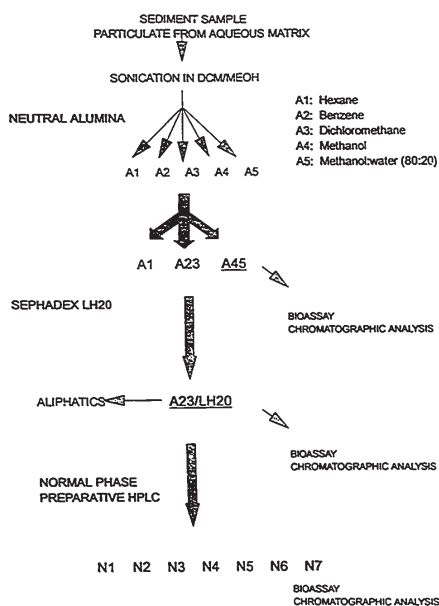
Metcalfe *et al* (10) used genotoxicity testing of a Hamilton Harbour sediment extract using the Salmonella assay to complement *in vitro* DNA adduct and *in vivo* rainbow trout sac fry microinjection assays. A wet sediment sample was combined with sodium sulphate and extracted with 1:1 acetone:hexane using a polytron homogenizer. The extract was then dried using a sodium sulphate column, reduced in volume, and diluted with DMSO to the desired concentration for bioassay. The sediment extract was observed to be mutagenic in the TA100 strain both with and without the addition of rat liver S9 as evidenced by a doubling of the spontaneous background reversion rate and a

This approach has previously been used in our laboratory for the genotoxicity testing of PAC associated with respirable air particulate material (20). Bryant *et al* (20) utilized sequential Soxhlet extractions with methylene chloride then methanol in conjunction with an alumina column clean-up and compound class-selective fractionation procedure similar to that described in the experimental section of this thesis (Figure 5); this study concluded that only a small percentage of the total biological activity associated with extracts of respirable air particulate is due to homocyclic PAH compounds.

Bryant *et al* (20) reported that the mutagenic activity observed was approximately equally divided between the non-polar and polar PAC fractions resulting from the alumina column clean-up (fractions A23/LH20 and A45 respectively in Figure 5). These fractions were assayed using a TA98-like strain and positive responses were observed without the addition of rat liver microsomes (S9). The majority of the mutagenic activity observed in the non-polar PAC fraction (A23/LH20) was detected in the normal phase HPLC fractions in which nitro-substituted PAH and heterocyclic PAC compounds are known to elute. Collection of 30-second subfractions during reversed-phase HPLC separation of these N fractions, combined with bioassay of these subfractions, revealed the mutagenic activity to be localized in a small number of subfractions. The observed activity did not correlate with any of the UV absorption peaks in the RP-HPLC chromatograms. Subsequent chemical analysis of the biologically active subfractions was inconclusive, suggesting that potent mutagens responsible for mutagenic activity can be difficult to determine given their high polarity and their probable presence at very low concentrations.

McCalla *et al* (29) applied the same methodology for the detection and

Figure 5. Schematic of sample clean-up and fractionation scheme. The procedure was applied to sediment, sediment trap and airborne particulate material and is described in detail in the experimental section.



identification of steel foundry mutagens. Several hundred grams of Dofasco steel foundry dust consisting of airborne particulates and binder emissions was fractionated and assayed. The bulk of the mutagenic activity was found to be associated with particulate material of respirable size and to be localized in the non-polar aromatic A23/LH20 fraction (Figure 5). Similar to the study on respirable air particulate, the majority of the observed mutagenic response was observed in N fractions containing more polar and substituted PAC, as opposed to their homocyclic PAH counterparts. Reversed-phase HPLC separation of the N2 and N3 fractions and bioassay of 30-second subfractions with *Salmonella* strain TA98 showed localized bands of mutagenic activity. The addition of S9 was not needed to observe a strong positive response. Subsequent analysis of these active subfractions by GC-MS revealed that nitro-PAH, particularly 1-nitropyrene and the dinitropyrene isomers, were potentially responsible for the observed mutagenic activity. Bioassay of authentic nitroaromatic standards showed these compounds to be highly mutagenic. These compounds were very responsive when assayed with the *Salmonella* TA98 strain and the addition of S9 reduced their mutagenic responses.

Quilliam and Wright (30) successfully employed a bioassay-directed strategy to identify demoic acid as the toxin in blue mussels (*mytilus edulis L.*) that was responsible for an outbreak of food poisoning in Canada in 1987. Fernandez *et al* (31) used bioassay-directed chemical analysis for the determination of genotoxic components in Spanish coastal sediments. These authors employed a sonication extraction method coupled with gel permeation chromatography, normal phase HPLC and RP-HPLC fractionation techniques and GC-MS analysis techniques to determine mutagenic compounds such as

1-nitropyrene, 6-nitrochrysene, and 6-nitrobenzo[a]pyrene.

Samples selected for the present study including sediment, sediment trap material and airborne particulate material from the Hamilton Harbour area were extracted and fractionated using a compound class-selective procedure adapted from the procedures previously described by McCalla *et al* (29) and Bryant *et al* (20). The resulting fractions were analysed using chromatographic methods and the *Salmonella typhimurium*/microsome assay was used to identify fractions displaying mutagenic activity. These fractions were the focus of further chemical analysis to determine the compounds or compound classes responsible for this biological activity.

#### 1.6 Validation of Methodology

The bioassay-directed fractionation methodology employed in this study was previously used in the genotoxicity testing of polycyclic aromatic compounds (PAC) associated with respirable air particulate (20), and in the genotoxicity testing of airborne particulate and binder emissions generated in a steel foundry (29). Both of these studies employed sequential Soxhlet extractions with methylene chloride then methanol, a neutral alumina chromatography clean-up procedure, Sephadex LH-20 gel chromatography to remove aliphatic components, a normal phase HPLC compound class fractionation procedure, and further separation using RP-HPLC. Subsequent analysis of the fractions by RP-HPLC and GC-MS showed that the extracts were effectively fractionated into compound classes; aliphatics, PAH and alkyl-PAH, sulphur heterocycles and their alkyl

derivatives, polycyclic aromatic ketones, polyaromatic quinones, aza-aromatics, nitro-PAH, dinitro-PAH and phenols were all found to elute reproducibly in the seven N fractions resulting from the normal phase HPLC fractionation (Figure 5). The sample preparation scheme described in the experimental section of this thesis is an adaptation of those used in these studies.

The complexity of environmental samples necessitates a clean-up and fractionation procedure to produce meaningful analytical and bioassay results. It is difficult or impossible to determine compound classes such as nitro-PAC in the presence of high concentrations of their parent PAH compounds and other interfering compounds. Non-linear dose response curves commonly result from *Salmonella* assays of samples which contain many potentially genotoxic components if the test mixture has not been sufficiently fractionated. This makes the extrapolated dose response data unreliable.

The extraction procedure employing the Soxhlet apparatus proved simple and efficient in the aforementioned studies, but large volumes of organic solvent (several hundred mL of both methylene chloride and methanol for sample sizes of only several g) and long periods of time (2X24 hrs) were needed for efficient extractions. A methanol extraction was shown to be needed in addition to extraction with methylene chloride in the respirable air particulate (20) and steel foundry (29) studies. Significant amounts of mutagenic activity were extracted into methanol in these complex environmental samples, primarily attributed to polar compounds. Sequential extractions using a non-polar and polar solvent have been shown to yield higher percentages of extractable organic material than extractions employing a single solvent (32,33). Sequential extractions using

methylene chloride and methanol are efficient for the extraction of organic material from airborne particulate material (20,33,34).

The extraction of organics from solid samples using ultrasonication has been documented (35-37), but Soxhlet extraction and the more recently developed technique of supercritical fluid extraction (SFE) (38-41) have been the favoured methods. In some comparison studies the ultrasonic extraction method has proven to be equally efficient, or more efficient than, Soxhlet extraction (42,43). The major advantages of ultrasonic extraction are a) the reproducibility of the technique (40), b) the applicability of the method to a wide range of sample sizes, c) the much shorter periods of time needed to perform highly efficient extractions, and d) the efficient extraction of polar organic compounds.

The crude extract is fractionated into a non-polar and a polar PAC fraction using open column alumina chromatography. The alumina clean-up step is inexpensive, simple, and reproducible. Alumina chromatography is a popular choice for the clean-up of environmental samples. The Sephadex LH20 gel (polyhydroxylated dextran) column is used to remove aliphatics from the non-polar PAC fraction (affording fraction A23/LH20, Figure 5). The gel column uses adsorptive interactions for the separation instead of the size exclusion mode most commonly employed with this stationary phase. Adsorption interactions with the gel are promoted by adding methanol to the conventional methylene chloride mobile phase, causing the aromatic compounds to interact more strongly with the stationary phase than the aliphatics. Hexane is added to the mobile phase (hexane/methanol/methylene chloride, 6:4:3 v/v) to increase the solubility of organic

## II. RESULTS AND DISCUSSION

### II.1 Testing of the Proposed Methodology.

The extraction of PAH from sediments and from an urban dust standard reference material (SRM 1649) was compared using the methods of ultrasonication and Soxhlet extraction described in the experimental section. Sample weights of 0.5 g to 5 g were extracted using ultrasonication.

The yield of extracted organic material from the sediment samples using sequential ultrasonication with two solvents (methylene chloride and methanol) was  $2.53 \pm 0.10\%$  (three samples) while the Soxhlet method yielded  $2.41 \pm 0.14\%$  (three samples) of the initial sample weight. These weight ratios were found to be statistically invariant with the weight of sample extracted (0.5 g to 5 g) when using ultrasonication.

Figure 6 shows the RP-HPLC chromatogram obtained from the injection of an aliquot of the crude bulk extract of a 5 g Randle Reef sediment sample prepared by Soxhlet extraction. The sample was not subjected to the clean-up and fractionation procedures. The figure legend gives a list of homocyclic PAH determined in the sample crude extract. Figure 7 shows a comparison of the RP-HPLC chromatograms of the crude extracts of Randle Reef sediment prepared by ultrasonication (7A) and using a Soxhlet apparatus (7B). Figure 8 shows a comparison of the RP-HPLC chromatograms of the A23/LH20 aromatic fractions of the ultrasonication (8A) and Soxhlet apparatus (8B)

material.

The non-polar PAC are then fractionated into compound classes using normal phase semi-preparative HPLC with an amino-cyano column (affording the N fractions, Figure 5). This step results in fractions that can yield informative analytical and biological data on specific compound classes such as nitro-PAC, dinitro-PAC, aza aromatics, etc. These normal phase N fractions can be further separated by RP-HPLC and subfractions collected and assayed to yield data on the mutagenic potency of the individual compounds.

In the present study, the efficiencies of the ultrasonication and Soxhlet methods of extraction were compared for the extraction of PAH from equal weights of Randle Reef sediment (Figure 1) and from an urban dust Standard Reference Material (SRM 1649). The samples were extracted and the combined methylene chloride and methanol extracts were submitted to the clean-up, fractionation and chemical analysis procedures described in the experimental section to isolate the low to mid-molecular weight PAH for quantification. The levels of selected PAH extracted from the Randle Reef sediment by the two methods were compared, and the levels of PAH found in the SRM 1649 were compared with the certified values. This data was used to test the hypothesis that ultrasonic extraction is as efficient as a Soxhlet apparatus.

Figure 6. Reversed phase HPLC chromatogram of the Randle Reef sediment sample crude extract. Compound identification was based on comparison of UV absorption spectra with library spectra and retention time comparison with authentic standards. The sample was extracted with a Soxhlet apparatus using the procedure described in the experimental section. The UV absorption chromatogram was plotted at 254 nm; the fluorescence chromatogram resulted from excitation at wavelengths below 365 nm and emission above 418 nm. The concentrations of many of these compounds can be found in Table 2.

Peak Number	Compound Identification
1	naphthalene
2	fluorene
3	phenanthrene
4	anthracene
5	fluoranthene
6	pyrene
7	benzo[a]fluorene
8	benzo[a]anthracene
9	chrysene
10	benzo[b]fluorene
11	benzo[b]naphtho[2,1-cd]thiophene
12	benzo[b]fluoranthene
13	benzo[k]fluoranthene
14	benzo[a]pyrene
15	indeno[1,2,3-cd]pyrene
	benzo[ghi]perylene
	benzo[b]chrysene
16	picene
17	anthanthrene

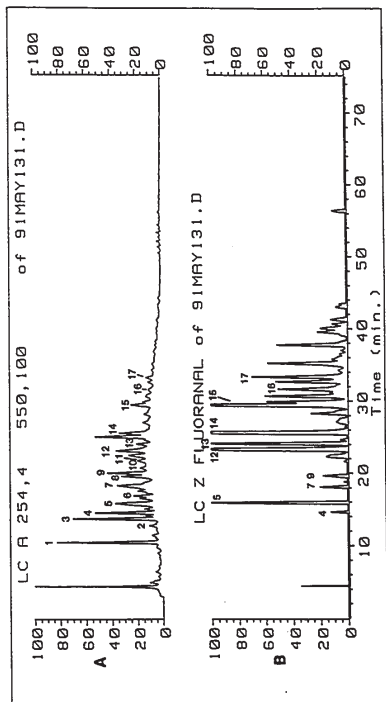


Figure 7. Reversed phase HPLC chromatograms of the crude methylene chloride/methanol extracts prepared from equal weights of Randle Reef sediment following Soxhlet extraction (A) and ultrasonic extraction (B). The extracts were not subjected to the clean-up and fractionation procedure. There are no statistical differences in the individual peak areas in the two chromatograms. The chromatograms were plotted at 254 nm. Peak identifications by number are as follows.

Peak Number	Compound Identification
2	fluorene
3	phenanthrene
4	anthracene
5	fluoranthene
6	pyrene
7	benzo[a]fluorene
8	benzo[a]anthracene
9	chrysene
10	benzo[b]fluorene
11	benzo[b]naphtho[2,1-cd]thiophene
12	benzo[b]fluoranthene
13	benzo[k]fluoranthene
14	benzo[a]pyrene
15	indeno[1,2,3-cd]pyrene
	benzo[ghi]perylene
16	benzo[b]chrysene
17	picene
18	anthanthrene

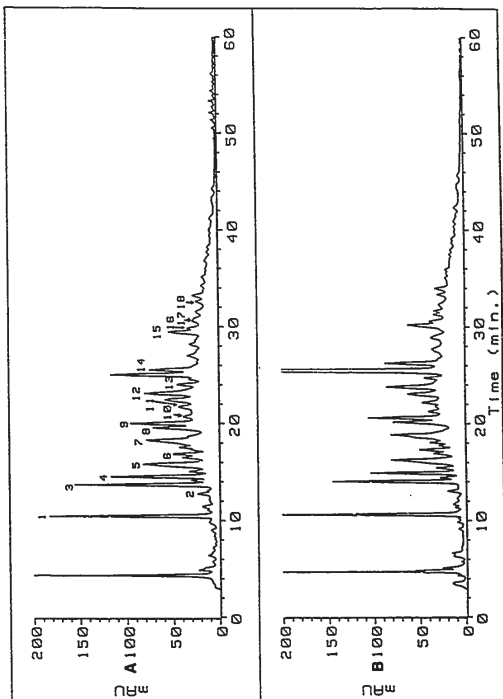
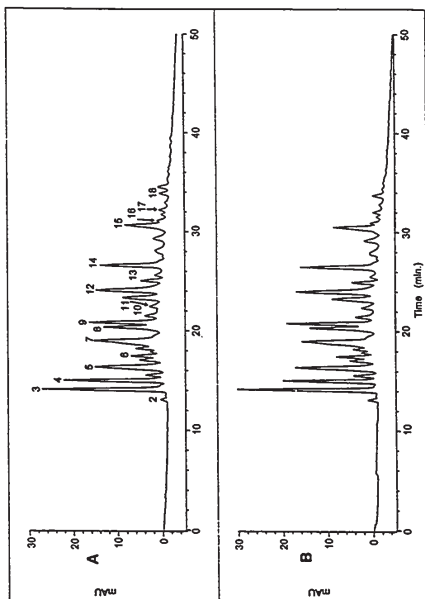


Figure 8. Reversed phase HPLC chromatograms of the polycyclic aromatic hydrocarbon extracts (fraction N1) prepared from equal weights of Randle Reef sediment following Soxhlet extraction (A) and ultrasonic extraction (B). There are no statistical differences in the individual peak areas in the two chromatograms. The chromatograms were plotted at 254 nm. Peak identifications by number are as follows.

Peak Number	Compound Identification
1	naphthalene
2	fluorene
3	phenanthrene
4	anthracene
5	fluoranthene
6	pyrene
7	benzo[a]fluorene
8	benzo[a]anthracene
9	chrysene
10	benzo[b]fluorene
11	benzo[b]naphtho[2,1-cd]thiophene
12	benzo[b]fluoranthene
13	benzo[k]fluoranthene
14	benzo[a]pyrene
15	indeno[1,2,3-cd]pyrene
	benzo[ghi]perylene
16	benzo[b]chrysene
17	picene
18	anthanthrene



extracts prepared using the described fractionation method. The large peak eluting just before benzo[a]pyrene (peak 14) is a solvent impurity.

A t-test was used for the comparison of the mean peak areas of the A23/LH20 fractions and an f-test was used for the comparison of the standard deviations of the peak areas. No statistical differences in the individual compound peak areas in the two chromatograms were found. The concentrations of naphthalene (peak 1, Figure 6) determined in the crude extract were approximately 95  $\mu\text{g/g}$  of dry sediment. During the subsequent clean-up and fractionation procedures, the majority of the volatile naphthalene was lost. The levels of phenanthrene and anthracene in fraction A23/LH20 are approximately 80% of those in the crude extract.

Table 1 shows a comparison of the quantitative PAH data obtained from the analysis of the extract of the standard reference material urban dust (SRM 1649) using the ultrasonic extraction method and the National Institute of Standards and Technology (NIST) certified values. These samples were subjected to the clean-up and fractionation procedure and the PAH were quantified by analyzing fraction A23/LH20. The PAH were quantified using an internal standard method (9,10-dimethylanthracene or 3-methylanthracene) with GC-MS and GC-FID analyses. Other PAH determined in the extracts were comparable with the non-certified values reported by the NIST (Table 1).

The extractions using the ultrasonication method required far less time (45 min) and far less organic solvent (150 mL in total) than extractions using the Soxhlet method (48 hours and 700 mL of solvent). Ultrasonic extraction using the developed methodology was performed in 45 min which made it comparable with SFE methods (39).

Table 1. A comparison of polycyclic aromatic hydrocarbon levels determined in Standard Reference Material 1649 urban dust/organics prepared by ultrasonic extraction with the certified values quoted by the National Institute of Standards and Technology. The numbers in parentheses represent the number of replicate analyses. The NIST values resulted from extracts prepared using a Soxhlet apparatus.

Compound	Concentration ( $\mu\text{g/g}$ )	Certified Value ( $\mu\text{g/g}$ )
fluoranthene	$7.2 \pm 1.0$ (4)	$7.1 \pm 0.5$
benzo[a]anthracene	$2.8 \pm 0.4$ (4)	$2.6 \pm 0.3$
benzo[a]pyrene	$3.4 \pm 0.3$ (5)	$2.9 \pm 0.5$
benzo[ghi]perylene	$4.1 \pm 0.5$ (5)	$4.5 \pm 1.1$
indeno[1,2,3-cd]pyrene	$3.4 \pm 0.8$ (5)	$3.3 \pm 0.5$
		Non-certified Value ( $\mu\text{g/g}$ )
phenanthrene	$3.7 \pm 0.5$ (5)	$4.5 \pm 0.3$ (by HPLC)
pyrene	$6.7 \pm 1.5$ (4)	6.6 (by HPLC and GC)
chrysene	$4.0 \pm 1.5$ (3)	3.6 (by HPLC)

Ultrasonic extraction does not suffer from the problems associated with SFE such as restrictor clogging or the need for sample matrix or fluid system modifiers. Previous work has shown that the Soxhlet extraction method using methylene chloride and methanol sequentially, efficiently extracts a substantial number of polar compounds (20,29). Based upon a comparison of weights of the methanol/methanol-water extracts (fraction A45) from the alumina column and the RP-HPLC chromatograms of these fractions, it was concluded that the extraction of polar compounds using ultrasonication is as efficient as Soxhlet extraction. Compared to SFE, the ultrasonication extraction method may be more efficient for the extraction of polar organic materials since modifiers such as alcohols must be added to conventional carbon dioxide SFE systems to achieve efficient extractions of mid-molecular weight PAH such as benzo[a]pyrene. More than one SFE fluid system may be needed for the extraction of samples containing compounds with a wide range of polarities. The SFE extraction of organic compounds containing polar functional groups such as carboxylic acids and hydroxyl groups can be difficult or impossible (44,45) and continues to be an area of active research.

The optimum conditions for ultrasonic extraction were found to be dependent upon the sample size and the matrix. For this study, 8 pulses of ultrasonic power and 50 mL of solvent per extraction cycle were used for the extraction of sample sizes varying from several hundred milligrams to 5 g of sample. An interval of one minute was maintained between pulses and the beaker containing the sample was immersed in an ice bath to minimize solvent heating. Solvent heating not only could result in the reduction of solvent volumes prematurely, but in the loss of volatile compounds or the alteration of

thermally labile compounds.

### II.1.1 Testing of Proposed Methodology: Summary.

The method of ultrasonication for the extraction of organic material from sediment and an urban dust standard reference material was found to be efficient. This conclusion was based upon a comparison with the Soxhlet method and a comparison of PAH levels determined in an SRM with the certified values. The statistical comparisons between the peak areas of the sediment A23/LH20 fractions extracted using the two methods (t-test and f-test) support the hypothesis that ultrasonication is equally efficient as a Soxhlet apparatus.

Ultrasonic extraction can be performed in a short period of time and is applicable to a wide range of sample sizes. The percentage of the original mass of material extracted was found to be constant over a ten-fold sample weight range. The ultrasonic probe apparatus is easy to operate and the technique has been applied to a variety of sample matrices including air particulate material as discussed later. The clean-up and fractionation procedure was effective in separating the components of the highly complex sediment sample into chemical compound classes. The recovery of PAH from an SRM was efficient as evidenced by the comparison of the observed values with the certified values.

Although the complete clean-up and fractionation procedure can be somewhat labour intensive, it has many characteristics making it attractive for use in bioassay

directed fractionation. These characteristics, as described by McCalla *et al* (29) include: a) high sample loading capacity b) high resolution c) selectivity for compound classes d) reproducibility e) nondestructive procedure and f) compatibility with the bioassay-directed fractionation methodology.

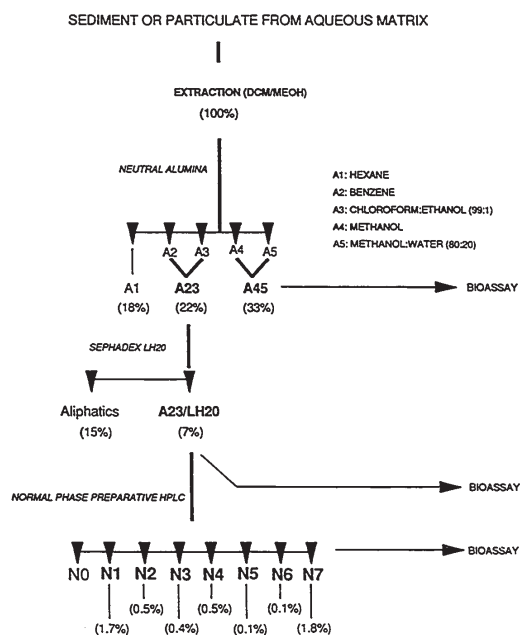
## II.2 Extraction and Chemical Analysis.

### II.2.1 Randle Reef Sediment Sample.

The sediment sample was collected with an Eckman dredge from an area east of Randle Reef adjacent to the Stelco coking pier (Figure 1). The sediment sample was a black oily slurry (52% water by weight) with a strong odour that was still apparent after drying. Extraction of the dried material resulted in an extract that was 2.5% of the dry sediment weight; 73% of this extracted material was removed by methylene chloride, the remaining 27% by methanol. No PAH were determined in the methanol extract when it was analysed by RP-HPLC (data not shown), but studies with air particulate material have shown that polar compounds extracted by methanol can account for significant amounts of mutagenic activity (20). Murphy *et al* (2) have observed organic solvent extractables from the Randle Reef area to be as high as 16% of the original dry weight of sediment.

The methylene chloride and methanol extracts were combined and chromatographed on alumina; approximately 73% of the total mass of the extract was recovered from the alumina clean-up procedure. Figure 9 shows the sample preparation

Figure 9. Schematic of the sample extraction, alumina open column clean-up and normal phase semi-preparative HPLC compound class fractionation procedure. This figure is identical to that of Figure 5 with the addition of the percentages of extracted material contained in each fraction. The values are expressed as a percentage of the original weight of extracted material (100%) from the Randle Reef sediment sample.



scheme with the percentages of extracted material contained in each fraction. The values are expressed as a percentage of the original weight of extracted material from the Randle Reef sediment sample. The remainder of the extract (approximately 27%) was irreversibly adsorbed to the alumina.

Fraction A45, which contains the polar organic compounds, accounted for 33% of the mass of extracted material but was difficult to analyze given the polar nature of the compounds present. The UV absorption and fluorescence profiles resulting from the RP-HPLC analysis of fraction A45 were observed to contain few compounds (Figure 10). Analysis of similar alumina fractions from air particulate materials has shown that fraction A45 contains alkylphenols, nitrophenols, naphthols, and acids (20).

Fraction A23 contained approximately 22% of the mass of the crude extract. The aliphatics contained in fraction A1 (Figure 11) and additional aliphatics removed from fraction A23 by the Sephadex LH20 chromatography step represented 15% of the original mass of extracted material; the aromatic compounds (fraction A23/LH20) represented only 7% of the mass of original extracted material (Figure 9).

Quantitative analysis of the PAH in fraction A23/LH20 was achieved by GC-MS. Figures 12 and 13 show GC-MS and RP-HPLC chromatograms of the A23/LH20 fraction of the sediment extract. The profiles of these chromatograms are indicative of coal tar contamination. The quantitative measurements of PAH determined in fraction A23/LH20 are shown in Table 2. These results are similar to those of Murphy *et al* (2), who characterized PAH in a large number of samples from the Randle Reef area. A number of substituted PAH and sulphur heterocyclic PAC (thia-PAC) were also identified in the

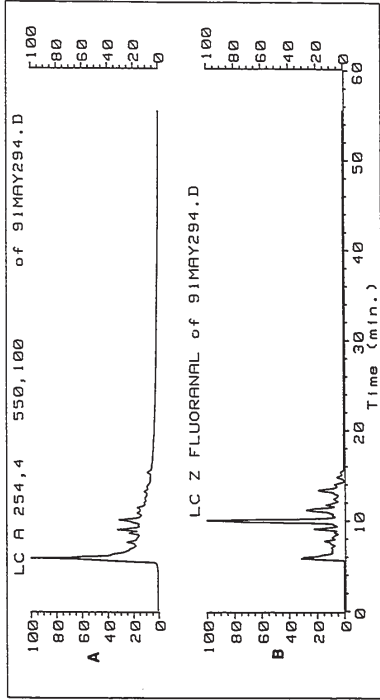


Figure 10. Reversed phase HPLC chromatogram of fraction A45 of the Randle Reef sediment sample extract showing the UV absorption (A) and fluorescence (B) profiles. The UV absorption profile was plotted at 254 nm. The amount of sample injected was equivalent to the extract derived from 23 mg of sediment. None of the compounds were identified.

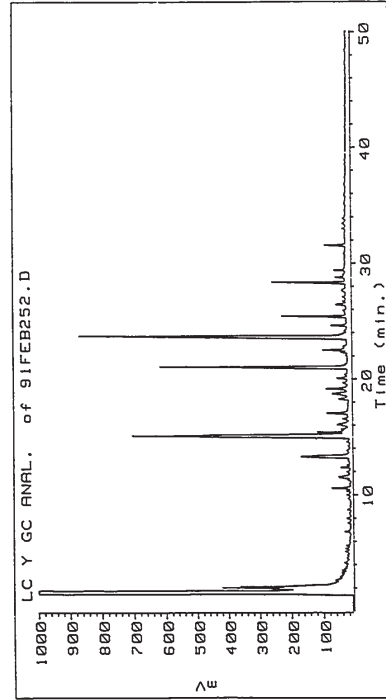


Figure 11. GC-FID chromatogram of fraction A1 of the Randle Reef sediment sample extract. Most of the compounds identified using supplemental analysis by GC-MS were low molecular weight aliphatic hydrocarbons and carboxylic acids and low molecular weight aromatic di-carboxylic acid esters (phthalic acid esters).

Figure 12. GC-MS total ion current chromatogram of the Randle Reef sediment sample extract fraction A23/LH20. The peaks are numbered to correspond with those listed in Table 2, which also lists the concentrations of PAH expressed in  $\mu\text{g/g}$  of dry sediment.

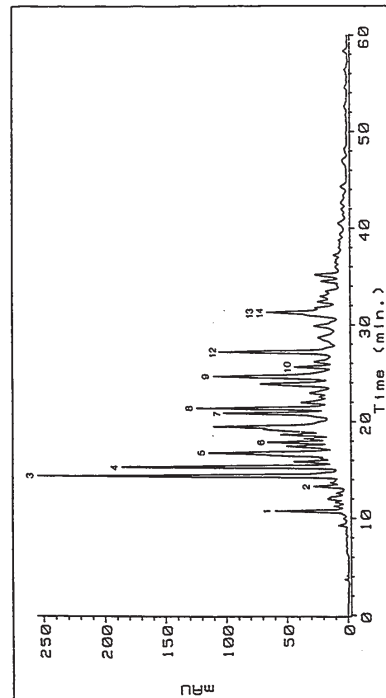
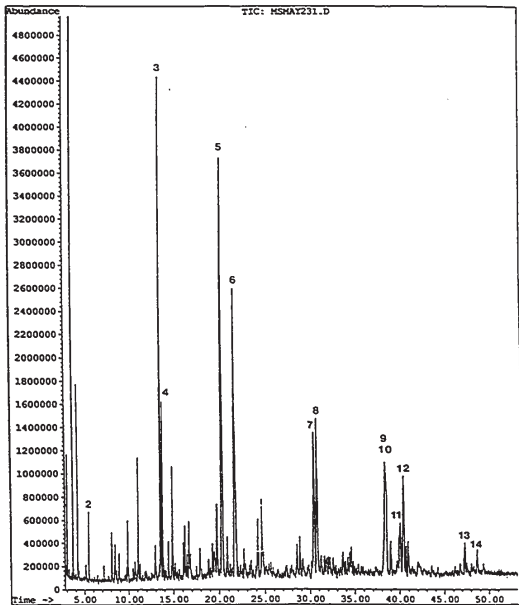


Figure 13. Reversed phase HPLC chromatogram of fraction A23/LH20 of the Randle Reef sediment sample extract. The UV absorption profile was plotted at 254 nm. The peaks are numbered to correspond to those listed in Table 2, which also lists the concentrations of PAH expressed in  $\mu\text{g/g}$  of dry sediment.



Table 2. Common PAH determined in the Randle Reef sediment sample. The peaks are numbered as to correspond to those in the figures. Concentrations are expressed in  $\mu\text{g/g}$  of dry sediment. Naphthalene, due to its volatility, was quantitated in the bulk extract using RP-HPLC. The total PAH content, expressed as the summation of the reported values in the table, was 583  $\mu\text{g/g}$ .

Compound	Molecular Weight	Concentration ( $\mu\text{g/g}$ )
1. Naphthalene	128	93.9
2. Fluorene	166	7.1
3. Phenanthrene	178	55.6
4. Anthracene	178	14.5
5. Fluoranthene	202	80.3
6. Pyrene	202	55.2
7. Benzo[a]anthracene	228	40.6
8. Chrysene	228	40.5
9. Benzo[b]fluoranthene	252	87.4 (UNR)
10. Benzo[k]fluoranthene	252	87.4 (UNR)
11. Benzo[e]pyrene	252	27.3
12. Benzo[a]pyrene	252	44.9
13. Indeno[1,2,3-cd]pyrene	276	22.2
14. Benzo[ghi]perylene	276	14.3

'UNR' denotes peaks unresolved by GC-MS.

sediment extract (46). Because of the likelihood of loss due to its volatility, naphthalene was determined in the crude extract by RP-HPLC immediately after sample extraction and solvent reduction. The total PAH concentration (defined as the sum of the concentrations of the individual unsubstituted PAH) was approximately 600  $\mu\text{g/g}$  (Table 2).

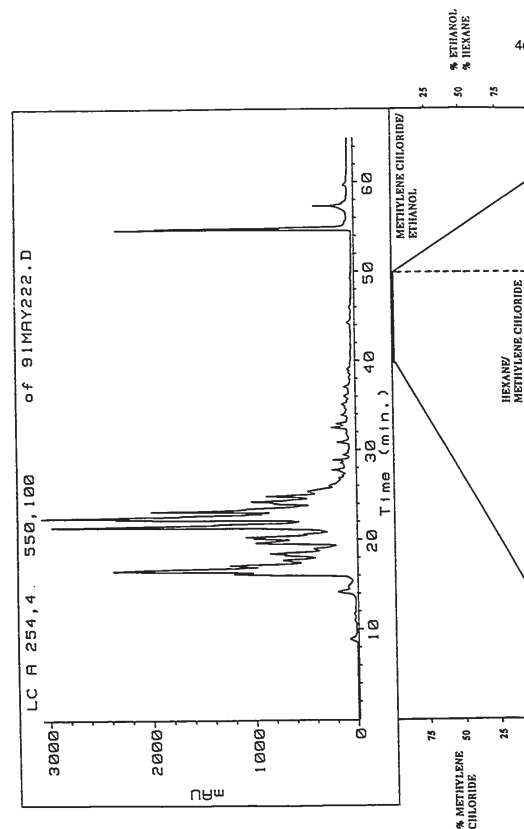
The non-polar PAC fraction (fraction A23/LH20) was further fractionated into compound classes using normal phase semi-preparative HPLC (Figure 14). The RP-HPLC chromatogram of fraction N1 showed that it contained the low to mid-molecular weight PAH (MW 128 to MW 276 amu). Fraction N1 also contained the alkyl-substituted low to mid-molecular weight PAH and sulphur heterocycles. The RP-HPLC chromatogram of fraction N1 is very similar to that of fraction A23/LH20 (Figures 13 and 15).

The analysis of fraction N2 by RP-HPLC with UV absorption and fluorescence detection (Figure 16) and GC-MS (Figure 17) revealed the presence of very high molecular weight PAH (greater than 278 amu) and assorted aza-aromatics and keto-PAC. These compounds are commonly found in coal-tar extracts. A number of these compounds were also detected in an N2 fraction prepared from a solvent extract of a Sydney Harbour, Nova Scotia sediment sample (47). Like Hamilton Harbour, large areas of Sydney Harbour contain sediments that are grossly contaminated by coal tar as a result of coking operations at a steel mill. The high molecular weight PAH (greater than MW 278) are observed only in the RP-HPLC chromatogram (Figure 16); the N2 fraction corresponding to the GC-MS chromatogram shown in Figure 17 was collected from the NP-HPLC column with a modified collection time so that the high molecular weight PAH

Figure 14. Normal phase semi-preparative HPLC chromatogram showing the fractionation of the Randle Reef sediment sample extract fraction A23/LH20. The injection represents approximately one tenth of the total extract and is equivalent to the extract derived from 566 mg of sediment. The UV absorption profile was plotted at 254 nm. Collection times for the N fractions (also described in the experimental section) are as follows.

Fraction	Collection Time
N0	0 minutes to 7.5 minutes
N1*	7.5 minutes to 24 minutes
N2	24 minutes to 30 minutes
N3	30 minutes to 35 minutes
N4	35 minutes to 40 minutes
N5	40 minutes to 45 minutes
N6	45 minutes to 50 minutes
N7	50 minutes to 65 minutes

\*These collection times result in PAH in the molecular weight range of 152 daltons to 278 daltons being collected in fraction N1. If the collection time for this fraction is extended to 25 minutes, PAH of molecular weight 302 daltons and higher will be collected in fraction N1 instead of fraction N2.



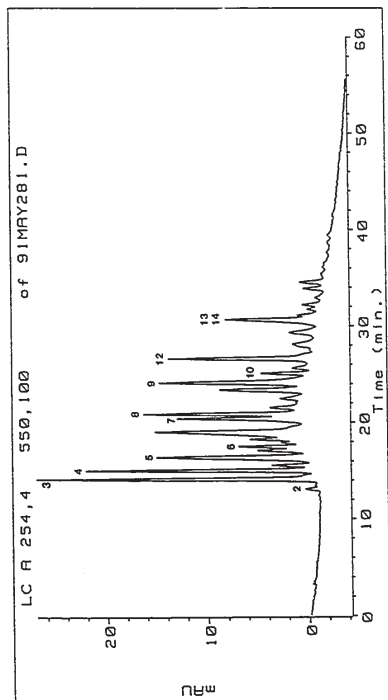


Figure 15. Reversed phase HPLC chromatogram of fraction N1 of the Randle Reef sediment sample extract. The UV absorption profile was plotted at 254 nm. The peaks are numbered to correspond to those listed in Table 2. The amount of sample injected was equivalent to the extract derived from 2 mg of sediment.

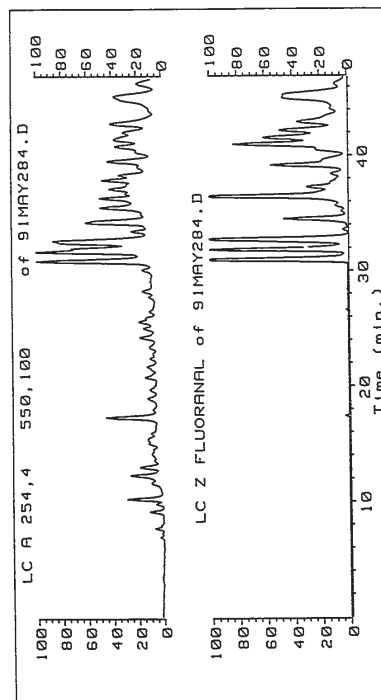
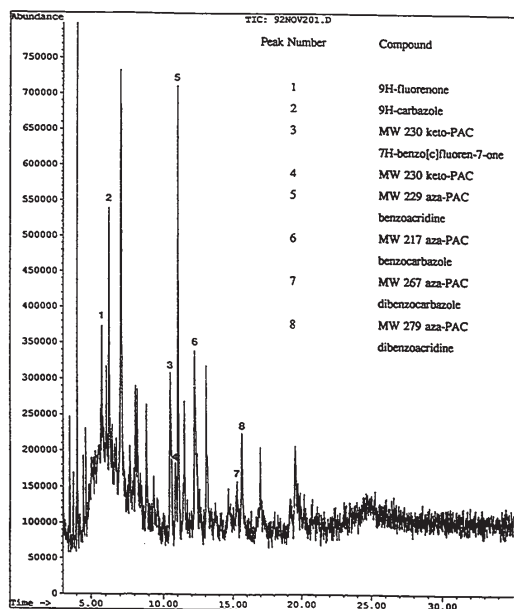


Figure 16. Reversed phase HPLC chromatogram showing the UV absorption profile at 254 nm (A) and the fluorescence profile (B) of fraction N2 of the Randle Reef sediment sample extract. The large number of peaks observed at elution times greater than 30 minutes are high molecular weight PAH with molecular masses greater than 278 daltons. The amount of sample injected was equivalent to the extract derived from 23 mg of sediment.

Figure 17. GC-MS total ion current chromatogram resulting from the analysis of the Randle Reef sediment sample extract N2 fraction. Compound identification was based upon comparison of mass spectra with library spectra.



were eluted in fraction N1 (see footnote to caption in Figure 14).

Fraction N3 was also analysed by both RP-HPLC (Figure 18) and GC-MS (Figure 19). This fraction was also observed to contain keto-PAC and aza-aromatics. Fractions N4, N5, N6, and N7 were analysed by RP-HPLC but none of the compounds observed were identified (data not shown).

## II.2.2. Station 910 Sediment Sample

Sediment was also sampled from the western end of the harbour (station 910) to provide both chemical and biological comparison data from an area far less contaminated by PAH than the Randle Reef area. The PAH levels in sediment sampled from this area range from undetectable levels to 17 µg/g (2). Approximately 11.5 g of dry sediment was extracted and cleaned-up using the described ultrasonication/clean-up/fractionation procedure. Figure 20 is the reverse phase HPLC chromatogram resulting from the analysis of fraction A23/LH20 of the station 910 sediment extract. The individual PAH determined in this extract were the same as those found in the Randle Reef sediment extract and the chromatographic profiles are similar. The total PAH content in the station 910 extract was found to be approximately 85 times lower than the Randle Reef sample.

## II.2.3 Sediment Trap Samples

Three sediment trap samples from station 53, collected at three depths near the

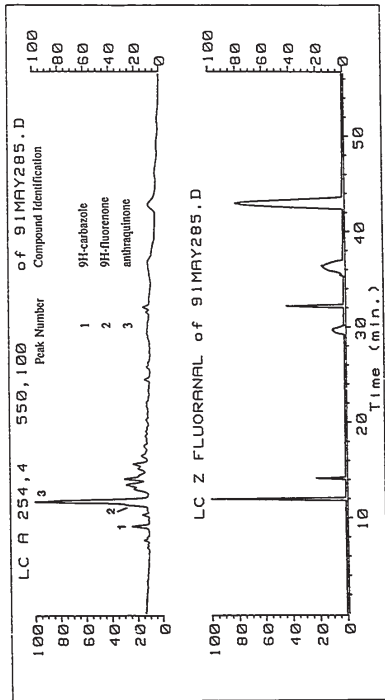
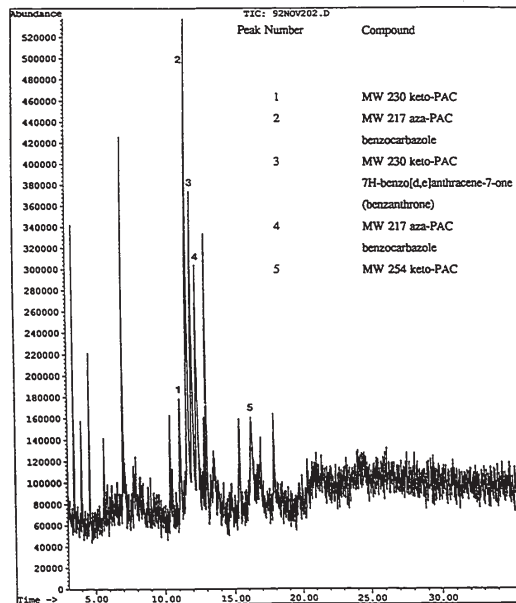


Figure 18. Reversed phase HPLC chromatogram showing the UV absorption profile at 254 nm (A) and the fluorescence profile (B) of fraction N3 of the Randle Reef sediment sample extract. Compound identification was based upon UV absorption spectra comparison with library spectra and retention time comparison with authentic standards. The amount of sample injected was equivalent to the extract derived from 23 mg of sediment.

51

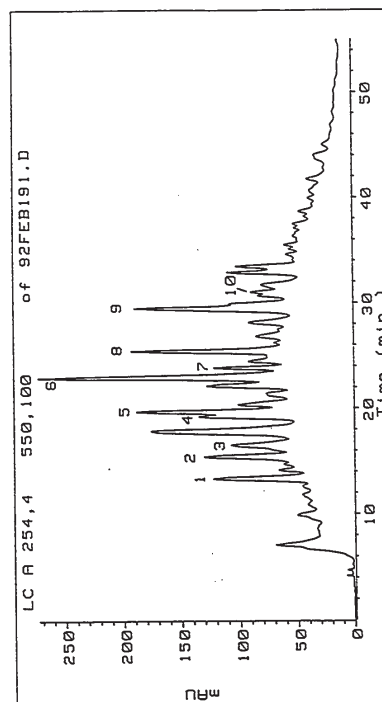
Figure 19. GC-MS total ion chromatogram resulting from the analysis of the Randle Reef sediment sample extract N3 fraction. Compound identification was based upon comparison of mass spectra with library spectra.



52

Figure 20. Reverse phase HPLC chromatogram of the A23/LH20 fraction of the station 910 sediment sample extract. The UV absorption profile was plotted at 254 nm. The amount of sample injected was equivalent to the extract derived from 1.15 g of sediment. Peak identifications by number are as follows.

Peak Number	Compound Identification
1	phenanthrene
2	fluoranthene
3	pyrene
4	benzo[a]anthracene
5	chrysene
6	benzo[b]fluoranthene
7	benzo[k]fluoranthene
8	benzo[a]pyrene
9	indeno[1,2,3-cd]pyrene
	benzo[ghi]perylene
10	picene



53

54

mouth of the Windemere Arm (Figure 1), were subjected to an extensive chemical characterization to provide data for comparison with the Randle Reef sediment sample. Quantitative analysis of the PAH in fraction A23/LH20 was achieved by GC-MS. Figures 21 and 22 provide comparisons of the three station 53 sediment trap samples and the Randle Reef sediment sample. Figure 21 is a set of four GC-MS total ion current chromatograms of the A23/LH20 fractions while Figure 22 is a set of four RP-HPLC chromatograms of the same samples. The chromatograms in each of the figures are very similar indicating that the sediment traps received substantial contributions due to the resuspension of coal tar contaminated sediment from the Randle Reef area.

Quantitative measurements of PAH present in the sample extracts are shown in Table 3. Table 4 lists the relative amounts of material contained in the crude extracts and A23/LH20 fractions of the sediment trap extracts, and are expressed as percentages of the masses of extracted organic material from each sample. The results of the PAH analysis of the sediment trap sample extracts were similar to those obtained by the National Water Research Institute (48). As with the Randle Reef sediment sample, alkyl-substituted PAH and thia-PAC were also identified in the sediment trap sample extracts (46).

The similarity of the chromatographic profiles is further illustrated in Table 5, which shows the relative PAH concentrations from Figure 21 normalized to chrysene (peak area 100%). With the exception of the more volatile PAH, phenanthrene and fluoranthene, the relative peak areas show a similar trend in all 4 samples. A comparable chromatographic profile was also observed in sample extracts of the station 50 sediment traps (Figure 24). It is interesting to note that in addition to PAH, high concentrations

Figure 21. GC-MS total ion current chromatograms showing the comparison between the Randle Reef sediment sample extract fraction A23/LH20 (D) and the station 53 top (A), middle (B) and bottom (C) sediment trap sample extracts fraction A23/LH20. The compound identifications can be found by referring to the individual GC-MS chromatograms of the Randle Reef fraction A23/LH20 (Figure 12) and station 53 sediment trap fraction A23/LH20 (Figure 23) chromatograms.

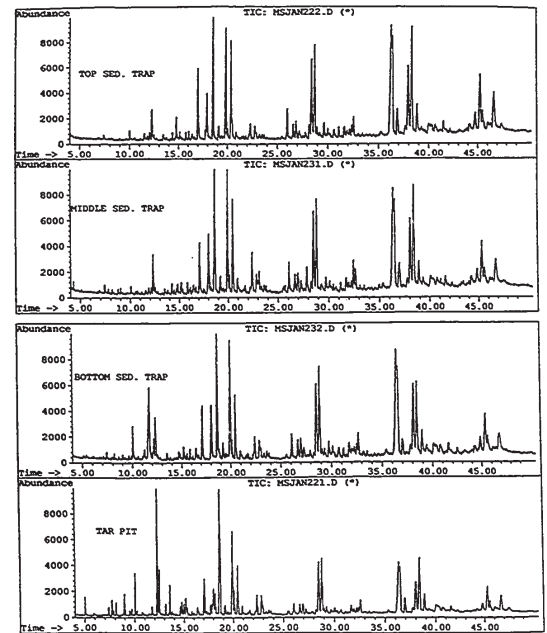


Figure 22. Reversed-phase HPLC chromatograms showing the comparison between the Randle Reef sediment sample extract fraction A23/LH20(D) and the station 53 top (A), middle (B) and bottom (C) sediment trap sample extracts fraction A23/LH20. The UV absorption chromatograms were plotted at 254 nm. Peak identifications by number are as follows.

Peak Number	Compound Identification
1	phenanthrene
2	fluoranthene
3	benzo[a]anthracene
4	chrysene
5	benzo[b]fluoranthene
6	benzo[a]pyrene
7	indeno[1,2,3-cd]pyrene
	benzo[ghi]perylene

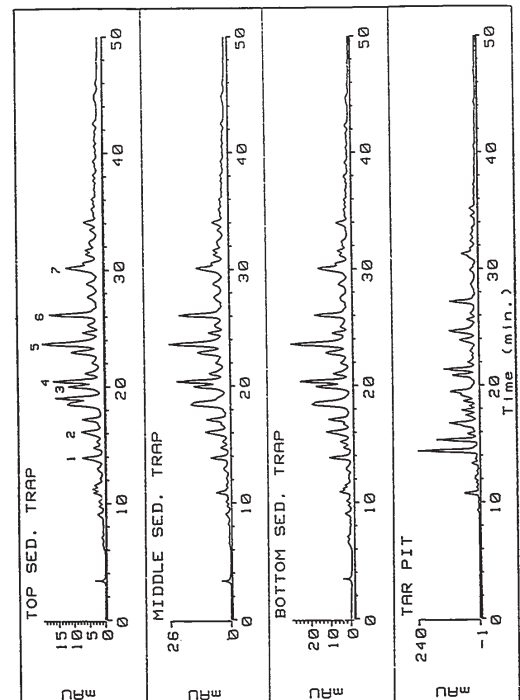


Figure 23. GC-MS total ion current chromatogram of the station 53 middle sediment trap extract fraction A23/LH20. Compound identification was based upon retention time comparison with authentic standards and mass spectra comparison with library spectra. Compounds were quantified using an internal standard method (9,10-dimethylanthracene).

Peak Number	Compound Identification
1	phenanthrene
2	fluoranthene
3	pyrene
4	9,10-dimethylanthracene
5	benzo[a]anthracene
6	chrysene
7	benzo[j,k]fluoranthenes
8	benzo[e]pyrene
9	benzo[a]pyrene
10	indeno[1,2,3-cd]pyrene
11	benzo[ghi]perylene

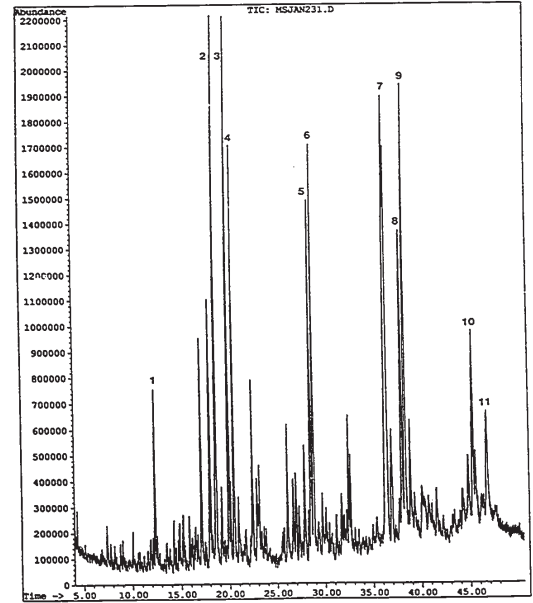


Table 3. Common polycyclic aromatic hydrocarbons determined in Hamilton Harbour sediment trap samples. Concentrations are expressed in µg/g of dry material.

Compound	Station 53 Top	Station 53 Middle	Station 53 Bottom	Station 50 Top	Station 50 Bottom
phenanthrene	2.48	1.63	2.53		0.57
anthracene					0.19
fluoranthene	9.75	6.47	8.22	0.92	1.33
pyrene	9.92	5.86	8.88	0.81	1.24
benzo[a]anthracene	8.29	4.47	6.48	0.30	0.55
chrysene	9.31	5.05	7.82	0.33	0.79
benzo[j,k]fluoranthene					1.86
benzo[a]pyrene	13.35	6.91	7.60	0.23	0.43
benzo[e]pyrene				0.22	0.33
indeno[1,2,3-cd]pyrene	6.86	3.11	4.65	0.15	0.25
benzo[ghi]perylene	6.21	2.29	3.04	0.13	0.21

Table 4. Weight of material in each fraction expressed in milligrams (mg). The numbers in parentheses are the weights expressed as a percentage of the weight of material originally extracted.

Fraction	Station 53 Top	Station 53 Middle	Station 53 Bottom	Station 50 Top	Station 50 Bottom
Crude Extract	57.0 mg (100%)	34.3 mg (100%)	70.0 mg (100%)	87.5 mg (100%)	94.8 mg (100%)
A23/LH20	0.625 mg (1.10%)	0.875 mg (2.7%)	1.0 mg (1.1%)	3.84 mg (4.4%)	2.5 mg (2.6%)
A45	17.8 mg (31%)	18.8 mg (59%)	22.0 mg (31%)		
N1	0.875 mg (1.5%)	0.50 mg (1.6%)	0.75 mg (0.8%)	1.44 mg (1.6%)	
N2				0.94 mg (1.1%)	
Total Percentage Extracubic	1.07%	0.94%	1.77%	1.00%	1.10%

Table 5. Concentrations of polycyclic aromatic hydrocarbons determined in the Randle Reef sediment sample extract and the station 53 sediment trap extracts normalized to chrysene (100%).

Compound	Percentage Concentration Relative to Chrysene Concentration (100%)			
	Randle Reef	Station 53 Top	Station 53 Middle	Station 53 Bottom
phenanthrene	137	26	32	32
fluoranthene	198	105	128	105
pyrene	136	107	116	114
benzo[ <i>a</i> ]anthracene	100	89	89	83
chrysene	100	100	100	100
benzo[ <i>b</i> ]pyrene	111	143	137	97
indeno[1,2,3- <i>cd</i> ]pyrene	55	74	62	59
benzo[ <i>ghi</i> ]perylene	35	67	45	39

of elemental sulphur (approximately 25 µg/g dry weight of sediment trap material) were quantified in the station 50 sediment trap sample extracts. Sulphur was not found in the sediment trap material extracts from the other sites or in the Randle Reef sediment extract.

As was the case with the A23/LH20 fractions, many of the compounds determined in the sediment trap N2 and N3 fractions were also determined in the corresponding extracts of the Randle Reef sediment sample. Many of these compounds identified in fractions N2 and N3 are commonly determined in extracts of coal tar. Various keto-PAH were determined in fraction N2 using GC-MS (Figure 25) while aza-PAH, quinones and larger keto-PAH were determined in fraction N3 (Figure 26). The analysis of the station 50 bottom sediment trap extract fraction N2 by GC-MS in selected ion monitoring mode failed to detect the presence of nitrated PAH (Figure 27). The analyses of selected sediment trap fractions using GC-MS and RP-HPLC are shown in Appendix 1.

### II.2.3 Extraction and Chemical Analysis, Summary

The detailed chemical analyses of the Randle Reef sediment sample and the station 53 sediment trap samples using GC-MS and RP-HPLC with UV absorption and fluorescence detection revealed dramatic similarities in the chromatographic profiles of these samples. The chromatographic profiles of the non-polar PAC fractions (A23/LH20) are dominated by homocyclic PAH. The chromatographic profiles of the more polar PAC N2 and N3 fractions revealed the presence of compounds common to all samples and are

Figure 24. GC-MS total ion current chromatogram of the station 50 top sediment trap extract fraction A23/LH20. Compound identification was based upon retention time comparison with authentic standards and mass spectra comparison with library spectra. Quantification was achieved using an internal standard method (9,10-dimethylanthracene).

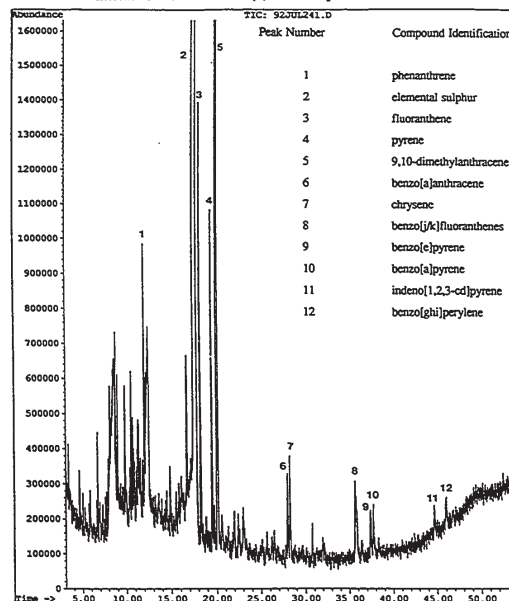


Figure 25. GC-MS total ion chromatogram of the station 53 top sediment trap fraction N2. Compound identification was based upon retention time comparison with authentic compounds and mass spectra comparison with library spectra.

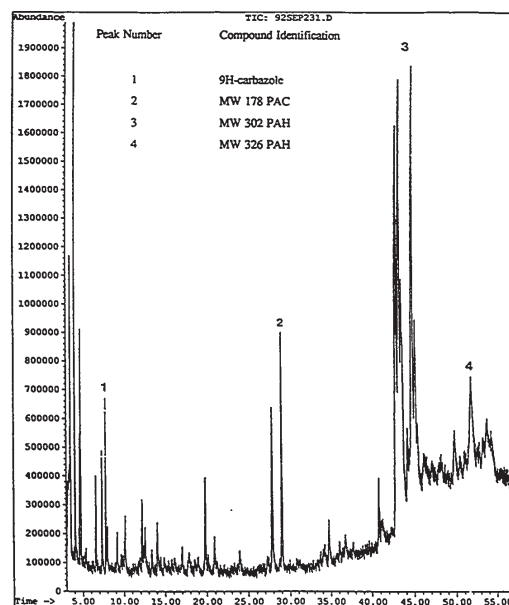


Figure 26. GC-MS total ion chromatogram of the station 53 top sediment trap extract fraction N3. Compound identification was based upon retention time comparison with known compounds and mass spectra comparison with library spectra.

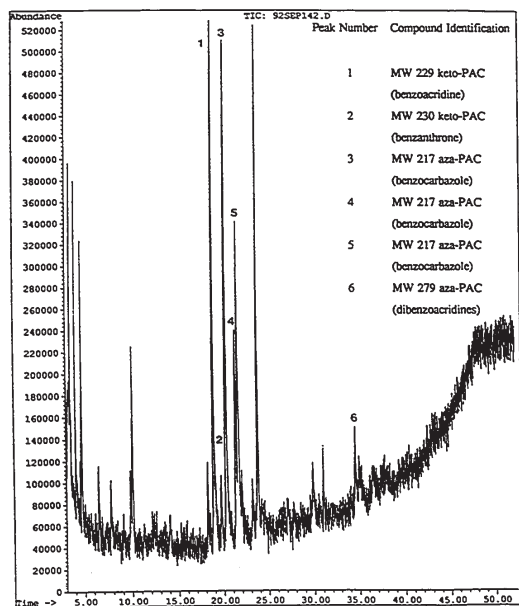
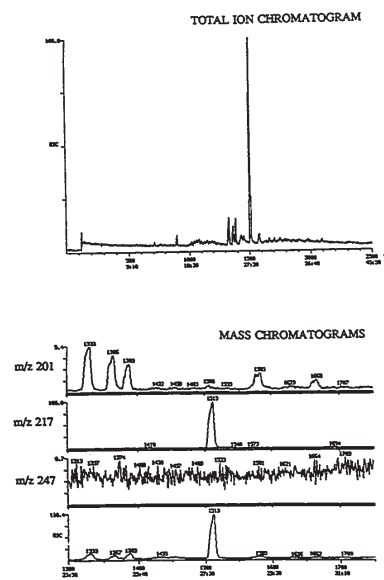


Figure 27. GC-MS selected ion monitoring chromatogram of ions  $m/z$  247,  $m/z$  217 and  $m/z$  201 of the station 50 bottom sediment trap extract fraction N2. These data show no evidence for the presence of nitrofluoranthenes or nitropyrenes as evidenced by the absence of peaks in the TIC that exhibit ions of  $m/z$  247 and  $m/z$  217 or  $m/z$  201.



commonly determined in extracts of coal tar contaminated samples (24,49). These data show that using conventional GC and HPLC methods, it is reasonable to conclude that coal tar contamination is the predominant if not essentially exclusive source of organic pollutants in these samples. Furthermore, the determination of contaminants from sources other than coal tar in Hamilton Harbour using conventional analytical techniques would be difficult. The normalized PAH data shown in Table 5 appear to support the hypothesis that resuspended material from coal tar contaminated areas is the principal contributor to the chemical profiles exhibited by extracts of suspended sediments.

### IL3 Biological Assays with *Salmonella Typhimurium*

#### IL3.1 Randle Reef Sediment Sample

The crude sediment extract was tested for either frameshift mutagens using strain YG1020, a strain similar to the Ames strain TA98, or for base substitution mutagens using YG1025, a strain similar to TA100 (50-52) (Figure 28). The mutagenic potency of the crude extract expressed as revertants per milligram of extracted material is shown in Table 6. The values were calculated by regression analysis of linear portions of the dose response curves. In both strains, the dose response curves for these complex samples were non-linear. Dose response profiles of complex PAH-rich samples such as coal tar extracts have been reported to result in nonlinear responses (53). This result may be due to the complexity of the sample mixture and the resulting inability of the bacteria

Figure 28. Dose response curves obtained from the bioassay of the Randle Reef sediment sample crude extract with the YG1020 (TA98-like) and YG1025 (TA100-like) strains both with and without metabolic activation (S9). The sample was not subjected to the alumina and Sephadex LH20 clean-up procedures. The mutagenic potency value is shown in Table 6 and was obtained by regression analysis of the linear portions of the dose response curves.

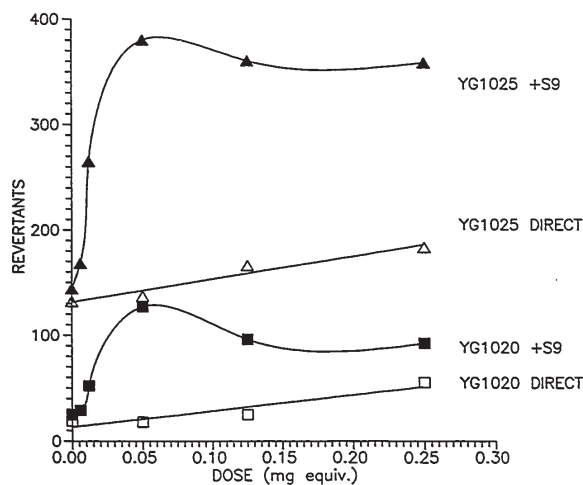


Table 6. Net mutagenic potency of Randle Reef sediment fractions expressed as revertants per milligram of extracted material. The values were calculated by regression analysis of the linear portions of the dose response curves. Positive and spontaneous control values are expressed as revertant colonies per plate. Standard deviations for positive and spontaneous control values were based on cumulative laboratory results from 25 replicate experiments.

FRACTION	YG1020		TA98-LIKE STRAINS YG1021 Nitroreductase		YG1024 O-acetyltransferase	
	DIRECT (-S9)	DIRECT (+S9)	DIRECT (-S9)	DIRECT (+S9)	DIRECT (-S9)	DIRECT (+S9)
Crude	149±23	2088±171				
A23/LH20	406±46	1770±383	215±57	1352±228	256±48	1654±4
A45	56±26	60±16	236±192	174±45		
N1	186±34	1514±128			50±9	662±18
N2	10±19	0			396±51	132±34
N3	0	63±26			24±2	92±11
Spontaneous	22±11	27±10	34±23	42±23	40±13	109±38
1,8-DNP (7.2X10 <sup>-4</sup> µg/plate)	436±149	39±19	368±153	62±38	3721±203	240±57
2-AF (3.6 µg/plate)	58±39	350±262	54±28	2312±1234	448±214	1787±691
			TA100-LIKE STRAINS YG1026 Nitroreductase		YG1029 O-acetyltransferase	
	DIRECT (-S9)	DIRECT (+S9)	DIRECT (-S9)	DIRECT (+S9)	DIRECT (-S9)	DIRECT (+S9)
Crude	214±36	4880±855				
A23/LH20	566±82	6490±566		4490±110		4827±293
A45	12±73	48±61				
N1	441±60	4018±341				
N2	45±57	1117±171				
N3	65±68	147±46				
Spontaneous	158±16	190±15	209±138	254±30	161±78	183±19
Sodium Azide (5.0 µg/plate)	730±478	576±173	517±419	449±190	932±510	467±255
B[a]P (1.0 µg/plate)	232±169	993±256	190±46	861±217	181±60	969±275

to respond adequately to such an excessive number of compounds.

The high PAH levels in these extracts were also emphasized by the dramatic difference in the dose responses of the two tester strains when metabolic activation was provided by the addition of a microsomal preparation of oxidative enzymes (S9). As a class, homocyclic PAH compounds are base-pair substitution mutagens.

Table 6 shows the mutagenic responses for the crude extract and for several fractions derived from the Randle Reef sediment sample. In addition to strains related to the standard Ames strains TA98 and TA100 (YG1024 and YG1025 respectively), the fractions were tested in strains which had approximately 50 additional copies of two activating enzymes incorporated into their genetic material. Strains containing extra copies of a nitroreductase enzyme are strain YG1021 (TA98-type) and strain YG1026 (TA100-type) while strains containing extra copies of an O-acetyltransferase gene are strain YG1024 (TA98-type) and strain YG1029 (TA100-type). Since there was no increase in mutagenic response in these strains compared to the responses obtained with strains without the enzymes it can be concluded that the mutagenicity of the extracts is mainly due to homocyclic PAH and that the extracts do not contain significant levels of compounds such as nitro-PAH that show increased responses to acetyltransferase and/or nitroreductase. These results were confirmed using chemical analysis. GC-MS analysis in selected ion monitoring mode of the N2 fraction failed to detect any nitro-PAH (Figure 29).

The assays of fraction A23/LH20, particularly those using the TA100-type strains, still exhibited non-linear responses at higher doses (Figures 30 and 31), but this effect was

Figure 29. GC-MS selected ion monitoring chromatogram of ions m/z 247, m/z 217 and m/z 201 of the Randle Reef sediment sample extract fraction N2. These data show no evidence for the presence of nitrofluoranthenes or nitropyrenes as evidenced by the absence of peaks in the TIC that exhibit both the molecular ion m/z 247 and either of the two fragment ions.

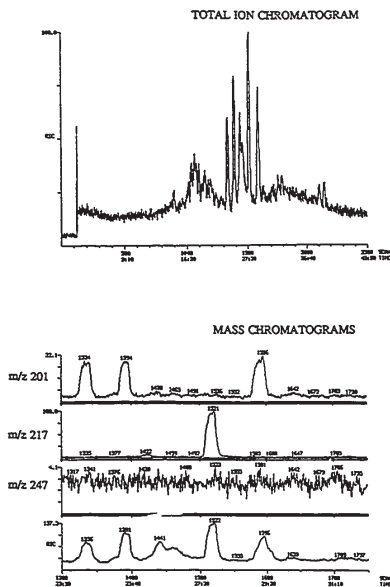


Figure 30. Dose response curves exhibited by fraction A23/LH20 of the Randle Reef sediment trap extract when assayed with the TA98-like strains. Doses were normalized to the amount of organic material originally extracted (milligram equivalents). Mutagenicity values for these assays are reported in Table 6.

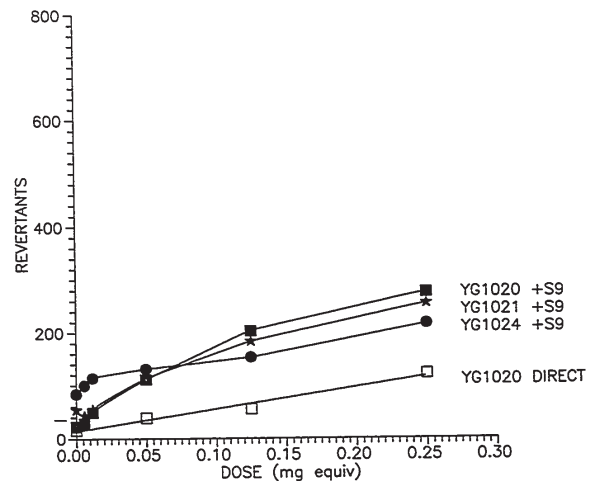




Figure 31. Dose response curves exhibited by fraction A23/LH20 of the Randle Reef sediment trap extract when assayed with the TA100-like strains. Doses were normalized to the amount of organic material originally extracted (milligram equivalents). Mutagenicity values for these assays are reported in Table 6.

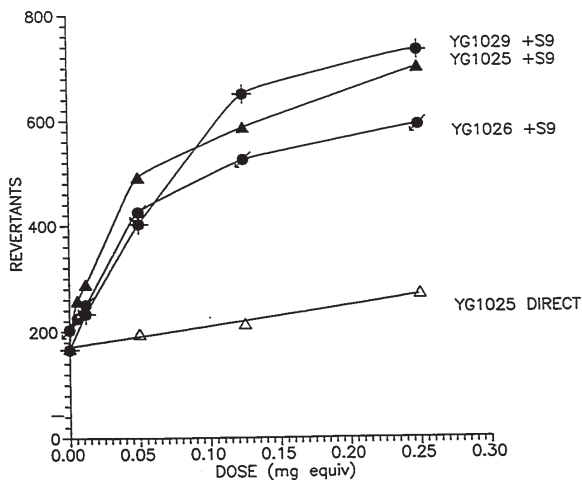
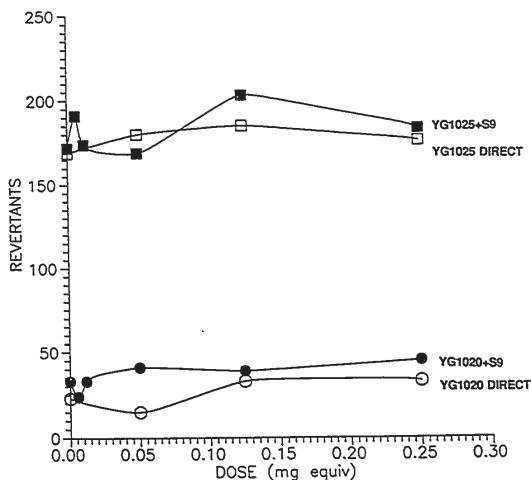


Figure 32. Dose response curves exhibited by fraction A45 of the Randle Reef sediment sample extract when assayed with strain YG1020 (TA98-like) and strain YG1025 (TA100-like). Doses were normalized to the amount of organic material originally extracted (milligram equivalents). Mutagenicity values for these assays are reported in Table 6.



less pronounced than was observed in the assays of the crude extract. The addition of S9 to the A23/LH20 fraction when assayed with the TA98-like strains produced positive dose response curves which only achieved a doubling of spontaneous mutation frequency at the highest doses. The lack of increased sensitivity in the TA98 derivative strains again showed the absence of frameshift mutagens which require O-acetyltransferase or nitroreductase enzymes to be metabolized to mutagenic intermediates (Figure 30). The lack of increased response to strains containing multiple copies of these enzymes underscores the absence of frameshift mutagens in the Randle Reef sediment extract.

The strong response of TA100-type strains to the A23/LH20 fraction revealed that this fraction contained primarily base pair substitution mutagens (Figure 31). While metabolic activation with S9 was required to obtain a positive dose response, there was no noticeable increase in mutagenic response in strains containing additional copies of either the nitroreductase or the O-acetyltransferase genes.

Fraction A45, which contained polar PAC, was tested for mutagenic activity with strains YG1020 and YG1025 but showed no positive response with or without S9 activation (Figure 32 and Table 6).

Selected normal phase N fractions derived from the A23/LH20 fraction were assayed to further confirm the identity of the compounds responsible for the activity observed in the crude extract (Figures 33-35). None of the N fractions exhibited significant responses in the TA98-like strains without metabolic activation with the exception of fraction N2 when assayed with strain YG1024 (Figure 35). This response may be due to the presence of nitro-PAH at levels in the extract that were below the

Figure 33. Dose response curves exhibited by selected N fractions of the Randle Reef sediment trap extract when assayed with strain YG1020 (TA98-like). Doses were normalized to the amount of organic material originally extracted (milligram equivalents). Mutagenicity values for these assays are reported in Table 6.

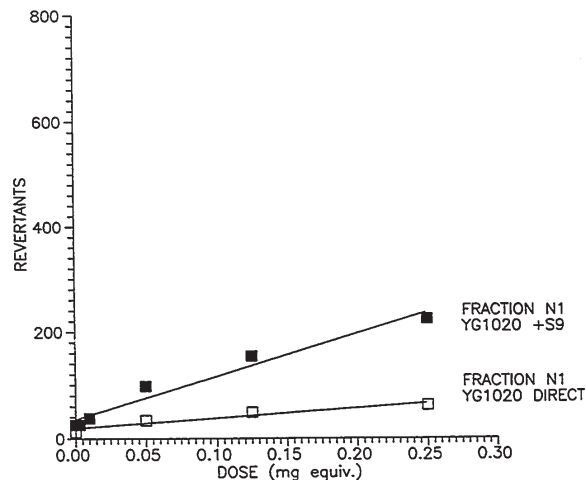
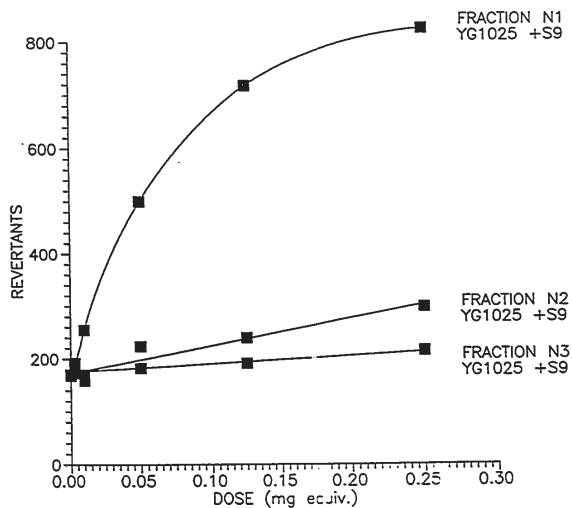


Figure 34. Dose response curves exhibited by selected N fractions of the Randle Reef sediment trap extract when assayed with strain YG1025 (TA100-like). Doses were normalized to the amount of organic material originally extracted (milligram equivalents). Mutagenicity values for these assays are reported in Table 6.



detection limits of the GC-MS instrumentation. The large responses exhibited by the N1 fraction in the TA98-like strains with the addition of metabolic activation are due to PAH (Figure 33); these responses are lower than observed in the TA100-like strains.

Fraction N1 contained most of the mutagenic potency observed in fraction A23/LH20 with the TA100-like strains with metabolic activation (Figure 34 and Table 6). The regression values for the N fractions given in Table 6 indicate that fractions N1 and N2, which contained the PAH, accounted for approximately 80% of the mutagenic activity observed in fraction A23/LH20 of the Randle Reef sediment sample. Figure 36 illustrates the relative mutagenic contributions of the N fractions to the total activity observed in the parent A23/LH20 fraction when assayed with strain YG1025+S9.

II.3.2 Randle Reef Sediment Sample Fraction N1

Mutachromatogram

Since fraction N1 contained most of the mutagenic activity exhibited by fraction A23/LH20 (Table 6), this fraction was the focus of further separations and bioassays to determine the individual compounds responsible for the activity. Fraction A23/LH20 was again chromatographed on the normal phase PAC column and the collection time for fraction N1, normally 7.5 minutes to 24 minutes, was extended to 25 minutes (see footnote to caption to Figure 14). This resulted in the high molecular weight PAH greater than MW 278 amu being collected in fraction N1. This was done to concentrate all of the PAH, and all of the mutagenic activity of fraction A23/LH20, in fraction N1. The

Figure 35. Dose response curves exhibited by selected N fractions of the Randle Reef sediment extract when assayed with strain YG1024 without metabolic activation. Doses are expressed in milligram equivalents of extracted material. Mutagenicity values are reported in Table 6.

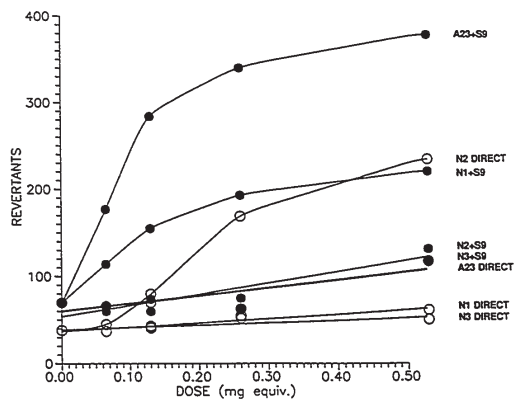
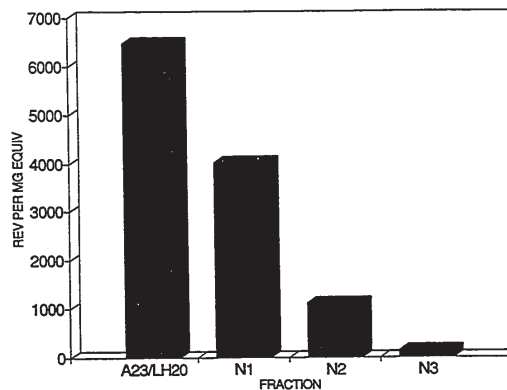


Figure 36. Histogram showing the relative contributions of the Randle Reef sediment N fractions to the total mutagenic activity observed in the parent fraction A23/LH20 when assayed with strain YG1025+S9. The mutagenic activities exhibited by each of these fractions are listed in Table 6.



mutagenic activity previously observed in fraction N2 was likely due to the high molecular weight PAH previously collected in that fraction.

This freshly collected fraction N1 was further fractionated by RP-HPLC and one minute subfractions, collected between 12 and 48 minutes elution times, were assayed in duplicate using strain YG1025 with the addition of S9. Figure 37 is a "mutachromatogram" showing the RP-HPLC UV absorption profile (254 nm) of fraction N1 (Figure 37B) and the net mutagenic responses of each of the one minute subfractions (Figure 37A). The number of spontaneous revertant colonies (150) was subtracted from the mutagenic response of each subfraction to result in a net mutagenic response per subfraction. Subfractions exhibiting significant positive responses in the mutachromatogram can be identified as those exceeding 150 net revertants (double the spontaneous reversion rate).

The majority of the mutagenic activity was observed in subfractions with retention times between 30.5 minutes and 36.5 minutes. Three subfractions showing net mutagenic responses of approximately 150 revertants elute in the 25 minutes to 27 minutes retention time range. This range corresponds to the known retention time for benzo[a]pyrene (peak 12, Figure 37). This compound, a known carcinogen and mutagen, was found to be a primary mutagen in a Sydney Harbour, Nova Scotia sediment sample (47) but was present at higher concentration in that sample extract relative to the higher molecular weight PAH.

The 30.5 minutes to 36.5 minutes subfractions were pooled and analysed using GC-MS. A total ion current chromatogram produced in full scan mode revealed that

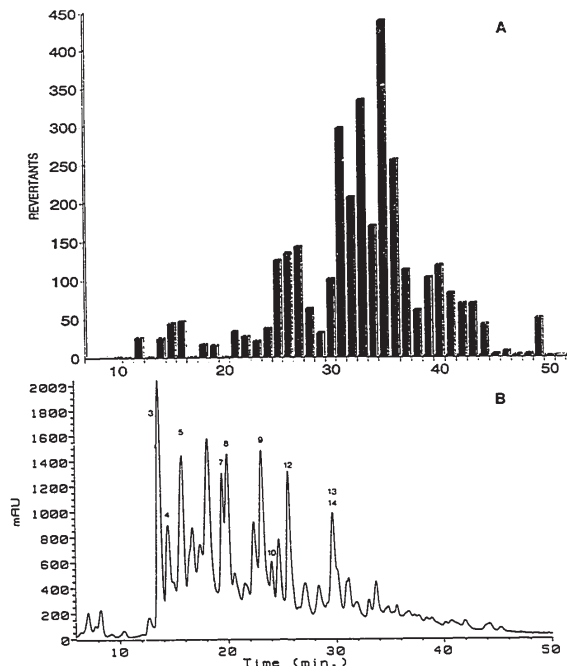


Figure 37. Randle Reef sediment sample extract fraction N1 mutachromatogram. One minute subfractions were collected between 12 minutes and 48 minutes elution times using RP-HPLC and assayed using strain YG1025 (TA100-like) with the addition of S9. The mutagenic response of the individual subfractions is expressed as net revertants per plate (number of revertant colonies minus the number of spontaneous revertant colonies) and is the average of duplicate measurements. The RP-HPLC UV absorption profile was plotted at 254 nm. Peaks are numbered to correspond with those in Table 2. Peak identifications are based on retention time comparisons with authentic standards and comparison of UV spectra with library spectra.

Peak Number	Compound
3	phenanthrene
4	anthracene
5	fluoranthene
7	benzo[a]anthracene
8	chrysene
9	benzo[b]fluoranthene
10	benzo[k]fluoranthene
12	benzo[a]pyrene
13	indeno[1,2,3-cd]pyrene
14	benzo[ghi]perylene

compounds of molecular weights 276, 278, and 302 were present (Figures 38 and 39). Indeno[1,2,3-cd]pyrene and benzo[ghi]perylene were identified. Compounds with a molecular weight of 278 amu may include picene, dibenz[ah]anthracene, dibenz[ac]anthracene, and benzo[b]chrysene, all of which have been determined in extracts of Hamilton Harbour sediment samples (2). The molecular weight 278 compounds were not sufficiently resolved to make positive identifications. The profile of the molecular weight 302 compounds showed a striking similarity to the profile observed by Wise *et al* (54) in fractions isolated from coal tar samples.

Data for the genotoxicity of benzo[ghi]perylene, indeno[1,2,3-cd]pyrene, and dibenz[ah]anthracene have been reported in studies using the *Salmonella*/microsome assay and other short-term biological tests (55-58). The lowest effective doses for these individual compounds in TA100 with S9 activation are in the range of the concentrations in the N1 subfractions isolated from the fraction N1 mutachromatogram.

### IL3.3 Station 910 Sediment Sample

Fraction A23/LH20 of the station 910 sediment sample extract was assayed with strain YG1024 (TA98-like) and YG1025 (TA100-like) (data not shown). No significant direct response was observed with strain YG1024 (66 rev/mg equivalent) but positive dose response curves were observed in both strains with the addition of oxidative metabolism. The extrapolated mutagenicity values for the two strains with S9 were very similar (strain YG1024+S9 - 229 rev/mg equivalent, strain YG1025+S9 - 220 rev/mg equivalent). These

Figure 38. GC-MS total ion chromatogram of the Randle Reef fraction N1 mutachromatogram subfractions collected in the 30.5 minutes to 36.5 minutes retention time range.

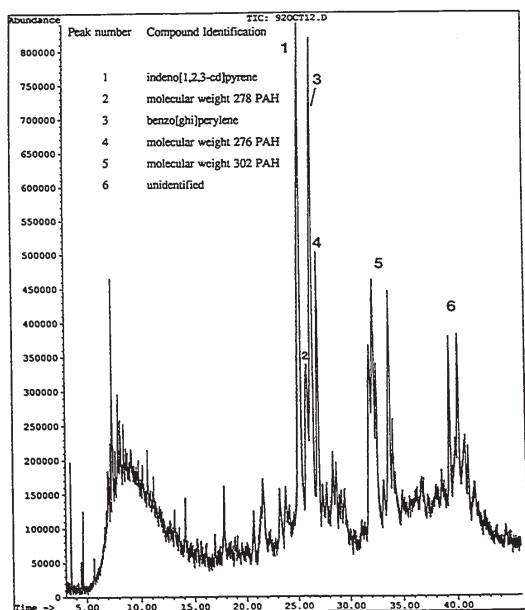
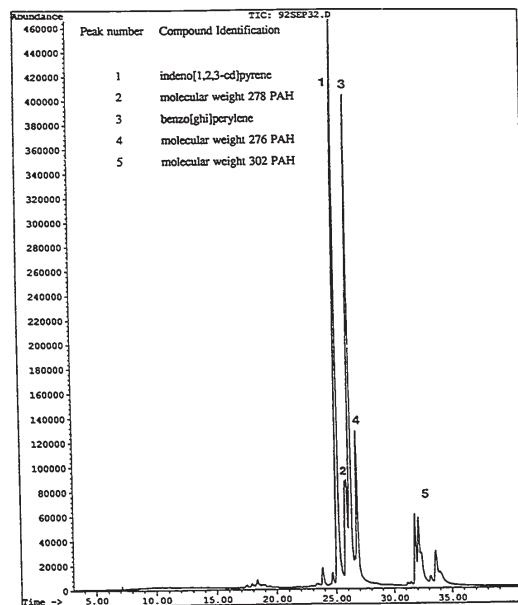


Figure 39. GC-MS selected ion monitoring chromatogram of the Randle Reef fraction N1 mutachromatogram subfractions collected in the 30.5 minutes to 36.5 minutes retention time range. Selected ions were  $m/z$  276,  $m/z$  278 and  $m/z$  302.



data do not provide evidence for the presence of mutagenic compounds other than PAH.

### IL3.4 Sediment Trap Samples

#### IL3.4.1 Mutagenicity Tests: TA100-Like Strain.

The A23/LH20 fractions from five sediment trap samples (station 50 and station 53 samples, Figures 40 and 41) were tested for base-pair substitution mutagens using *Salmonella* strain YG1025 (TA100-like strain)(50-52). These assays resulted in data that were similar to those produced with the Randle Reef sediment sample extract. In the YG1025 strain, the dose response curves were non-linear. The high PAH levels in the sample extracts were also manifest by the dramatic difference in the dose responses with S9 activation. The addition of S9 to the A23/LH20 fractions produced dose response curves which achieved a doubling of spontaneous mutation frequency at the higher doses.

As with the Randle Reef sediment sample, the positive response of TA100-type strains to the A23/LH20 fractions revealed that the samples contained base pair substitution mutagens. The mutagenic potencies of the extracts were determined from regression values calculated for the linear portions of the dose response curves (Tables 7 and 8).

The sediment trap samples contain lower concentrations of PAH than the Randle Reef sediment sample by factors of 5-fold to 200-fold. To provide data for comparison purposes, normalization factors for PAH were calculated based on the levels of five

Figure 40. Dose response curves for the station 50 sediment trap extracts fraction A23/LH20 when assayed with strain YG1025 (TA100-like) with and without metabolic activation (S9). Doses are expressed in revertants per milligram equivalents of extracted material. The mutagenic responses extrapolated from the linear portions of the dose response curves are shown in Table 7.

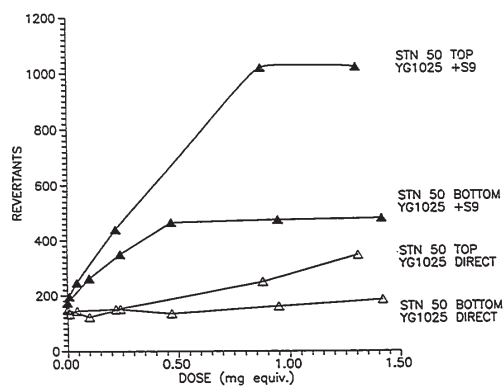


Figure 41. Dose response curves exhibited by the station 53 sediment traps fraction A23/LH20 when assayed with strain YG1025 (TA100-like).

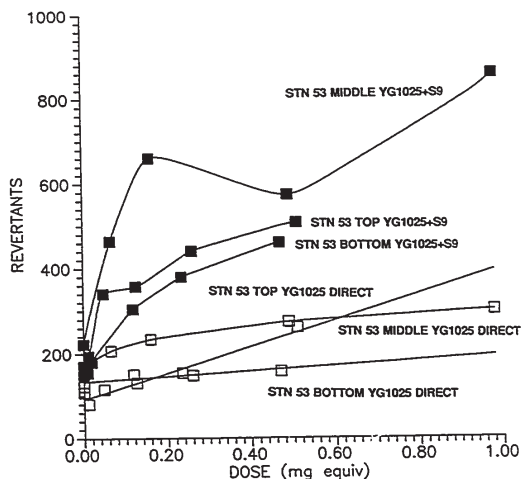


Table 7. Mutagenic potencies of station 53 sediment trap extract fractions expressed in revertants per milligram equivalent. NR denotes no response.

Strain/Fraction	Top		Middle		Bottom	
	Direct	+S9	Direct	+S9	Direct	+S9
YG1024 (TA98-like)						
A23/LH20	220±25	745±58	145±35	976±82	399±37	1098±54
Reconstructed A23/LH20	1283	1886				
A45	NR	154±18	NR			
N1	NR	698±60	35±4	427±113	NR	222±13
N2	NR	NR	1165±109	185±36	82±19	NR
N3	375±9	230±30	2647±894	1455±183	2100±138	689±69
N456	NR	NR	NR	NR		
N7	150		214±20	NR	277±10	
YG1025 (TA100-like)						
A23/LH20	310±41	1513±113	NR	1329±39	NR	1326±65

\*Based on a single 0.50 mg equivalent dose measurement

Table 8. Mutagenic potencies of station 50 sediment trap extract fractions expressed in revertants per milligram equivalent. NR denotes no response.

Strain/Fraction	Top		Bottom	
	Direct	+S9	Direct	+S9
YG1024 (TA98-like)				
A23/LH20	18435	4680	1342±151	1685±162
A45	43±8	NR	34±3	NR
N1	NR		NR	225±40
N2	9510±252	1260±250	675±45	NR
N3	12675±891	2071±417	1390±15	138±21
N456	125±5	NR	59±5	
N7	204±40	504±97	204±40	
YG1025 (TA100-like)				
A23/LH20	153±13	945±35	NR	608±51

The top and bottom N7 fractions were combined to form a composite fraction.

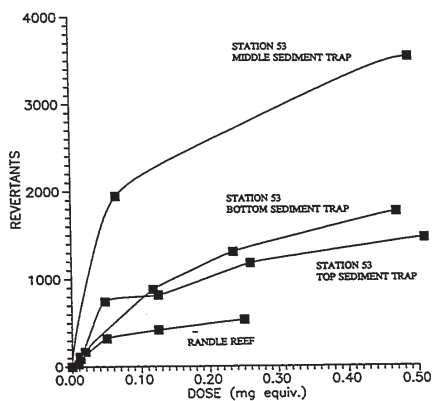
selected homocyclic PAH in the Randle Reef sediment sample and the station 53 sediment trap samples: pyrene, benzo[a]anthracene, chrysene, benzo[ghi]perylene, and indeno[1,2,3-cd]pyrene. These compounds were chosen to avoid disproportionately high normalization constants due to decreased levels of more volatile PAH in the sediment trap sample extracts relative to the Randle Reef sediment sample extract. The normalized sediment trap data results in dose response curves that have similar slopes for the Randle Reef sediment sample and the station 53 sediment trap sample extracts (Figure 42). This data does not provide conclusive evidence that PAH are the only source of base pair substitution type mutagens in the station 53 sediment trap sample extracts. The normalized response values for the Station 50 sediment trap samples resulted in dose response curves that were much greater in slope than the slope exhibited by the Randle Reef sediment sample (Figure 43).

The results of the assays with strain YG1025 did not reveal any significant differences in the biological profile between the Randle Reef sample extract and the extracts from station 50 and station 53. Further investigation of the sediment trap sample extracts in the form of assays of the N fractions using strain YG1025 was deemed unnecessary. It was concluded that the compounds identified in the Randle Reef sediment sample extract fraction N1 mutachromatogram were likely those responsible for the TA100-like strain activity observed in the sediment trap sample extracts. Due to the low PAH levels in the sediment trap samples and the relatively small weight of extract obtained from these samples, fraction N1 mutachromatograms could not be produced.

Figure 42. Comparison of responses of station 53 sediment trap and Randle Reef sediment fractions A23/LH20 normalized for PAH content. The dose response curves are for normalized assay results with strain YG1025+S9. The normalization factors, defined as the averages of the ratios in PAH concentrations of pyrene, benzo[a]anthracene, chrysene, benzo[a]pyrene and indeno[1,2,3-cd]pyrene between the Randle Reef sediment sample and the station 53 sediment trap samples are as follows:

- Station 53 top sediment trap sample - 4.3:1
- Station 53 middle sediment trap sample - 8.0:1
- Station 53 bottom sediment trap sample - 5.7:1

The bioassay results for the sediment trap A23/LH20 fractions were multiplied by these normalization factors to result in the dose response curves shown in the figure.



IL3.4.2 Mutagenicity Tests: TA98-Like Strain.

The Randle Reef sediment and sediment trap extracts were tested for frameshift mutagens using *Salmonella* strain YG1024, a strain similar to the Ames strain TA98 (50-52). We believe this strain to be a suitable choice for the detection of mutagenic activity in complex environmental mixtures. The initial bioassays of the station 53 sediment trap sample extracts fraction A23/LH20 with strain YG1024 indicated that there was marginally greater biological activity in two of the sediment trap samples as compared to the Randle Reef sediment sample (Figure 44). As a result of this preliminary data, fresh samples of the station 53 sediment traps were extracted, cleaned up and fractionated and the resulting N fractions were assayed (Figures 45-47). These assays yielded significant results. Large positive responses were observed, particularly in the N3 fractions. The response of the N3 fractions was also observed to be greater without the addition of oxidative metabolism in the form of S9. The mutagenicity values for the station 53 sediment trap extracts are shown in Table 7.

The large positive direct-acting response exhibited by the N fractions was not observed when the A23/LH20 fractions were assayed (Figure 44 and Table 7), but when the station 53 top sediment trap N fractions were re-combined to form a reconstructed A23/LH20 fraction, a large positive response was observed when this fraction was assayed (Table 7). It is possible that this activity was suppressed in the previously assayed A23/LH20 fraction.

The assays of the station 50 sediment trap A23/LH20 fractions with strain YG1024

Figure 43. Comparison of responses of station 50 sediment trap and Randle Reef sediment fractions A23/LH20 normalized for PAH content. The dose response curves are for normalized assay results with strain YG1025+S9. The normalization factors, defined as the averages of the ratios in PAH concentrations of pyrene, benzo[a]anthracene, chrysene, benzo[a]pyrene and indeno[1,2,3-cd]pyrene between the Randle Reef sediment sample and the station 53 sediment trap samples are as follows:

- Station 50 top sediment trap sample - 134:1
- Station 50 bottom sediment trap sample - 73:1

The bioassay results for the sediment trap A23/LH20 fractions were multiplied by these normalization factors to result in the dose response curves shown in the figure.

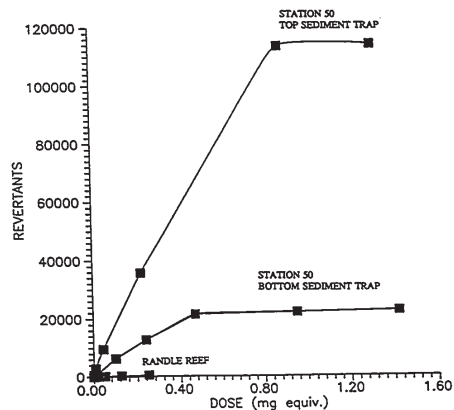


Figure 44. Dose response curves exhibited by station 53 sediment trap samples and the Randle Reef sediment sample fraction A23/LH20 when assayed with strain YG1024 (TA98-like) without the addition of S9.

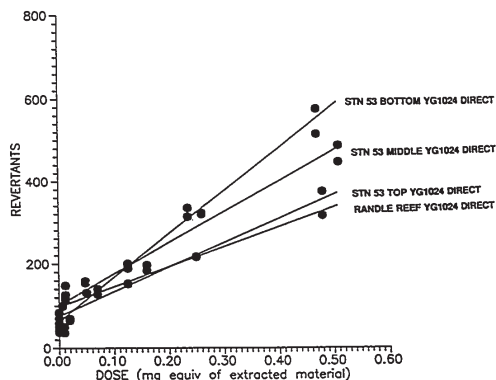


Figure 45. Dose responses exhibited by the station 53 top sediment trap extract N fractions when assayed with strain YG1024 (TA98-like) with and without the addition of S9. Doses are expressed in milligram equivalents of extracted material. The mutagenicity values for these fractions are reported in Table 7.

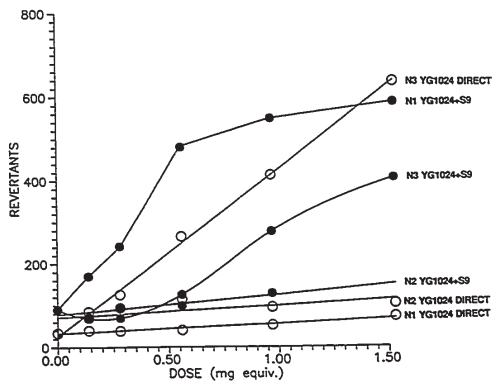


Figure 47. Dose responses exhibited by the station 53 bottom sediment trap extract N fractions when assayed with strain YG1024 (TA98-like) with and without the addition of S9. Doses are expressed in milligram equivalents of extracted material. The mutagenicity values for these fractions are reported in Table 7.

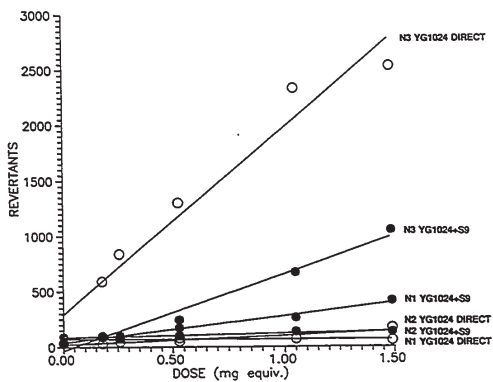
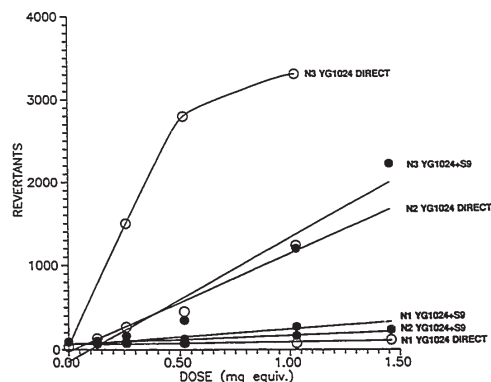


Figure 46. Dose responses exhibited by the station 53 middle sediment trap extract N fractions when assayed with strain YG1024 (TA98-like) with and without the addition of S9. Doses are expressed in milligram equivalents of extracted material. The mutagenicity values for these fractions are reported in Table 7.



also resulted in the detection of significant biological activity. The responses of strain YG1024 to the A23/LH20 extracts resulted in linear dose response curves with steep slopes which indicated the presence of frameshift type mutagens in both samples (Figure 48 and Table 8). The fraction A23/LH20 responses for the station 50 sediment trap extracts were much greater than those obtained with the Randle Reef sample extract as evidenced by the large mutagenic potencies listed for these fractions in Table 8. The dose response curves for the corresponding station 50 sediment trap N fractions show that the majority of the direct mutagenic activity is contained in fractions N2 and N3 (Figures 49 and 50). These data show a similarity with those obtained from the station 53 sediment trap N fractions. The dose response curves for the Randle Reef sediment sample A23/LH20 and N fractions when assayed with strain YG1024 (TA98-like) are shown in Figure 51 and have been plotted on the same scale as the station 50 top sediment trap N fraction dose response curves for comparative purposes.

The A23/LH20 fractions from the station 51 sediment trap extracts were assayed with strain YG1024 (Figure 52). The top and bottom extracts both exhibited positive dose responses, but the mutagenic potencies of these fractions (station 51 top - 101 rev/mg equivalent, station 51 bottom - 71 rev/mg) were far lower than those of the station 53 and station 50 samples (Tables 7 and 8). The station 51 sample site is at the western end of the harbour in an area where contaminant levels in the sediments, and likely in the suspended sediments, are lower. The location of the sampling site may be the dominant reason for the observed lower mutagenic potencies of the station 51 sediment trap extracts.

Figure 48. Dose responses exhibited by the station 50 sediment traps A23/LH20 fractions when assayed with strain YG1024 (TA98-like) with and without the addition of S9. Doses are expressed in milligram equivalents of extracted material. The mutagenicity values for these fractions are reported in Table 8.

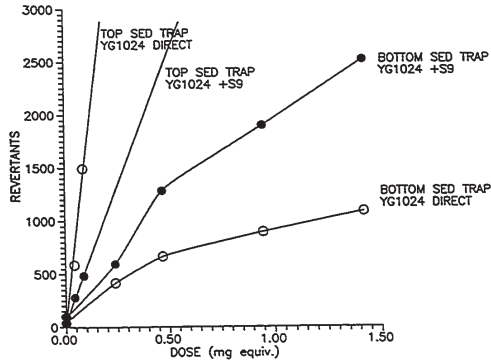


Figure 50. Dose responses exhibited by the station 50 top sediment trap extract N fractions when assayed with strain YG1024 (TA98-like) with and without the addition of S9. Doses are expressed in milligram equivalents of extracted material. The mutagenicity values for these fractions are reported in Table 8.

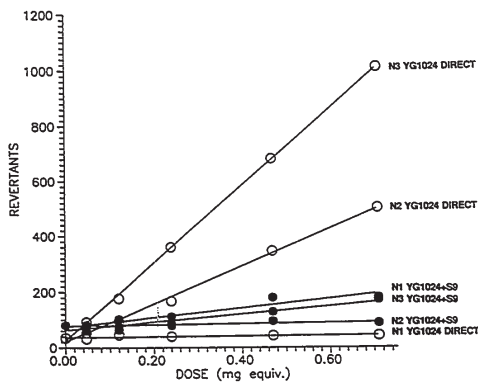


Figure 49. Dose responses exhibited by the station 50 bottom sediment trap extract N fractions when assayed with strain YG1024 (TA98-like) with and without the addition of S9. Doses are expressed in milligram equivalents of extracted material. The mutagenicity values for these fractions are reported in Table 8.

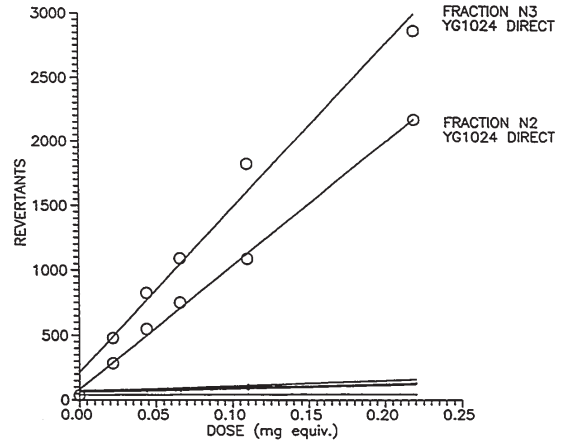


Figure 51. Dose response curves exhibited by Randle Reef sediment sample extract fractions when assayed with strain YG1024 without S9. These curves are identical to those shown in Figure 34 but have been plotted with a Y axis scale the same as that of the station 50 top sediment trap A23/LH20 fractions (Figure 46) to provide a comparison between the two sets of data.

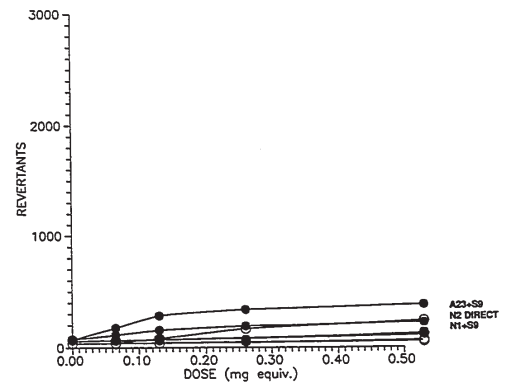




Figure 52. Dose response curves exhibited by the station 51 sediment trap A23/LH20 fractions when assayed with strain YG1024. The doses are expressed in milligram equivalents of extracted material. The mutagenicity values were 71 rev/mg equivalent for the bottom sediment trap extract and 101 rev/mg for the top sediment trap extract.

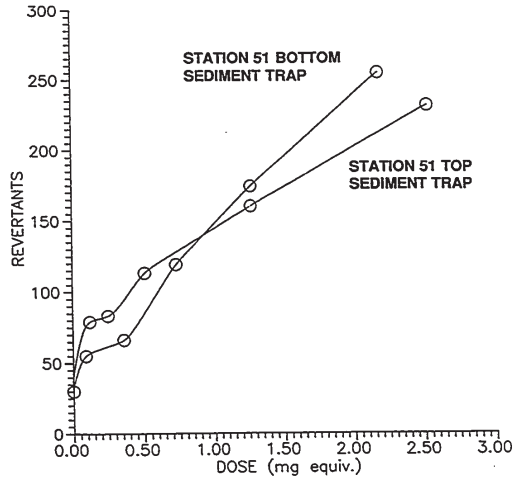
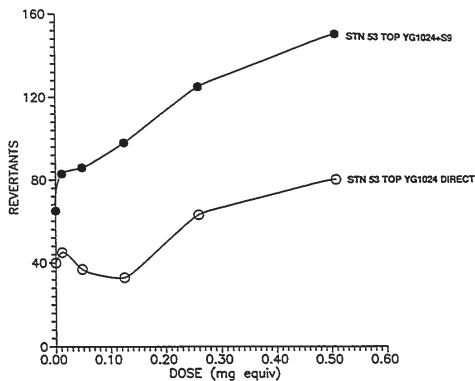


Figure 53. Dose response curves exhibited by fraction A45 of the station 53 top sediment trap extract when assayed with strain YG1024 (TA98-like). Doses were normalized to the amount of organic material originally extracted (milligram equivalents). Mutagenicity values for these assays are reported in Table 7.



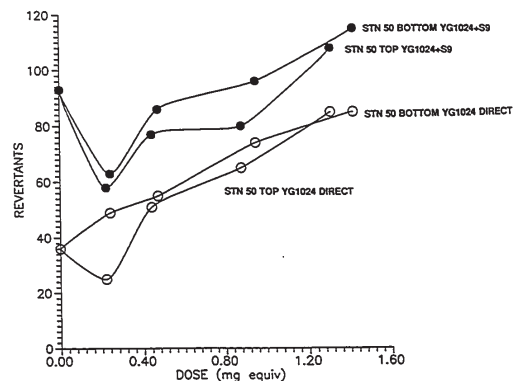
The sediment trap extracts A45 fractions showed no significant positive responses with or without S9 activation using strain YG1024 (Tables 7 and 8 and Figures 53 and 54).

II.3.4.3 TA98-Like Strain Bioassay Data: Summary

In contrast to the results obtained with the TA100-like strain, the assays of the sediment trap sample N fractions with strain YG1024 resulted in dramatically different results as compared to the Randle Reef sediment sample. The assays of the N<sub>1</sub> fractions with strain YG1024 resulted in dramatically varying results for the different samples. The Randle Reef sample displayed minimal activity in fractions N1 and N2 and showed no significant activity in fraction N3. Extracts of the station 50 and station 53 sediment trap samples displayed dramatically higher responses in all of the N3 fractions and some of the N2 fractions (Tables 7 and 8). The compound(s) responsible for this activity did not require metabolic activation by S9 to manifest their response. These data indicated the presence of compounds not present in the Randle Reef sediment sample. These results are among the most significant presented in this thesis. The station 51 sample extracts exhibited relatively low responses compared to stations 50 and 53.

After these results were obtained, a fresh sample of Randle Reef sediment was extracted, cleaned up and fractionated for immediate bioassay. The assays of the A23/LH20 and N1, N2 and N3 fractions of this extract failed to detect significant amounts of direct-acting activity in the YG1024 strain. Mutagenicity values of 31±12

Figure 54. Dose response curves exhibited by fraction A45 of the station 50 top and bottom sediment trap extracts when assayed with strain YG1024 (TA98-like). Doses were normalized to the amount of organic material originally extracted (milligram equivalents). Mutagenicity values for these assays are reported in Table 8.



rev/mg equivalent and  $1021 \pm 174$  rev/mg equivalent were obtained for fraction A23/LH20 directly and with S9 respectively. The mutagenic potencies of the N1, N2 and N3 fractions are reported in Table 6. This experimental work was performed to confirm the earlier results obtained from the bioassays of the Randle Reef sediment sample extract and to discount the possibility of a reduction of mutagenic activity in the previously assayed extract due to prolonged sample storage.

### II.3.5 Sediment Trap Fraction N3 Mutachromatograms.

In contrast to the dramatic differences in mutagenic profiles between the sediment trap and Randle Reef sediment samples, there appeared to be no apparent differences in the chemical profiles of the samples. As discussed previously, the analysis of the A23/LH20 and N fractions from the Randle Reef sediment and sediment trap extracts revealed similar compounds and compound classes to be present in all sample extracts. In an attempt to determine the source of the observed direct mutagenic activity, the N3 fraction of the station 50 top sediment trap was further fractionated by RP-HPLC (using the described gradient elution program) and one minute subfractions were collected and subjected to bioassay. This specific sample was chosen for further fractionation because it displayed the greatest direct mutagenic activity of the sediment trap extracts, based on the number of revertants per milligram equivalent of extracted material (Table 8).

Figure 55 is the station 50 fraction N3 mutachromatogram with the RP-HPLC chromatogram (Figure 55A) and the net mutagenic responses displayed by the one minute

subfractions when assayed with strain YG1024 (TA98-like strain) without metabolic activation (Figure 55B). The mutagenic activity displayed by the station 50 sediment trap N3 fraction was contained in 2 one minute subfractions with elution times from 13 to 15 minutes. Further analysis of these subfractions (pooled to form a single fraction) by GC-MS (Figure 56) revealed that few compounds were present.

Benzanthrone (7H-benz[de]anthracen-7-one) was determined in both the RP-HPLC and GC-MS chromatograms, but was not responsible for the observed mutagenic activity although this compound has been found to be highly active in the *paramecium caudatum* photodynamic assay (59). The inactivity of benzanthrone in the *Salmonella* assay was confirmed by bioassay of an authentic benzanthrone standard. No response was observed. The other compounds observed in the GC-MS chromatogram have not been positively identified, and may or may not be responsible for the observed mutagenic activity. If the active compounds are highly mutagenic, they may be present at the picogram level making them difficult to detect. Another possibility is that the mutagenic compounds may not elute from the GC column and remain irreversibly adsorbed to the stationary phase.

Several fractions from the station 53 sediment traps were pooled to isolate more sample to produce a mutachromatogram. The Station 53 middle sediment trap extract N2, middle sediment trap extract N3 and bottom sediment trap extract N3 fractions were pooled to form a single extract. This combined fraction was separated using RP-HPLC and 30-second subfractions (note that one minute fractions had been collected for the station 50 top sediment trap N3 mutachromatogram) were collected and assayed using strain YG1024 without metabolic activation. The resulting mutachromatogram is shown

Figure 55. Station 50 top sediment trap extract fraction N3 mutachromatogram produced by assaying 1 minute subfractions from RP-HPLC with strain YG1024 (TA98-like) without S9. The mutagenic responses (B) are expressed as net revertants per plate and are the averages of duplicate measurements. The RP-HPLC UV absorption chromatogram (A) was plotted at 254 nm. Peak number 1 in the RP-HPLC chromatogram was identified as benzanthrone.

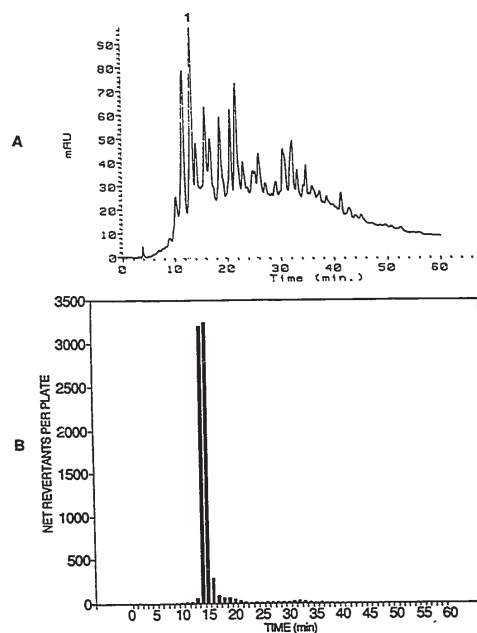
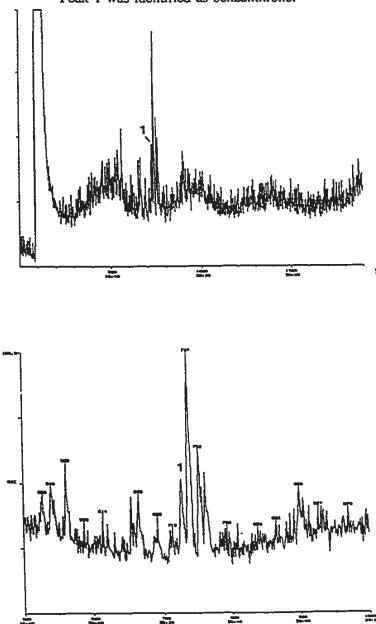


Figure 56. GC-MS total ion chromatogram resulting from the analysis of the pooled active subfractions (13 minutes to 15 minutes elution time from RP-HPLC) from the station 50 top sediment trap fraction N3 mutachromatogram. The analysis was performed on a Hewlett-Packard 5890 GC with a Finnigan quadrupole mass spectrometer equipped with an on-column injector as described in the experimental section. The chromatogram has been plotted on two different time scales to highlight the retention time range of interest. Peak 1 was identified as benzanthrone.

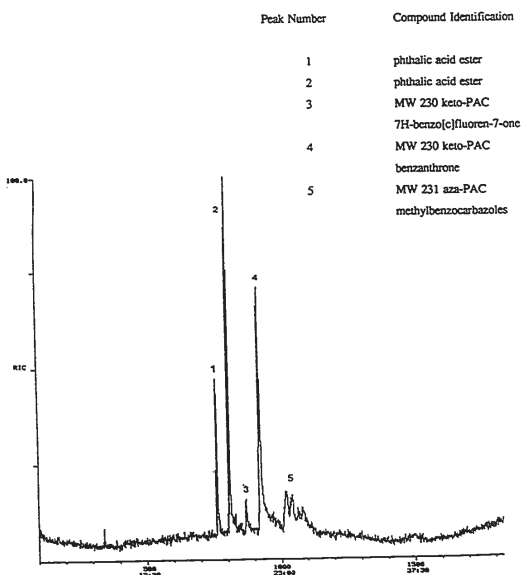


in Figure 57.

The mutagenic activity was eluted from the HPLC column in two 30-second subfractions. This similar result to the station 50 top sediment trap N3 mutachromatogram shows that the activity exhibited by some of the sediment trap N2 fractions was due to material that was mostly collected in fraction N3. It can thus be concluded that the mutagenic compound(s) eluted at an approximate elution time of 35 minutes on the NP-HPLC column. The 30-second subfraction exhibiting the highest activity was analysed using GC-MS (Figure 58). The GC-MS analysis again resulted in the determination of benzanthrone in the sample. A group of compounds of molecular weight 231 amu were observed in the total ion chromatograms of the most active subfractions and identified as methylbenzocarbazole isomers (Figure 59). Re-examination of the GC-MS total ion chromatogram of the mutagenic subfraction from the station 50 top sediment trap mutachromatogram revealed that the methylbenzocarbazoles were also present in that sample (Figure 60). Analysis by GC-MS of the 30-second subfractions collected before, during and after the elution of the mutagenic activity from the HPLC column showed that these compounds co-elute with the mutagenic activity (Figures 61 and 62). However, methylbenzocarbazoles are base-pair substitution type mutagens (TA100-active) and require oxidative metabolism to transform them into mutagens (60). Upon re-examination of the GC-MS data from the analysis of the Randle Reef sediment sample N2 and N3 fractions, it is apparent that the methylbenzocarbazole isomers were also present in this sample (Figure 63). This is further evidence that these compounds are not responsible for the observed mutagenic activity in the sediment trap fraction N3

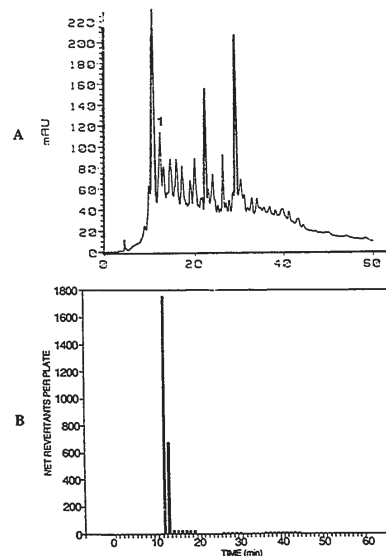
117

Figure 58. GC-MS total ion chromatogram resulting from the analysis of the most active 30 second subfraction from the station 53 sediment trap fraction N3 mutachromatogram. The analysis was performed using the Finnigan quadrupole GC-MS instrument with on-column injection (as described in the experimental section).



116

Figure 57. Mutachromatogram resulting from selected station 53 sediment trap N2 and N3 fractions that were pooled to form a single fraction. Thirty second subfractions were collected from RP-HPLC and assayed in duplicate with strain YG1024 without metabolic activation. The mutagenic responses are expressed in net revertants per plate and are the averages of duplicate measurements. The RP-HPLC UV absorption chromatogram (a) was plotted at 254 nm. Peak 1 in the RP-HPLC chromatogram was identified as benzanthrone.



118

Figure 59. Mass spectrum (A) of molecular weight 231 PAC (methylbenzocarbazoles) determined in the total ion chromatogram of the most active subfraction (12.5 minutes to 13 minutes) from the station 53 sediment trap fraction N3 mutachromatogram. All of the peaks of the MW 231 PAC were observed to exhibit this mass spectrum. The library mass spectrum of methylbenzo[c]carbazole is shown in figure (B). The m/z 149 and m/z 167 ions in the library spectrum are likely a result of phthalate contamination of the standard.

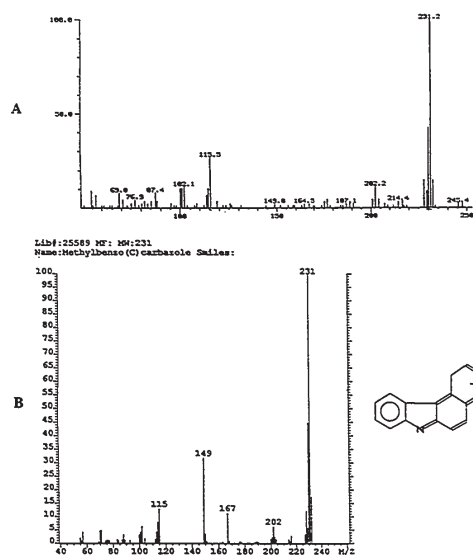


Figure 60. GC-MS total ion chromatogram (B) and m/z ion chromatogram (A) resulting from the analysis of the station 50 top sediment trap fraction N3 mutachromatogram pooled active subfraction (13 minutes to 15 minutes elution time on RP-HPLC). Peak identifications are as follows.

Peak Number	Compound Identification
1	benzanthrone
2	methylbenzocarbazoles (MW 231)

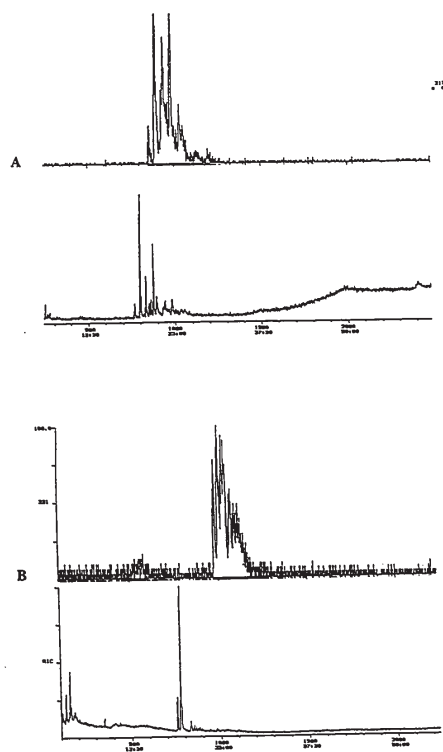
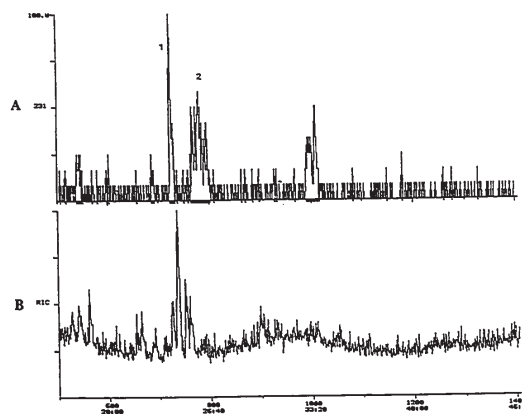
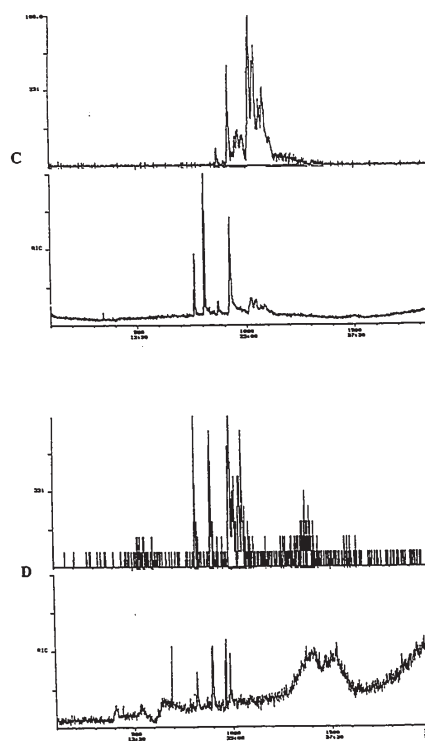


Figure 61. GC-MS chromatograms resulting from the analysis of the 30 second subfractions collected from the station 53 sediment trap fraction N3 mutachromatogram. These analyses illustrate the co-elution of the methyl benzocarbazoles of molecular weight 231 with the observed mutagenic activity. The figures show the total ion chromatograms at the bottom of the figures and selected individual ion chromatograms at the top of the figures.

- (A) 11.5 minutes to 12 minutes subfraction; 3 net revertants. The m/z 217 ion chromatogram shows the parent benzocarbazole isomers. The m/z 231 ion chromatogram did not show any significant ion abundances.
- (B) 12 minutes to 12.5 minutes subfraction; 662 net revertants.
- (C) 12.5 minutes to 13 minutes subfraction; 2780 net revertants.
- (D) 13 minutes to 13.5 minutes subfraction; 1024 net revertants.
- (E) 13.5 minutes to 14 minutes subfraction; 268 net revertants.



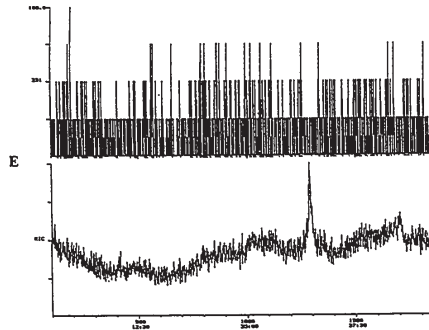


Figure 63. GC-MS  $m/z$  231 ion chromatogram resulting from the analysis of the Randle Reef sediment sample extract fraction N3 (see Figure for the total ion chromatogram). Peak number 1 is the M+1 ion of benzanthrene. The large  $m/z$  231 ion abundances are the methylbenzocarbazole isomers.

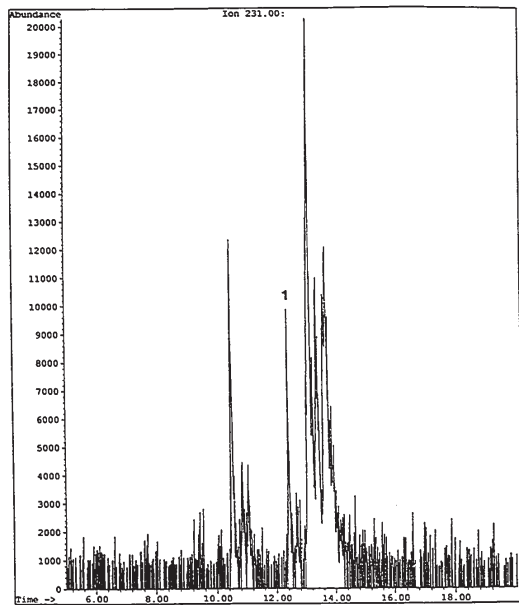
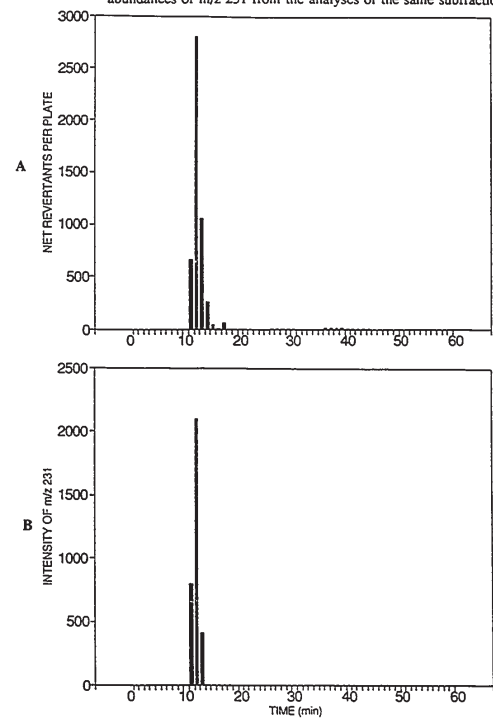


Figure 62. Plot of the mutagenic responses of subfractions from the station 53 sediment trap fraction N3 mutachromatogram (A) versus the relative ion abundances of  $m/z$  231 from the analyses of the same subfractions (B).

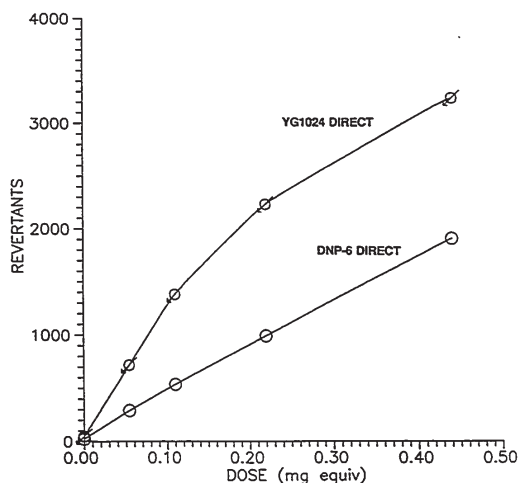


mutachromatograms. Each individual ion chromatogram over a range of  $m/z$  100 to  $m/z$  350 was reviewed but this procedure failed to identify any other compounds in the GC-MS TIC chromatograms of subfractions from either N3 mutachromatogram.

The active subfractions from the station 53 fraction N3 mutachromatogram were also analysed at the Canada Center for Inland Waters laboratories using a Hewlett-Packard 5890 GC equipped with a Varian Saturn ion trap mass spectrometer. This analysis failed to detect additional compounds that were likely to be responsible for the observed mutagenic activity, i.e., compounds that are probable direct-acting frameshift mutagens.

The elution time range for the mutagenic activity in the station 50 and station 53 sediment trap extracts fraction N3 mutachromatograms was very close to that of 1,8-dinitropyrene (1,8-DNP, 13.9 minute retention time on RP-HPLC, elutes in fraction N3 in NP-HPLC), a potent direct-acting frameshift mutagen. This compound was determined in Dofasco steel foundry sample extracts by McCalla *et al* (29) who employed a methodology similar to that described in the experimental section of this thesis. Although no evidence for the presence of 1,8-DNP was found in the GC-MS analyses of the active subfractions from the N3 mutachromatograms, it could not be discounted as a source of mutagenic activity as its presence at sub-detection limit levels (sub-ng) could still result in significant mutagenic activity. The pooled subfractions from the station 50 top sediment trap N3 mutachromatogram were assayed with strain DNP<sub>6</sub> (Figure 64). This strain is totally devoid of genes that code for acetyltransferase enzymes, which results in no response when 1,8-DNP is assayed. As seen in Figure 64, a strong positive response

Figure 64. Dose response curves exhibited by the pooled subfractions from the station 50 top sediment trap fraction N3 mutachromatogram when assayed with strain YG1024 and strain DNP<sub>6</sub> without S9.



acetonitrile. This elution time is quite close to that of benzanthrone, which was determined in the analyses of the active subfractions from the mutachromatograms.

### IL3.6 CCIW Air Sample

A total of approximately respirable air particulate samples collected at the Canada Center for Inland Waters over a period from September 1991 to April of 1993 were pooled to form a single sample. This sample was extracted using a Soxhlet apparatus and subjected to the clean-up and fractionation procedure. The bioassays of the A23/LH20 and A45 fractions with strain YG1024 (TA98-like) resulted in the detection of significant biological activity in both of these fractions (Figure 65). The determination of mutagenic activity in fraction A45 was in contrast to results from the analyses of the Randle Reef sediment sample and the sediment trap samples, but is in agreement with other studies that have concluded that polar compounds are responsible for up to half of the biological activity in air particulate material (20).

The A23/LH20 fraction was fractionated and the resulting N fractions were assayed with strain YG1024. Significant mutagenic activity was observed in fractions N2, N3, N456 and N7 (Figure 66). The mutagenicity values for these fractions are shown in Table 9. The fraction N2 activity was due to the presence of nitro-PAH, particularly 2-nitrofluoranthene which has been quantified in extracts of Hamilton air particulate (61). The majority of the activity in fraction N456 may also be the result of the presence a single compound, 2-nitrobenzopyranone (61). The analytical chemistry and bioassay

is still exhibited by the subfraction when assayed with DNP<sub>6</sub>. The bioassay approach was used in this case because of the rapidity and selectivity of the technique and the lowest detectable quantity of 1,8-DNP (sub-nanogram) in the assay was much lower than that of the detection limits for this compound using GC-MS. The positive responses observed in the sediment trap N3 fractions when assayed with strain YG1024 with S9 added (Table 7 and Table 8) is further evidence that 1,8-DNP is not present as S9 significantly reduces response from 1,8-DNP.

### IL3.5.1 Summary of Sediment Trap N3 Mutachromatogram Data

A complete summary of the analytical data from the analysis of the station 50 top and station 53 sediment traps fraction N3 mutachromatograms is given in Appendix 2. Although no compounds were identified that were likely to be responsible for the observed mutagenic activity, information about the compound(s) in question was obtained. The compound(s) eluted from the normal phase PAC semi-preparative HPLC column at approximately 30 minutes. An elution time of 30 minutes is the boundary between the collection of fractions N2 and N3. This accounts for some of the N2 fractions of the sediment trap samples exhibiting high mutagenic activity. The compound(s) is active in the YG1024 (TA98-like) and DNP<sub>6</sub> strains, both with and without metabolic activation. This excludes 1,8-DNP as a possible candidate. The compound(s) co-eluted with methylbenzocarbazole isomers in the 13 minute to 15 minute retention time range in RP-HPLC. This corresponds to a mobile phase composition of approximately 70-71%

Figure 65. Dose response curves exhibited by fractions A23/LH20 and A45 of the CCIW air particulate extract when assayed with strain YG1024 (TA98-like).

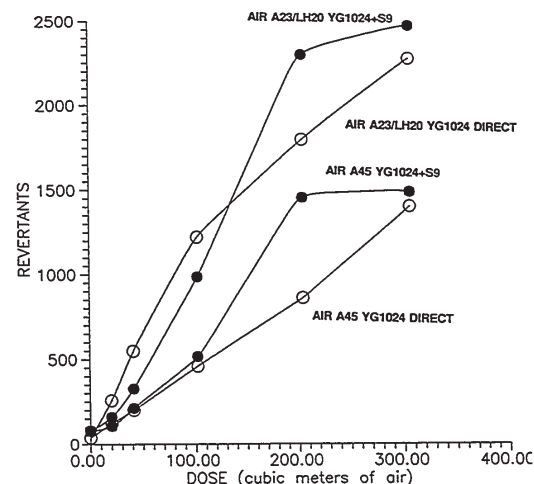
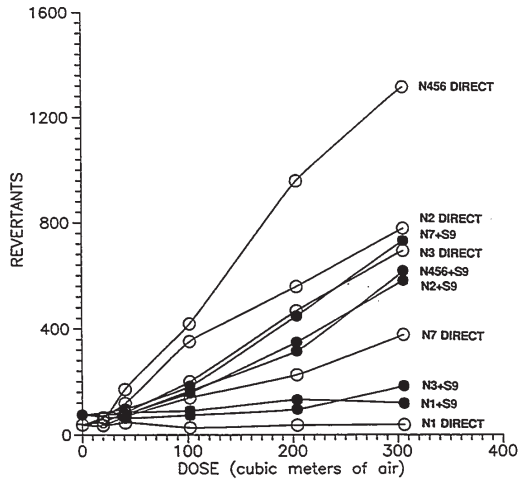


Figure 66. Dose response curves exhibited by N fractions of the CCIW air particulate extract when assayed with strain YG1024 (TA98-like).



data from the corresponding fractions from the Randle Reef and sediment trap extracts failed to provide any evidence for the presence of these compounds.

Comparison of mutachromatogram data from 1988 Hamilton air extracts fraction N3 and the sediment traps fraction N3 reveals dramatic similarities in the profiles (Figure 67). These mutachromatograms all show the mutagenic activity to be contained in a narrowly defined elution time ranging from 13 minutes to 15 minutes on RP-HPLC. This offers the possibility of a common mutagenic compound being present in both sample matrices.

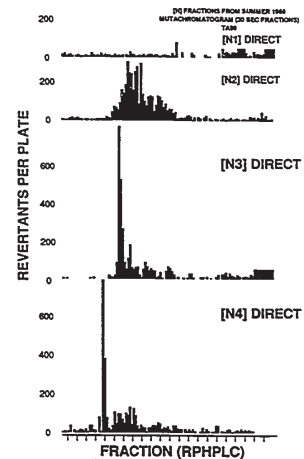
**II.3.7 Polycyclic Aromatic Hydrocarbon Content and Genotoxicity of Extracts of Zebra Mussels Sampled from Hamilton Harbour**

This chapter describes a study of PAH contamination and genotoxicity of extracts of tissues of Zebra mussels sampled from Hamilton Harbour. This ancillary data presents a unique perspective of the effects of chemical contamination in the harbour on living members of the ecosystem. An introduction to mussels as biological indicators is presented as well as a briefing on one of Hamilton Harbours newest inhabitants, *Dreissina Polymorpha* (Zebra mussel). An adaptation of the extraction procedure for the Zebra mussels is described and the results of the PAH determinations and the bioassays are discussed.

Table 9. Mutagenic activity of organic extract fractions of air particulate material sampled from the Canda Center for Inland Waters site. The extracts were assayed with strain YG1024. The values are expressed in revertants per cubic meter of air.

Fraction	Direct	+S9
A23/LH20	11.6 ± 0.35	8.66 ± 0.91
A45	4.38 ± 0.13	6.88 ± 0.74
N1	NR	NR
N2	2.49 ± 0.12	1.71 ± 0.23
N3	2.22 ± 0.21	0.35 ± 0.05
N456	4.37 ± 0.32	1.77 ± 0.17
N7	1.17 ± 0.09	2.21 ± 0.11

Figure 67. Mutachromatograms of N fractions of Hamilton air particulate extracts. Subfractions collected from RP-HPLC were assayed with strain YG1024 (TA98-like). The samples were collected by Bryant *et al* in 1988 (20).



### IL3.7.1 Mussels as Indicators of Pollution in Aquatic Environments

The use of mussels as bioindicators of pollution in aquatic environments has been described previously (62-64). Both freshwater and marine mussels have been shown to display multi-xenobiotic resistance and to accumulate non-polar organic contaminants in their tissues (65,66). This ability to bio-accumulate organic compounds can result in tissue concentrations of these contaminants that exceed those found in the surrounding waters and sediments. Mussels feed by filtering large volumes of water and their sedentary nature results in the sampling of the contaminants in a specific area. Mussels can also provide time-integrated data of contaminant levels in particle or water fluxes over long periods of time. Water sampling by either grab sampling or centrifugation permits the evaluation of contaminant concentrations in that sample matrix at that specific time. The sampling of suspended sediments using apparatus such as sediment traps requires sampling times which may vary from weeks to a year and the infrastructure requirements can be prohibitive. In contrast, the analysis of contaminant levels in mussel tissue can provide time-integrated samples for the bioconcentration of xenobiotics by a living organism in the environment.

### IL3.7.2 Zebra Mussels in the Great Lakes and Hamilton Harbour

In recent years the Great Lakes have been invaded by the exotic freshwater mussel Dreissina polymorpha (Zebra mussel) which is native to Europe. Since its initial

137

seconds each. The sample was then centrifuged at 4000 rpm and the methylene chloride was decanted and reduced in volume by rotary evaporation under reduced pressure. The extracts were then subjected to the alumina/Sephadex LH20 clean-up procedure.

The homogenate of the Zebra mussels sampled from station 7 was extracted a second time using ultrasonication. The solvent extracts from the ultrasonic extraction procedures were combined, reduced in volume, and subjected to the alumina clean-up procedure.

The A23/LH20 fractions of the mussel extracts were assayed using the two O-acetyltransferase Salmonella typhimurium bacterial strains; strain YG1024 (TA98-like) and strain YG1029 (TA100-like) using the same procedure that was employed for the sediment and sediment trap sample extracts.

### IL3.7.4 Sampling Sites

Seven Zebra mussel sampling sites were chosen in Hamilton Harbour. Mussels were sampled in late November from the following locations (Figure 68): Station 1. Floating tire booms at a marina on the north shore of the harbour. Stations 2, 3, 4 and 5. Navigational buoys at selected sites in the Windermere arm of the harbour. Station 6. A buoy in an area east of Randle Reef close to the site where the Randle Reef sediment was sampled. Station 7. A bio-box at the East Side Filtration Plant at the Stelco Co. steel plant Hilton Works on the south shore of the harbour. The Zebra mussels at this site had been continuously exposed to recirculated bay water from the harbour.

detection in 1990, this mussel has become firmly established in Hamilton Harbour. The mussel's high spawning rate, great mobility, and high population densities (67-69) have resulted in an immediate impact on the Harbour and its ecosystem. Research is currently underway to develop methods for the control of the Zebra mussel and to project its future distribution in North American waterways (67,70,71). In some areas, the Zebra mussel population has risen to a level where it has become a major food source for fish and wildlife; this new food source has resulted in the disruption of bird migration cycles and exposure of fish and wildlife to the contaminants accumulated in mussel tissue.

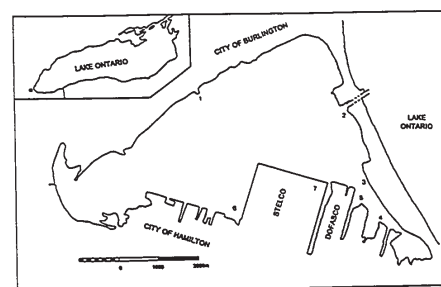
### IL3.7.3 Methodology

The Zebra mussels (250 g) were processed immediately after collection. The mussels were drained of excess water and then homogenized in a Waring blender. The homogenate was centrifuged at 10,000 rpm for 15 min and the supernatant decanted and discarded.

The extraction procedure was modified to include the use of a tissue homogenizer. This protocol was based on a National Oceanographic and Atmospheric Administration standard procedure for the extraction of toxic organic compounds from marine mussels (72). Aliquots of homogenate (125 g) were suspended in centrifuge bottles by the addition of 50 mL of HPLC grade methylene chloride and were extracted using a Janke and Kunkel Ultraturax T50 tissue homogenizer with an S50 head (Terochem Inc., Toronto, Ontario). The homogenizer was operated for several cycles at 100 rpm for 45

138

Figure 68. Map of Hamilton Harbour showing the sites at which Zebra mussels were sampled.





The homogenate from the mussels sampled at station 7 was further extracted sequentially with methylene chloride and methanol using ultrasonication in an attempt to remove additional PAH. This secondary extraction procedure yielded on average an additional 18% of PAH from the mussel homogenate. These results indicated that extraction using the tissue homogenizer alone is adequate for preparing extracts for preliminary determinations of PAH in mussel tissues and for bioassays. The mussels sampled at the other sites were extracted with methylene chloride using the tissue homogenizer alone.

### II.3.7.5 Determination of Polycyclic Aromatic Hydrocarbons

Figure 69 is a GC-MS selected ion monitoring (SIM) chromatogram from the analysis of the PAH-containing fraction (fraction A23/LH20) from the Zebra mussels sampled at station 4. The chromatogram is relatively free from interfering compounds which simplifies the accurate quantitation of the PAH. Table 10 shows the homocyclic PAH determined in the mussel extracts from each site, and the individual concentrations expressed in ng per gram (ppb) of wet mussel homogenate. The total PAH concentrations, expressed as the summation of the individual PAH concentrations, ranged from 0.34  $\mu\text{g/g}$  for the mussels sampled at station 1 to 10.0  $\mu\text{g/g}$  for the mussels sampled at station 6.

The profiles of the GC-MS chromatograms were very similar to those of the extracts of material collected in sediment traps in Hamilton Harbour. The sediment traps

Figure 69. GC-MSD selected ion monitoring chromatogram of fraction A23/LH20 of the extract of the Zebra mussels sampled from site 4. The sample was processed using the described sample preparation scheme. The peaks are numbered to correspond to those PAH compounds listed in Table 10. The + identifies the internal standard peak of 9,10-dimethylanthracene.

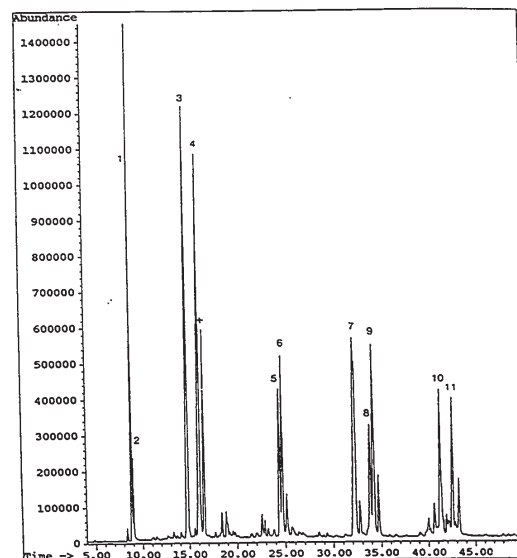


Table 10. Concentrations of homocyclic PAH determined in extracts of Zebra mussels sampled from Hamilton Harbour. Concentrations are expressed in ng/g of mussel homogenate. Quantitation was achieved using an internal standard in conjunction with the described sample clean-up and analysis procedure.

	Station 1	Station 2	Station 3	Station 4	Station 5	Station 6	Station 7
1. Phenanthrene	81	22	66	774	5	472	30
2. Anthracene	11	6	19	165	3	115	16
3. Fluoranthene	49	143	237	1318	65	1399	109
4. Pyrene	44	136	237	1002	74	1312	144
5. Benzo[a]anthracene	32	79	160	486	50	747	88
6. Chrysene	48	93	172	501	56	753	132
7. Benzofluoranthenes (UNR)	38	170	404	1178	134	1957	162
8. Benzo[e]pyrene	14	72	169	467	52	686	76
9. Benzo[a]pyrene	27	82	227	701	64	1076	54
10. Indeno[1,2,3-cd]pyrene	4	35	181	613	37	802	7
11. Benzo[ghi]perylene	3	32	131	466	31	720	8
TOTAL (ng/g)	342	870	2003	7671	571	10039	825

UNR denotes peaks unresolved by GC-MS

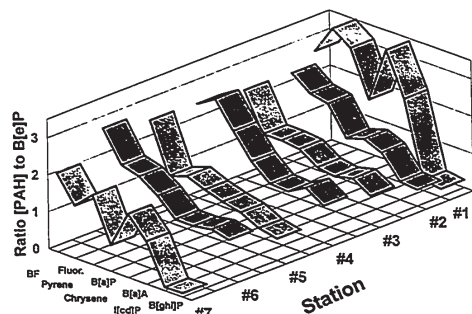
provide a parallel to the filter feeding mechanism by which Zebra mussels are exposed to PAH contamination. The resuspension of PAH-contaminated benthic sediments and industrial discharges result in total PAH concentrations in suspended sediments in some areas of the harbour that are comparable to those of the bottom sediments. Mayer and Nagy (73) have determined total PAH concentrations in suspended sediments as high as 106  $\mu\text{g/g}$  at a site near station 3 and we have quantified total PAH concentrations of 90  $\mu\text{g/g}$  in this same area. High concentrations of PAH have also been determined in the harbour water (74).

The GC-MS chromatograms of the extracts of mussels from all sites were similar in profile. This similarity in profile is illustrated in Figure 70 which shows the relative concentrations of the individual PAH normalized to the concentration of benzo[e]pyrene in each sample. The highest PAH levels determined in the extracts were found in mussels sampled from station 6 (near Randle Reef).

### II.3.7.6 Genotoxicity of Mussel Extracts

Mussel extracts from stations 2,3,4,5 and 6 were subjected to bioassay with *Salmonella* strain YG1024 (TA98-like) and strain YG1029 (TA100-like), both with and without the addition of metabolic activation in the form of a rat liver supernatant (S9). A range of seven concentrations of each A23/LH20 fraction was assayed in duplicate. All of the extracts assayed exhibited positive responses in both strains in the presence of S9 (Figure 71). No response was detected at the highest doses in the absence of S9.

Figure 70. Graph showing the relative concentrations of PAH in extracts of mussels sampled from each site. The concentrations of the individual PAH were normalized to the concentration of benzo[e]pyrene (given the value of 1) in each of the extracts.



The mutagenic potencies of the extracts are expressed in revertants per gram of wet mussels and were obtained from the linear regression of the linear portions of the dose response curves (Table 11). The requirement for oxidative metabolism to manifest a positive response and the non-linear nature of the dose response curves at the higher doses is reminiscent of the Randle Reef sediment sample extract.

The mussel extract from station 2 showed significantly higher activity in strain YG1024 (TA98-like) with S9 than did the extracts from other sites but exhibited relatively low levels of PAH contamination. These results suggest the presence of a mutagenic compound(s) not present in the extracts of mussels sampled at the other sites or the presence of a compound(s) at higher concentrations than in mussels sampled from the other sites. There appears to be no correlation between the between the magnitude of the observed mutagenic responses and the PAH concentrations in extracts of Zebra mussels sampled from any of the sites. The presence of mutagenic compounds other than PAH in these complex extracts may account for this poor correlation.

**IL3.7.7 Summary**

The tissue homogenizer extraction coupled with the alumina/Sephadex LH20 clean-up methodology afforded extracts of Zebra mussels that were free of interfering compounds and allowed for the accurate quantitation of PAH. All of the mussel extracts analyzed in the study contained significant levels of PAH contamination and all of the extracts that were assayed exhibited positive mutagenic responses with the addition of

Figure 71. Dose response curves exhibited by the PAH-containing fractions (A23/LH20) of selected Zebra mussel extracts when assayed with *Salmonella typhimurium* strains with the addition of 4% rat liver S9. The doses are expressed in milligrams of mussels extracted.

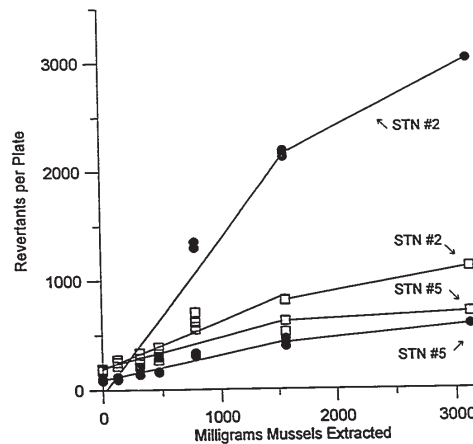


Table 11. Mutagenic potencies of A23/LH20 fractions of Zebra mussel extracts expressed in revertants per gram of mussels extracted. ND denotes no activity detected at the highest dose. The values were determined from the slopes of the linear portions of the dose response curves.

Station	YG1024 (TA98-like)		YG1029 (TA100-like)	
	Direct	+S9	Direct	+S9
Station 2	ND	1792±163	ND	259±18
Station 3	ND	202±22	ND	117±27
Station 4	ND	179±30	ND	46±18
Station 5	ND	170±18	ND	165±35
Station 6	12±12	421±45	ND	330±67

oxidative metabolism. These results show that Zebra mussels in Hamilton Harbour are accumulating genotoxic contaminants and could potentially be used as bioindicators of contamination.

mutachromatogram. These subfractions each contained several compounds and the observed positive responses likely represented the sum of their individual mutagenic potencies. The surprising complexity of these subfractions made positive identification of individual compounds responsible for the observed biological activity very difficult. Future work should employ methodologies that decrease the complexity of chromatographic subfractions collected for mutachromatograms. An initial separation of fraction A23/LH20 based on the molecular weight of PAH could serve this purpose. Molecular weight classes of PAH that are biologically active would be identified and the analysis of mutachromatogram subfractions would be more facile as fewer compound would be present. The mutachromatograms of these fractions should be generated using a 5 micron packing size analytical column as opposed to the 10 micron dual column procedure currently used. The resulting increase in separation efficiency should aid in identifying individual mutagens in these types of samples.

The analyses of the sample extracts by chromatographic methods and the genotoxicity data obtained using strain YG1025 (TA100-like strain) indicated that PAH are a significant source of chemical and genotoxic contamination in Hamilton Harbour. However, the dramatic differences in the mutagenic profiles exhibited by the Randle Reef sediment sample and the sediment trap samples shows that the resuspension and transport of coal tar contaminated sediment is not the only major contribution to the genotoxic burden on the harbour. The station 50 and station 53 sediment trap sample extracts displayed high direct-acting mutagenic responses in some N2 fractions, and particularly in the N3 fractions. The active compounds or compound classes present in these fractions

### III. FUTURE WORK AND CONCLUSIONS

The clean-up and fractionation methodology described in the experimental section was shown to be effective in quantitatively separating the components of complex mixtures into compound classes. The method of ultrasonication for the extraction of organic material from sediments and from an urban dust standard reference material was efficient, based upon comparison with extraction using the Soxhlet method and the comparison of quantified PAH levels with the certified values. The statistical comparisons of the experimental means and standard deviations of the individual PAH peak areas in sediment extracts prepared using both extraction methods supported the hypothesis that the two methods were equally efficient. Ultrasonic extraction was found to be facile, efficient, reproducible, fast and applicable to a variety of sample matrices.

The chemical analysis of the Randle Reef sediment extract revealed that the sample was dominated by low to intermediate molecular weight homocyclic PAH. The bioassays indicated the presence of base-pair substitution type mutagens requiring metabolic transformation to mutagenic by-products to obtain a positive dose response. These data show that PAH were the principal contributors to both the chemical and biological profiles of the Randle Reef sediment.

The majority of the mutagenic activity displayed by the Randle Reef sediment crude extract was contained in the PAH-containing fractions (fractions N1 and N2). Higher molecular weight PAH of masses of 252, 276, 278 and 302 daltons were identified by GC-MS in the most biologically active subfractions of the fraction N1

are frameshift type mutagens that do not require oxidative metabolism to manifest their genotoxic response.

The bulk of the direct-acting mutagenic activity observed in the sediment trap sample extracts fraction N3 was confined to a very narrow elution time range in RP-HPLC. However, detailed chemical analyses of these mutagenic fractions failed to identify compound or compound classes that would likely have been responsible for the observed activity. Potent mutagens need only be present at the sub-nanogram level to result in high mutagenic responses of sample extracts. These levels of contamination are difficult to determine in complex mixtures, particularly when employing mass spectrometric detection in full scan mode.

Figure 68 shows a map of Hamilton Harbour that presents a brief overview of the chemical and biological characteristics of the sample extract from each site sampled in the harbour. The histograms show the relative total PAH content, direct-acting mutagenic activity observed in strain YG1024 (TA98-like), and the mutagenic activity observed in strain YG1025 (TA100-like) with the addition of metabolic activation (S9). The histogram bars were normalized to the highest level observed in any sample extract e.g. the total PAH content (sum of seven individual PAH concentrations) determined in the Randle Reef sediment sample extract (308 µg/g) was given the value of 100 and the PAH concentrations at the other sample sites were normalized to this value. These histograms emphasize the high PAH levels and the corresponding high mutagenic responses in strain YG1025 with S9 exhibited by the Randle Reef sediment extract; these data are in contrast to the station 50 and station 53 sediment trap extracts which exhibited much lower PAH

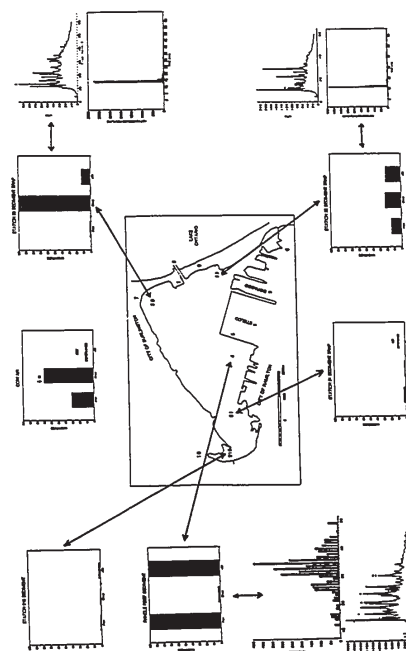
Figure 72. Map of Hamilton Harbour with histograms illustrating PAH levels and mutagenic activities exhibited by samples from each site. The numbers on the map correspond to those identified in the legend from Figure 1. The bars on the histograms represent:

**PAH** The level of PAH contamination, defined as the sum of the concentrations of fluoranthene, pyrene, benzo[a]anthracene, chrysene, benzo[a]pyrene, indeno[1,2,3-cd]pyrene and benzo[ghi]perylene. The levels at all sites were normalized to that of the Randle Reef sediment sample (308 ug/g). The PAH levels in the station 51 sediment trap extracts were estimated from RP-HPLC analysis (data not shown). The PAH levels in the CCIW air extract were calculated from GC-MS analysis of fraction A23/LH20

**Direct** The direct-acting mutagenic activity in fraction A23/LH20 in strain YG1024 (TA98-like) was normalized to the station 50 sediment traps (average of 9888 rev/mg equivalent for the top and bottom traps). The CCIW air extract is shown at 70 times less than its true value. The station 53 sediment trap values are the summation of the activities observed in the N fractions as the minimal activity observed in fraction A23/LH20 did not reflect the total activity in the extract.

**+S9** The mutagenic activity in fraction A23/LH20 in strain YG1025 with S9 (TA100-like) was normalized to the Randle Reef sediment sample (6500 rev/mg equivalent).

The values for the sediment trap extracts were averaged over the number traps at the site i.e. 3 depths for station 53 and 2 depths for the station 50 and station 51 sites. Also shown are the mutachromatograms from the most active fractions of the station 50 and station 53 sediment traps and the Randle Reef sediment sample.



and YG1025 with S9 response levels but much higher direct-acting responses in the YG1024 strain (TA98-like). The station 50 sediment trap and station 910 sediment samples from the western end of the harbour are characterized by low PAH levels and low mutagenic activities. The CCIW air particulate extract exhibited direct-acting mutagenic activity in strain YG1024 that was approximately 70 times higher than that observed in the station 50 sediment traps when expressed in revertants per milligram equivalent of extracted material instead of revertants per cubic meter of air. A comparison of the fraction N3 mutachromatograms of the station 50 and station 53 sediment traps and an air particulate material suggests the presence of a mutagenic compound common to all of these samples.

The material collected in the sediment traps must also contribute to the composition of the surficial sediments in Hamilton Harbour. Future experimental work should focus on the extraction and fractionation of large weights of surficial sediments sampled from sediment trap sites within the harbour. This might be a more cost and time-effective approach than to pursue instrumental methods that have lower theoretical detection limits. Large scale centrifugation (e.g. Westphalia centrifugation) could also result in the sampling of large weights of suspended solids from the water column. These approaches could result in the isolation of significant quantities of the unknown compound(s) responsible for the mutagenic activity observed in the sediment trap extracts fraction N3. This would make the identification of these compounds by HPLC or GC-MS more facile and allow the use of definitive identification techniques such as nuclear magnetic resonance spectroscopy and/or high resolution mass spectrometry.

The sediment trap extracts fraction N3 mutachromatograms showed a dramatic similarity to fraction N3 mutachromatograms of extracts of air particulate material prepared by Bryant *et al* (20). The potential presence of a contaminant that is common to both the air particulate material and the material isolated from the sediment traps should be explored. The infrastructure requirements for the sampling of air particulate are considerably less prohibitive than those required for the sampling of suspended material in the water column using sediment traps. Similar to the approach that would be used for surficial sediments, a large composite sample of air filters could be extracted, cleaned up and fractionated resulting in the potential isolation of a large weight of material from the fraction N3 mutachromatogram. An identification of this component(s) would not only result in the determination of a potent environmental mutagen, but also establish a potential link between genotoxic contamination in Hamilton Harbour and the deposition of air particulate material.

## IV. MATERIALS AND METHODS

### IV.1 Samples

Standard Reference Material 1649, urban dust/organics, was obtained from the National Institute of Standards and Technology (NIST, Washington, DC). The sediment and sediment trap samples used in the study were kindly provided by Drs. Mike Fox, Murray Charlton, Tom Murphy, and Mr. Wynn Booth of the National Water Research Institute, Canada Center for Inland Waters, Burlington, Ontario.

### IV.2 Gases

High purity helium, nitrogen, argon, air, and hydrogen were obtained from Canadian Liquid Air Ltd. (Toronto, Ontario).

### IV.3 Solvents

Solvents used in the study were HPLC grade or were distilled in glass in the laboratory. Methylene chloride and acetonitrile (HPLC grade) were obtained from Fisher Scientific (Fairlawn, New Jersey). Hexane (HPLC grade) was obtained from BDH Inc. (Toronto, Ontario). Benzene, chloroform and ethanol (reagent grade, Caledon

157

### IV.5 Extraction Methods

#### IV.5.1 Soxhlet Extraction

Soxhlet thimbles were pre-rinsed in methylene chloride. Air filters were cut into 1 cm<sup>2</sup> squares and placed in a Soxhlet thimble. The dried sample was extracted with a Soxhlet apparatus using 350 mL of methylene chloride for 24 hrs, followed by extraction with 350 mL of methanol for 24 hrs. Cycle times were approximately 12 minutes for methylene chloride and 20 minutes for methanol. The resulting solvent extracts were pooled and reduced in volume by rotary evaporation. The extract was then made up to 50.00 mL volumetrically with methylene chloride and a 1 mL aliquot removed to determine the percentage of extractable organic material. The aliquots were dispensed into pre-weighed aluminum boats, evaporated to dryness under nitrogen or argon, and then immediately re-weighed. The procedure was repeated until constant weight was achieved.

#### IV.5.2 Ultrasonic Extraction

The dried sample was suspended in 50 mL of methylene chloride in a glass beaker. The probe tip was placed approximately 1 cm from the bottom of the beaker to maximize cavitation. Eight consecutive pulses, each of 15 seconds duration, were applied at full power. One minute intervals were maintained between sonication cycles. The beaker was immersed in an ice bath to prevent solvent heating. The resulting suspension

Laboratories, Georgetown, Ontario), acetone (reagent grade, J.T. Baker Inc., Phillipsburg, New Jersey) and toluene (reagent grade, Fisher Scientific) were distilled in glass in the laboratory before use. A Milli-Q purification system (Waters Associates, Millford, Massachusetts) was used to further purify distilled water.

### IV.4 Instrumentation

Reversed and normal phase HPLC were performed on a Hewlett-Packard Model 1090 liquid chromatograph with a built-in diode array detector, Chemstation data system (Hewlett Packard Co., Mississauga, Ontario), and a Kratos Model FS950 fluorometric detector (Kratos Inc., Westwood, New Jersey). Gas chromatography-mass spectrometry (GC-MS) experiments were performed using the following instruments: 1. splitless injection on a Hewlett-Packard Model 5890 Series II gas chromatograph equipped with a Hewlett-Packard Model 5971A mass selective detector 2. On-column injection on a Hewlett-Packard 5890 gas chromatograph interfaced with a Finnigan Mat Model 4023 quadrupole mass spectrometer with an IncoS MSDS data system (Finnigan Corp., San Jose, CA). Gas chromatography with flame ionization detection was performed with a Hewlett-Packard Model 5890 Series I gas chromatograph equipped with an on-column injector. A Beckman Model 110A HPLC pump equipped with a Beckman Model 153 ultraviolet absorption detector (Beckman Instruments, Fullerton, California) was used in the Sephadex LH20 procedure.

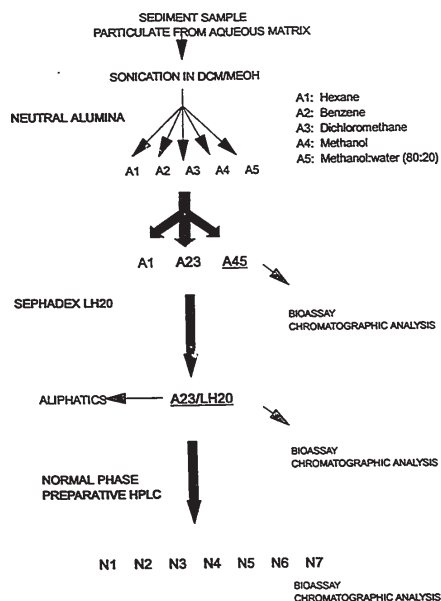
158

was filtered through a Whatman #1 filter paper using a Buchner funnel and a vacuum aspirator. The filter paper containing the sediment was then re-extracted using 50 mL of fresh methylene chloride. The procedure was repeated a third time with 50 mL of methanol. The solvent extracts were then pooled to form a single extract. This extract was reduced in volume by rotary evaporation, made up to 50.00 mL volumetrically and a 1 mL aliquot removed for the determination of the percentage of extractable organic material.

### IV.6 Alumina/Sephadex LH20 Clean-up

The alumina clean-up procedure is represented in Figure 68. The organics were adsorbed to alumina (3 g) by solvent evaporation under reduced pressure. The sample, adsorbed to alumina, was then applied to the top of fresh alumina (6 g) contained in a glass column (1 cm X 30 cm with glass wool at the bottom). Organic components were eluted using solvents of increasing polarity. Hexane (60 mL), added to the column to elute aliphatics, afforded a fraction designated as fraction A1. The polycyclic aromatic compounds (PAC) were eluted by the sequential addition of benzene (50 mL, fraction A2) and methylene chloride/ethanol (70 mL, 99:1 v/v, fraction A3), which were combined to afford fraction A23. Polar PAC were eluted from the column with methanol (50 mL, fraction A4) and methanol/water (50 mL, 3:1 v/v, fraction A5), which were combined to afford fraction A45. The solvents were allowed to pass through the column by gravity. Fraction A23 was subjected to an additional chromatographic step using Sephadex LH20

Figure 73. Schematic of the sample clean-up and fractionation scheme.



Clifton, New Jersey) using the described gradient elution program. Eight fractions, designated as N (normal phase) fractions (N0, N1,...up to N7) were collected. A 100 microliter sample loop and a mobile phase flow rate of 4.2 mL/min was used with the following linear gradient elution program (elapsed time, composition of mobile phase): initial, 100% hexane; 5 min, 100% hexane; 10 min, 99% hexane and 1% methylene chloride; 15 min, 95% hexane and 5% methylene chloride; 40 min, 100% methylene chloride; 50 min, 100% methylene chloride; 60 min, 100% ethanol; 65 min, 100% ethanol.

The N fractions were collected during the following time intervals: N0, 0-7.5 min; N1, 7.5-24 min; N2, 25-30 min; N3, 30-35 min; N4, 35-40 min; N5, 40-45 min; N6, 45-50 min; N7, 50-65 min. The low to intermediate molecular weight PAH eluted between 7.5 min and 24 min (fraction N1). For some samples, the collection time for fraction N1 was extended until 25 minutes to allow all of the PAH, including the very high molecular weight compounds (greater than 278 amu) to be collected in fraction N1. In some cases, the N4, N5 and N6 fractions were pooled to form a single fraction designated as fraction N456.

#### IV.8 Analytical High Performance Liquid Chromatography, Gas Chromatography, and Gas Chromatography-Mass Spectrometry

Reversed phase HPLC was performed using two 10 micron 25 cm X 4.6 mm i.d. Vydac Reverse Phase analytical columns linked in series (Separations Group, Hesperia,

gel. Fraction A23 was evaporated to dryness using rotary evaporation under reduced pressure followed by a nitrogen blow-down step. The residue was reconstituted in 1 mL of the mobile phase (hexane/methanol/methylene chloride (6:4:3 v/v)) and injected onto a 4 cm X 30 cm glass column packed with Sephadex LH20 gel (flow rate 3 mL/min) to remove the remaining aliphatic material from the sample. Material eluting prior to naphthalene was rejected as aliphatic material. This was confirmed by GC-MS analysis. The Sephadex LH20 procedure afforded an aromatic PAC fraction designated as A23/LH20.

The weights of the alumina and volumes of solvent used in the open-column chromatography clean-up of the Randle Reef sediment sample were twice those described herein because of the extreme levels of contamination exhibited by this sample.

#### IV.7 Normal Phase Semi-Preparative HPLC

Components of the aromatic A23/LH20 fraction were further separated into compound classes using normal phase semi-preparative HPLC (Figure 68). The HPLC operating conditions were as follows; diode array UV absorption at a wavelength range from 211 nm to 400 nm; fluorescence excitation at 365 nm with emission cutoff filter of 418 nm; column temperature, 40 °C.

Normal phase HPLC was performed using an amino precolumn (Brownlee Labs, Santa Clara, California, 1.5 cm X 4.6 mm i.d.) and a 10 micron 25 cm X 9.4 mm i.d. Whatman Partisil M9 PAC semi-preparative normal phase HPLC column (Whatman,

CA). The HPLC operating conditions were as follows: diode array UV absorption at a wavelength range from 211 nm to 400 nm; fluorescence excitation at 365 nm with emission cutoff filter of 418 nm; column temperature, 40 °C. Compound identification was based on retention time comparison with standards and UV absorption spectra (211 nm to 400 nm) comparison with library spectra. A mobile phase flow rate of 1.0 mL/min was used with the following linear gradient elution program (elapsed time, composition of mobile phase): initial, 60% acetonitrile and 40% water; 30 minutes, 100% acetonitrile; 60 minutes, 100% acetonitrile. The RP-HPLC analysis procedure was also used to collect individual subfractions of selected N fractions for bioassay using *Salmonella typhimurium*.

Samples requiring GC-MS analysis were blown to dryness under nitrogen or argon and reconstituted in toluene or acetone. The GC-MS operating conditions were as follows: mass spectrometer transfer line temperature, 300 °C; 1 µl injection volume; helium carrier gas flow rate, 20 cm/sec; injector temperature, 300 °C. The following temperature program was used for GC-MS analysis of fraction A23/LH20: 50°C to 160°C at 20°C/min; 160°C to 290°C at 3°C/min; final time at 290°C, 10 min. The column was a 25 m X 0.25 mm i.d. DB-5 with a 0.25 micron stationary phase film coating (J and W Scientific, Folsom, CA). The following temperature program was used for GC-MS analysis of N1 subfractions: 80 °C to 200 °C at 20 °C/min; 200 °C to 290 °C at 3 °C/min; final time at 290 °C, 5 min. The column was a 12 m X 0.2 mm i.d. HP-1 with a 0.33 micron stationary phase film coating (Hewlett Packard Co., Mississauga, Ontario). Compound identification was based upon retention index comparisons and mass spectral library comparison. An internal standard method (9,10-dimethylanthracene) was used for

The GC-FID operating conditions were as follows: detector temperature, 300 °C; 1 µl on-column injection; helium carrier gas flow rate, 25 cm/sec; injector temperature, 250 °C. The following temperature program was used: 100 °C to 150 °C at 10 °C/min; 150 °C to 290 °C at 3 °C/min; final time at 290 °C, 10 min. Analysis was performed using a 30 m X 0.25 mm i.d. DB-5 column with a 0.25 micron stationary phase film coating (J and W Scientific, Folsom, California). Compound identification was based upon retention time comparison with standards and was confirmed by GC-MS. An internal standard method (2-methylanthracene or 9,10-dimethylanthracene) was used for quantitation. Relative weight responses were calculated for each of the analytes and the linearity of detector response was confirmed over three orders of magnitude.

#### IV.11 Bioassays.

The protocol used for the bioassays was adapted from that of Maron and Ames (75). Bacteria were grown in Oxoid Nutrient Broth #2 (15 mL) with ampicillin (50 µg/mL) and tetracycline (6.25 µg/mL) added in a shaker bath for 9 hrs at 37°C. Extracts were dissolved in 50 µL DMSO and were assayed in duplicate, both with and without metabolic activation (4% Aroclor 1254 induced rat liver S9)(75). During the test procedure, 2 mL of molten top agar (40 °C) was added to the test mixture (in 50 µL DMSO); 100 µL of the *Salmonella* bacteria was then added and the resulting solution was vortex mixed and poured onto a petri dish containing a minimal glucose agar substrate. To assay for indirect biological activity, a replicate of the test procedure was performed

response of twice the spontaneous reversion rate (background).

procedure, 2 mL of molten top agar (40 °C) was added to the test mixture (in 50 µL DMSO); 100 µL of the *Salmonella* bacteria was then added and the resulting solution was vortex mixed and poured onto a petri dish containing a minimal glucose agar substrate. To assay for indirect biological activity, a replicate of the test procedure was performed with the addition of 500 µL of the rat liver S9 solution. This procedure is represented in Figure 69. The petri dishes were then placed in an incubator at 37 °C for 48 hours. Revertant colonies were determined using a Biotran II colony counter (New Brunswick Scientific). Positive controls routinely used in the study included 1,8-dinitropyrene (LC Services, Woburn, MA), 2-aminofluorene (Sigma Corp., St. Louis, MO), benzo[a]pyrene (Sigma), and sodium azide (BDH Inc, Toronto, Ontario, Canada).

A total of six *Salmonella typhimurium* bacterial strains were used in this study (49-51). Strains YG1020 and YG1025 are TA98 and TA100 type strains respectively which are auxotrophic for histidine and contain pKM101, but have been modified by the addition of the plasmid pBR322. Strains YG1021 and YG1026 are TA98 and TA100 type strains respectively containing multiple copies of the plasmid pBR322 containing the gene for the activating enzyme nitroreductase. Strains YG1024 and YG1029 are TA98 and TA100 type strains respectively modified by the addition of pBR322 plasmid DNA containing the gene for the activating enzyme O-acetyltransferase. Table 6 lists the typical spontaneous reversion rates and positive control revertants for each of the *Salmonella* strains used. Figure 70 shows the dose response curves obtained from assays with selected *Salmonella* strains tested with standard mutagens. A positive response in the assay is evidenced by a positive dose response relationship that achieves a minimum

Figure 74. Representation of the Ames *Salmonella typhimurium* assay procedure.

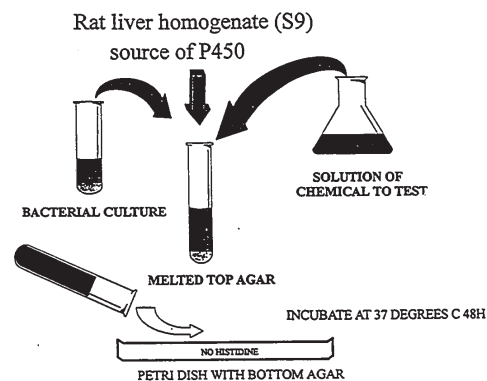
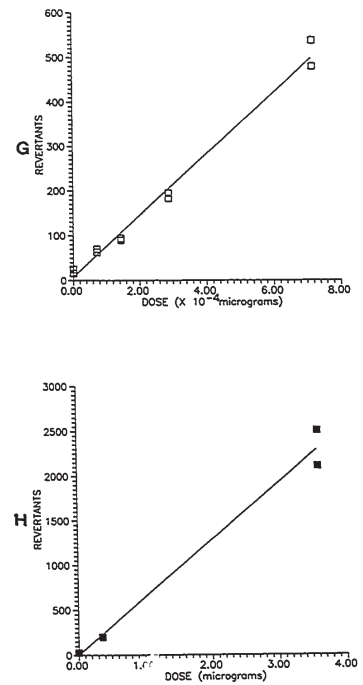
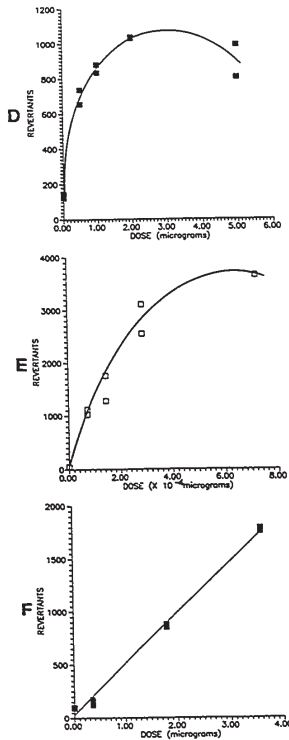
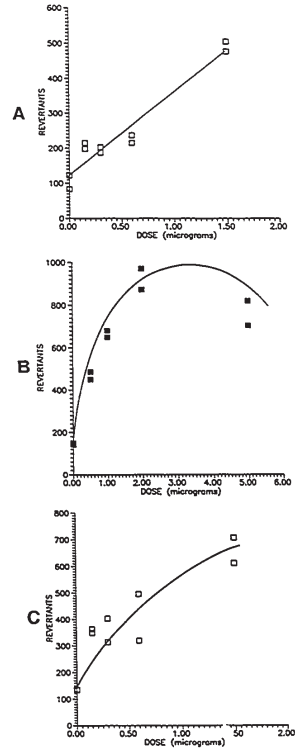


Figure 75. Dose response curves exhibited by standard mutagens when assayed with *Salmonella typhimurium* bacterial strains using the described procedure.

- A. YG1029 direct, sodium azide
- B. YG1029+S9, benzo[a]pyrene
- C. YG1025 direct, sodium azide
- D. YG1025+S9, benzo[a]pyrene
- E. YG1024 direct, 1,8-dinitropyrene
- F. YG1024+S9, 2-aminofluorene
- G. YG1020, 1,8-dinitropyrene
- H. YG1020+S9, 2-aminofluorene





## V. REFERENCES

1. Poulton, D.J., *J. Great Lakes Res.* 13(2), 193-201, 1987.
2. Murphy, T.P., Brouwer, H., Fox, M.E., Nagy, E., McArdle, L., and Moller, A. Coal tar contamination near Randle Reef, Hamilton Harbour. NWRI contribution No. 90-17, 1990.
3. Remedial Action Plan for Hamilton Harbour, Stage 1 Report, Environmental Conditions and Problem Definition. 1992.
4. Black, J.J. *J. Great Lakes Res.* 9(2), 326-334, 1983.
5. Couch, J.A., and Harshbarger, J.C., *Environ. Carcinogenesis Revs.* 3, 63-78, 1985.
6. Mix, M.C. Cancerous diseases in aquatic animals and their association with environmental pollutants: A critical review of the literature. Report for the American Petroleum Institute, Washington D.C., 239 pg. 1986.
7. Hayes, M.A., Smith, I.R., Crane, T.L., Rushmore, T.H., Thorn, C., Kocal, T.E., and Ferguson, H.W. *Sci. Tot. Env.* 94, 105-123, 1990.
8. Smith, I.R. and Ferguson, H.W.. The assessment of a point source discharge of suspected mutagenic and carcinogenic contaminants: An epidemiological approach. Proceedings of the Ontario Ministry of the Environment Technology Transfer Conference 6, 285-332, 1985.
9. Metcalfe, C.D., Cairns, V.W., and Fitzsimons, J.D. *Can J. Fish Aquat. Sci.* 45, 2161-2167, 1988.
10. Metcalfe, C.D., Balch, G.C., Cairns, V.W., Fitzsimons, J.D., and Dunn, B.P. *Sci. Tot. Env.* 94, 125-141, 1990.
11. Malins, D.C., McCain, B., Brown, D., Chan, S.L., Myers, M., Landahl, J., Prohaska, A., Friedman, A., Rhodes, L., Burrows, D., Gronlund, W., Hodgins, H., *Environ. Sci. Tech.*, 18, 705-713, 1984.
12. Baumann, P.C., Smith, W.D., Parland, W.K., *Trans. Am. Fish. Soc.*, 116, 79-86, 1987.

- 7, 529-543, 1988.
28. Schuetzle, D., and Lewtas, J. *Anal. Chem.*, 58(11), 1060A-1075A, 1986.
29. McCalla, D.R., Quilliam, M.A., Kaiser-Farrell, C., Tashiro, C., Hoo, K., Gibson, E.S., Lockington, N.J., Kerr, A.A. and Sheldrake, C. Integrated approach to the detection and identification of steel foundry mutagens. In King, C.M., Romano, L.J. and Schuetzle Eds. *Carcinogenic and Mutagenic responses to aromatic amines and nitroarenes*, Elsevier, pp 47-63, 1988.
30. Quilliam, M.A. and Wright, J.L.C., *Anal. Chem.*, 61(18), 1053A-1059A, 1989.
31. Fernandez, P., Grifoll, M., Solanas, A.M., Bayona, J.M. and Albaiges, J., *Environ. Sci. Technol.*, 26(4), 829, 1992.
32. Junk, G.A. and Richard, J.J., *Anal. Chem.*, 58, 962-965, 1986.
33. Grosjean, D., *Anal. Chem.*, 47, 797-805, 1975.
34. Breuer, G.M., *Anal. Lett.*, 17(A11), 1293-1306, 1984.
35. Eiceman, G.A., Viau, A.C., and Karasek, F.W., *Anal. Chem.*, 52, 1492-1496, 1980.
36. Koh, T.S., *Anal. Chem.*, 55, 1814-1815, 1983.
37. Junk, G.A., and Richard, J.J., *Anal. Chem.*, 58, 962-965, 1986.
38. Hawthorne, S.B., and Miller, D.J., *J. Chromatogr.*, 403, 63-76, 1987.
39. Hawthorne, S.B., and Miller, D.J., *Anal. Chem.*, 59, 1705-1708, 1987.
40. Davies, I.L., Raynor, M.W., Kithinji, J.P., Bartle, K.D., Williams, P.T., and Andrews, G.E., *Anal. Chem.*, 60, 683(A)-702(A), 1988.
41. Hawthorne, S.B., *Anal. Chem.*, 62, 633(a)-642(A), 1990.
42. Golden, C., and Sawicki, E., *Int. J. Environ. Anal. Chem.*, 4, 9-23, 1975.
43. Grimalt, J., Marfil, C., Albaiges, J., *Int. J. Environ. Anal. Chem.*, 18, 183-194, 1984.
44. Brignole, E.A., *Fluid Phase Equilib.*, 29, 133-144, 1986.

13. Myers, M.S., Landahl, J.T., Krahn, M.M., and McCain, B.B. *Env. Health Pers.*, 90, 7-15, 1991.
14. Stein, J.E., Reichert, W.L., Nishimoto, M., and Varanasi, U. *Sci. Tot. Env.*, 94, 51-69, 1990.
15. Baumann, P.C. *J. Great Lakes Res.*, 10(3), 251-253, 1984.
16. Gardner, W.D. *J. Mar. Res.* 38, 17-38, 1980.
17. Gardner, W.D. *J. Mar. Res.* 38, 41-52, 1980.
18. Eadie, B.J., Chambers, R.L., Gardner, W.S. and Bell, G.L. *J. Great Lakes Res.* 10, 307-321, 1984.
19. Baker, J.E., Eisenreich, S.J. and Eadie, B.J. *Environ. Sci. Technol.* 25, 500-509, 1991.
20. Bryant, D.W., McCalla, D.R., and McCarty, B.E. Classical PAH form a minor portion of mutagens detected in Hamilton air particulates. Interim report for Ontario Ministry of the Environment project 386G, 1989.
21. Vo-Dinh, T. Significance of chemical analysis of polycyclic aromatic compounds and related biological systems. In: *Chemical analysis of polycyclic aromatic compounds*, T. Vo-Dinh ed., J. Wiley & Sons, Toronto, 1989.
22. Chipman, J.K. and Marsh, J.W. *J. Biotech.* 17, 199-208, 1991.
23. *Polynuclear Aromatic Hydrocarbons: Chemistry, Metabolism and Carcinogenicity*, R. Freudenthal and P. Jones, Eds., Raven Press, New York, 1976.
24. West, W.R., Smith, P.A., Booth, G.M., and Lee, M.L. *Environ. Sci. Technol.* 22, 224-228, 1988.
25. Durant, J.L., Hemond, H.F., and Thilly, W.G. *Environ. Sci. Technol.* 26, 599-608, 1992.
26. Maccubbin, A.E., Ersing, N., and Frank, M.E. *J. Great Lakes Res.* 17(3), 314-321, 1991.
27. Fabacher, D.L., Schmitt, C.J., Besser, J.M., and Mac, M. *Environ. Tox. Chem.*

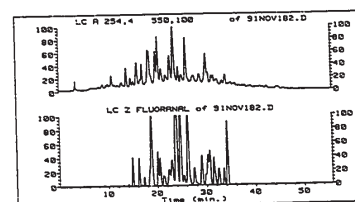
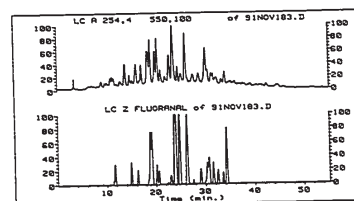
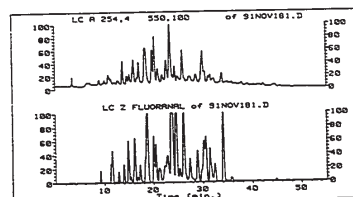
45. Stahl, E.A. and Quirin, K.W., *Fluid Phase Equilib.*, 8, 93-105, 1983.
46. Allan, L.M. Sulphur-containing aromatic compounds in the environment. B.Sc. thesis, Department of Chemistry, McMaster University, 1992.
47. Tessaro, M. A Bioassay-Directed Fractionation Investigation of Sydney Harbour. B.Sc. thesis, Department of Chemistry, McMaster University, 1993.
48. Fox, M. and Charlton, M., personal communication, 1993.
49. Ramdahl, T. *Environ. Sci. Technol.* 17, 666-670, 1983.
50. Watanabe, M., Ishidate, M. Jr., and Nohmi, T. *Mutat. Res.* 216, 211-221, 1989.
51. Watanabe, M., Ishidate, M. Jr., and Nohmi, T. *Mutat. Res.* 234, 337-348, 1990.
52. Watanabe, M., Einisito, P., Ishidate, M. Jr., and Nohmi, T. *Mutat. Res.* 259, 95-102, 1991.
53. Claxton, L.D., Creason, J., Leroux, B., Agurell, E., Bagley, S., Bryant, D.W., Courtois, Y.A., Douglas, G., Clare, C.B., Goto, S., Quillardet, P., Jagannath, D.R., Kataoka, K., Mohn, G., Nielson, P.A., Ong, T., Pederson, T.C., Shimizu, H., Nylund, L., Tokiwa, H., Vink, G.J., Wang, Y., and Warshawsky, D. *Mutat. Res.* 276, 23-32, 1992.
54. Wise, S.A., Benner, B.A., Liu, H., Byrd, G.D., and Colmsjo, A. *Anal. Chem.* 60, 630-637, 1988.
55. Zeiger, E., Anderson, B., Haworth, S., Liawlor, T., and Mortelmans, K., 1992. *Environ. Molec. Mutagen.* 19 Suppl., 21, 2-141, 1992.
56. Sakai, M., Yoshida, D., and Mizusaki, S. *Mutat. Res.* 156, 61-67, 1985.
57. Rice, J.E., Coleman, D.T., Hosted, T.J., Lavoie, J., McCausland, D.J., *Cancer Res.*, 45, 5421-5425, 1985.
58. Mersch-Sundermann, V., Mochayed, S., and Kevekordes, S. *Mutat. Res.* 278, 1-9, 1992.
59. Epstein, S.S., Mantel, N. and Stanley, T.W., *Environ. Sci. Technol.* 2, 132-138, 1968.
60. Warshawsky, D., *Environ. Carcino. and Ecotox. Revs.*, C10(1), 1-71, 1992.

61. Legzdins, A.E., McCarty, B.E. and Bryant, D.W. Polycyclic aromatic compounds in Hamilton air: their mutagenicity, ambient concentrations and relationships with atmospheric pollutants, 1994.
62. Butler, A.C. and Sibbald, R.R., *Bull. Environ. Contam. Toxicol.* 37, 570-578, 1986.
63. Dunn, B.P., *Environ. Sci. and Technol.* 10(10), 1018-1021, 1976.
64. Dunn, B.P. and Stich, H.F., *Bull. Environ. Contam. Toxicol.* 15, 398-401, 1976.
65. Hartley, D.M. and Johnston, B., *Bull. Environ. Contam. Toxicol.* 31:33-40, 1983.
66. Kurelec, B., *Crit. Rev. Toxicol.* 22, 23-43, 1992.
67. Griffiths, R.W., Schloesser, D.W., Leach, J.H. and Kovalak, W.P., *Can. J. Fish. Aquat. Sci.* 48, 1381-1388, 1991.
68. Cooley, J.M., *J. Great Lakes Res.* 17(1), 1-2, 1991.
69. Mackie, G.L., *Hydrobiologia.* 219, 251-268, 1991.
70. Neary, B.P. and Leach, J.H., *Can. J. Fish. Aquat. Sci.* 49, 406-415, 1992.
71. Strayer, D.L., *Can. J. Fish. Aquat. Sci.* 48, 1389-1395, 1991.
72. MacLeod, W.D., Jr., Brown, D.W., Friedman, A.J., Burrows, D.G., Maynes, O., Pearce, R.W., Wigren, C.A., and Bogar, R.G. Standard Analytical Procedures of the NOAA National Analytical Facility, 1985-1986, Extractable Toxic Organic Compounds, NOAA Technical Memorandum NMFSF/NWC-92, National Oceanic and Atmospheric Administration, National Marine Fisheries Service, United States Department of Commerce, Seattle, Washington, 1985.
73. Mayer, Y. and Nagy, E., *Water Poll. Res. J. Canada.* 27, 807-831, 1992.
74. Ontario Ministry of the Environment and Energy. Hamilton Harbour technical summary and general management options. Ontario Ministry of the Environment and Energy, Water Resources Branch, Toronto, Ontario, 1985.
75. Maron, D.M. and Ames, B.N., *Mutat. Res.* 113, 173-215, 1983.

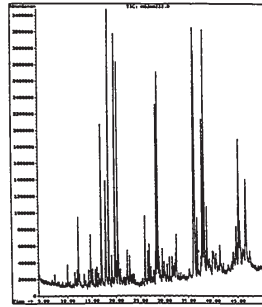
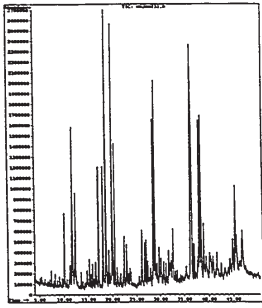
## VI. APPENDICES

Appendix 1. Analyses of Hamilton Harbour sediment trap sample extracts.

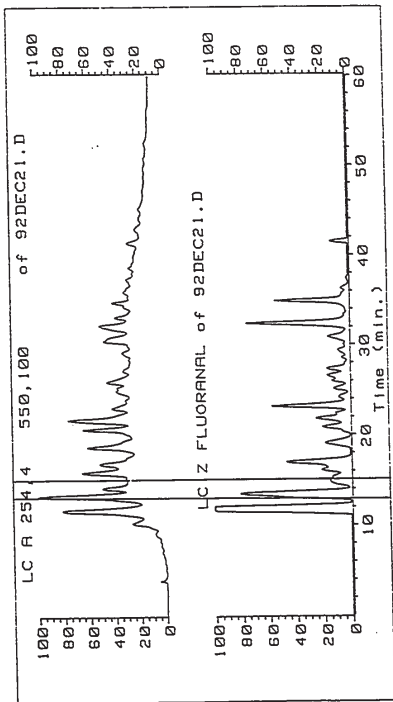
Reverse phase HPLC chromatograms of the A22/LH20 fractions of the station 53 top (A), middle (B) and bottom (C) sediment trap extracts. These analyses show the similarities in the chromatographic profiles of these extracts.



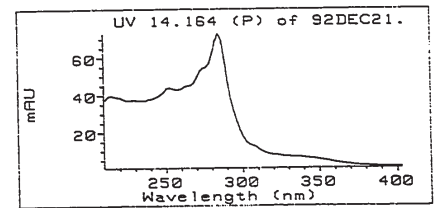
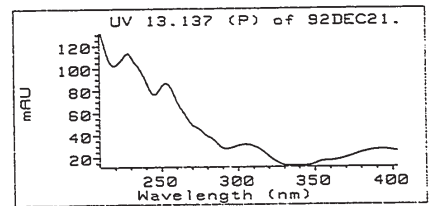
GC-MS total ion current chromatograms of the A23/LH20 fractions of the station 53 top (A) and bottom (B) sediment trap extracts. Peak identifications can be made by referring to Figure 26.



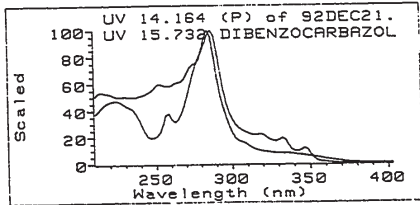
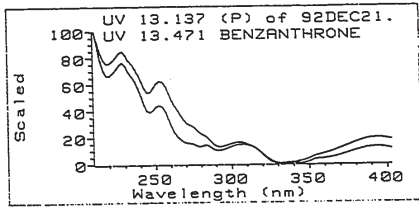
Appendix 2. Details of Hamilton Harbour sediment trap fraction N3 mutachromatogram.



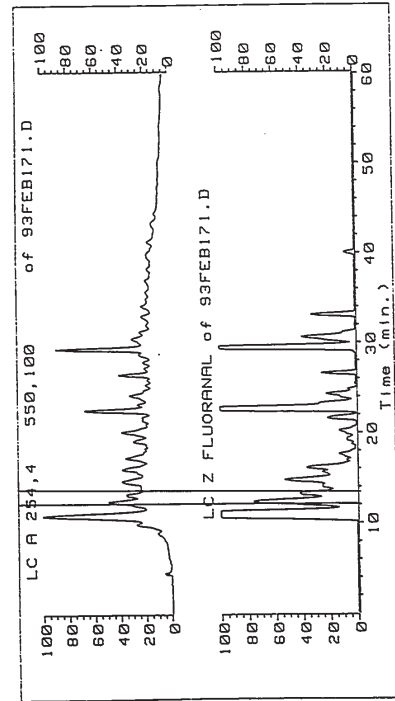
Reversed-phase HPLC UV absorption and fluorescence chromatograms from the station 50 top sediment trap fraction N3 mutachromatogram. The active subfractions are indicated.



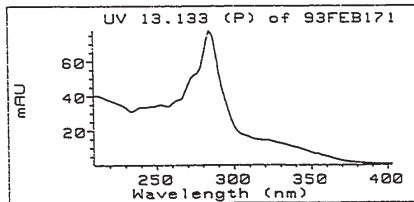
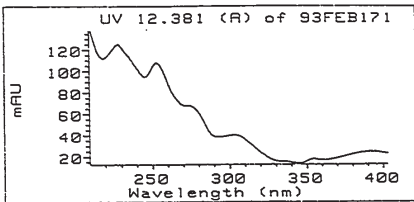
UV absorption spectra of peaks in active subfractions of the station 50 top sediment trap fraction N3 mutachromatogram. The elution times of the peaks are shown above the UV spectra.



UV absorption spectra of peaks in active subtractions of the station 50 top sediment trap fraction N3 mutachromatogram and their comparisons with library spectra of standard compounds. The elution times of the peaks are shown above the UV spectra.



Reversed-phase HPLC UV absorption and fluorescence chromatograms from the station 50 top sediment trap fraction N3 mutachromatogram. The active subtractions are indicated.



UV absorption spectra of peaks in active subtractions of the station 53 sediment trap fraction N3 mutachromatogram. The elution times of the peaks are shown above the UV spectra.